



MASTER THESIS

# STUDY OF DECOUPLED UPLINK AND DOWNLINK ACCESS IN 5G HETEROGENEUS SYSTEMS

A thesis submitted by Enric Pardo for the degree "Enginyeria de Telecomunicació" in Universitat politècnica de Catalunya (UPC)

---

This thesis has been supervised by Professor Mischa Dohler (KCL) and co-supervised by Dr Anna Umbert (UPC) and Dr Maria Lema (KCL)

London, May 2016

*If you can dream—and not make dreams your master;*
*If you can think—and not make thoughts your aim;*
*If you can meet with triumph and disaster*
*And treat those two imposters just the same;*
*If you can fill the unforgiving minute*
*With sixty seconds' worth of distance run*
*Yours is the Earth and everything that's in it,*
*And—which is more—you'll be a Man my son!*

*(Rudyard Kipling)*

# Abstract

Uplink and downlink decoupling (DUDe) is a disruptive technique that has been proposed recently to reduce the uplink and downlink imbalance problem, which occurs in HetNets due to the strong transmit power disparities between macro and small cells.

In this thesis, previous research done on DUDe, in particular the association probability derivation, is used to calculate how the capacity is affected when the association is made to any SCell in the scenario. This specific situation is highly realistic since one or several small cells might be unavailable due to overload reasons. Therefore, one of the main objectives of this thesis is to evaluate and compare the potential capacity gains of decoupling to any other small cell in the scenario with respect to the macro cell, association that follows classical downlink received power policies. Decoupling uplink from the macro cell can improve as well the uplink outage, metric also evaluated and compared in this study.

Moreover, there is a strong trend in research to empower multi-connectivity solutions, where one user has more than one uplink connection. We refer to this case as a dual connectivity scenario, and the uplink is further studied by allowing decoupled associations in dual connectivity scenarios. Dual connectivity in the uplink is highly controversial, since the user has limited power to share between two different access points. Therefore, a part from comparing the decoupled association performance with the downlink received power policies, this study compares the performance of multi-connectivity against having one single serving cell. In this case, comparison is done with respect to the best uplink serving cell.

Results show that decoupling the access increases the capacity even if there are some SCells unreachable and presents great performance on DC scenario

# Resum

*L'Uplink and downlink decoupling* (DUDe) és una innovadora tècnica que ha sigut proposada recentment per reduir el problema de *l'uplink and downlink imbalance*. *L'uplink and downlink imbalance* es dona a les *heterogeneous networks* (HetNets) degut a la disparitat de potències entre les diferents antenes.
Durant aquest projecte, tenint en compte la recent recerca sobre DUDe (sobretot sobre la probabilitat d'associació de lusuari), s'utilitza per calcular la capacitat a qualsevol *SCell*. Aquesta situació es molt important d'analitzar ja que pot ser possible que algunes no estiguin accessibles per sobrecàrrega. Per aquest motiu, un dels principals objectius del projecte és avaluar la millora de capacitat entre realitzar el DUDe a qualsevol *SCell* i mantenir l'associació amb la *MCell* com s'havia fet fins ara, el que es coneix com a *downlink receive power* (DRP). El DUDe també comporta moltes millores a la *outage probability*, indicador que també s'evalua a l'estudi.
En els estudis més recents també treballen amb *dual connectivity* per millorar les prestacions. Tot i que dividir la transmissió a l'enllaç de pujada pot comportar perdre capacitat degut a la baixa potència de l'usuari, es compara la capacitat amb el DUDe en un escenari de dual connectivity amb el cas de *single best association*. Els resultats mostren que el fet de desacoplar laccés aumenta la capacitat de la connexió tot i tenir algunes *SCells* inabastables. També s'ha mostrat que el DUDe funciona perfectament amb la *dual connectivity*.

# Resumen

El *Uplink and downlink decoupling* (DUDe) es una novedosa técnica propuesta recientemente para reducir el problema del *uplink and downlink imbalance*. El *uplink and downlink imbalance* ocurre cuando las potencias de una *heterogeneous network* (HetNet) son muy dispares.

En este proyecto, teniendo en cuenta la investigación realizada hasta la fecha sobre el DUDe (especialmente sobre la probabilidad de asociación), se calcula la capacidad asociándose a cualquier *SCell*. Esta situación es muy imporante ya que puede ser que algunas celdas sean inalcanzables por el usuario debido a que pueden estar sobrecargadas. Por este motivo, uno de los principales objetvos del proyecto es avaluar la mejora de capacidad al realizar el DUDe con cualquier *SCell* y mantener la asociación con la *MCell* tal y como se ha hecho hasta ahora. Esta técnica se llama *downlink receive power* (DRP). El DUDe también mejora la *outage probability*, indicador que también se evalua en el estudio.

En los estudios mas recientes también se trabaja con *dual connectivity* para mejorar las prestaciones de la conexión. Aunque dividir la transmisión en el enlace de subida entre dos antenas puede disminuir la capacidad debido a la baja potencia del usuario, se compara la capacitat de desacoplar el acceso en *dual connectivity* con el escenario de *single best association*.

Los resultados muestran que el DUDe aumenta la capacidad aun y teniendo algunas *SCells* inalcanzables. También se ha demostrado que el DUDe funciona perfectamente con la *dual connectivity*.

# Acknowledgements

This thesis is the result of 6 months of research in Centre of telecommunications research at KCL. I never imagined I could get the chance to study here and I would like to give some lines to thank all of those that helped me to fulfil this dream.
I want to first thank Professor Mischa Dohler, my thesis supervisor, for trusting in me and giving me the opportunity of carrying out this project at KCL. Also, I am deeply grateful to Dr Maria Lema, this thesis would have not been possible without your guidance and your patience. Besides the academic point of view, I also would like to thanks for making me feel part of the team from the very first moment I arrived. I am also very grateful to Anna Umbert, my thesis supervisor in Spain, for agree to carry this thesis and for her support and help from Barcelona.
I would also like to thanks Mabel Gómez for her advices on the report.
I would also like to acknowledge all my friends in London that made the best of this experience. This would not have been such great without you
To all my friends in the university, who have been here during these 7 years even in the darkest times. As this thesis is the result of all these years, I am completely sure that I would have not reach this final step without you.
Last, but not least, to my family. They always have been by my side, no matter what my decisions were, and have given everything to fulfil my dreams. I could not find enough words to express my gratitude
A tots vosaltres, gràcies.

# List of Figures


2.1 Uplink-Downlink imbalance . . . . . 8
2.2 Comparison DUDe and DRP . . . . . 9

3.1 PPP and PCP . . . . . 12
3.2 Centred device scenario . . . . . 13
3.3 Void probability SBA . . . . . 14
3.4 Void probability nth . . . . . 17

4.1 DUDe nth Single Best Association Scenario . . . . . 21
4.2 nth SBA, Case 1 . . . . . 23
4.3 nth SBA, Case 2 . . . . . 24
4.4 nth SBA, Case 3 . . . . . 25
4.5 nth SBA, Case 4 . . . . . 26
4.6 Association probability Best SBA, n=1 . . . . . 29
4.7 Association probability Nth SBA, n=2,3,4,5 . . . . . 30
4.8 Decoupling probability for n=1,2,3,4 and Pm/Ps = 20,200 . . . . . 31
4.9 Comparison capacity $n$-th Single Best Association, n=1,2,3,4 . . . . 32
4.10 Reliability capacity nth SBA DUDe/DRP . . . . . 32
4.11 Outage probability nth SBA DUDe/DRP . . . . . 33
4.12 Reliability Outage Probability: Outage probability nth SBA . . . . 33

5.1 Dual Connectivity scenario . . . . . 35
5.2 Association Case 1 . . . . . 38
5.3 Association Case 2 . . . . . 39
5.4 Association Case 3 . . . . . 41
5.5 Association Case 4 . . . . . 42
5.6 Association probability 2 Best Association . . . . . 45
5.7 Decoupling probability 2 Best Association . . . . . 45
5.8 PDF Density conditioned . . . . . 46
5.9 Capacity 2nd Association. Comparison DUDe/DRP. . . . . 47
5.10 Capacity 2 Best Association. Comparison SBA/DC. . . . . 47

# List of Tables

3.1 Notation . . . . . 19

4.1 Probability regions *nth*-SBA . . . . . 22

5.1 Probability regions in a Best Association Dual connectivity scenario 36

# Contents

**Abstract** **ii**

**Resum** **iii**

**Resumen** **iv**

**Acknowledgements** **v**

**List of Figures** **vi**

**List of Tables** **viii**

**1 Introduction** **1**

1.1 Motivation . . . . . 1

1.2 Main contributions . . . . . 3

1.3 Thesis outline . . . . . 3

**2 Background and State of the Art** **5**

2.1 Towards 5G mobile networks . . . . . 5

2.2 Heterogeneous networks . . . . . 6

2.3 UL/DL Imbalance . . . . . 7

2.4 Downlink and Uplink Decoupling . . . . . 7

2.5 Dual Connectivity . . . . . 9

**3 System model** **10**

3.1 Poisson Point process: Main definitions . . . . . 10

3.2 Our system model . . . . . 11

3.3 Void Probability . . . . . 14

3.4 Interference modelling . . . . . 16

3.5 Notation . . . . . 18

**4 The reliability of the decoupled access** **20**

4.1 Introduction . . . . . 20

4.2 Association probability . . . . . 21

4.3 Capacity . . . . . 26

4.4 Outage probability . . . . . 28

4.5 Performance evaluation . . . . . 29

**5 Decoupling access on Dual Connectivity scenario** **34**

5.1 Introduction . . . . . 34

5.2 Probability regions . . . . . 35

5.3 Capacity . . . . . 43

5.4 Performance evaluation . . . . . 44

**6 Conclusions and further work** **48**

**Appendices** **50**

**A Matlab code** **51**

**B Scientific paper related to the thesis** **68**

**Bibliography** **93**

# Chapter 1

# Introduction

## 1.1 Motivation

Since the 4th generation of mobile communications was launched, the data traffic over cellular networks has been increasing massively. Also, the services offered nowadays pose stringent requirements over the network, and current cellular deployments can not simply deliver the desired quality of service. The increase of data and this need for improved user experience, has driven the need to offload traffic from cells, and as well as to bring the cell closer to the user. To this end, the use of heterogeneous networks has been increasingly considered in today's network deployments. Essentially, a HetNet is a network that overlays high power and low power cells: macro and small cells, (MCell and SCell, respectively). However, due to the cell transmit power disparities, users can face what it is called the uplink-downlink imbalance problem: the best serving cell, based on the received signal, is different for both uplink and downlink, meaning that the DL received power is higher the MCell, whereas the UL received power decreases dramatically. One of the solutions proposed to solve this problem is Uplink and downlink decoupling (DUDe).

Many services involved in mobile communications were originally created for the user to consume content, rather than generate it. In such a context, traditionally networks have been planned based on downlink performance parameters and downlink capacity has always been maximized. Nowadays, there has been big

change in way the communications are understood. A lot of applications of the Internet of Things, the Tactile Internet or M2M Communications require also a high capacity in the uplink. For this reason, the research community has started to propose innovative solutions to reduce the capacity imbalance between the uplink and the downlink, and move towards a more symmetric connectivity [1].

On the road to the fifth generation (5G), features such as dual Connectivity (DC) are gaining interest in the context of radio access networks [15]. In a DC scenario, two different base stations are used to transmit information. DC allows the user either to split the information or to transmit the same information via different paths as a means to increase the reliability, this is known as multi-path. The fact that both transmissions are uncorrelated, multi-path decreases the probability of errors. If DC is used as a means to aggregate traffic, the user is likely to improve capacity, since it will opt to a higher bandwidth being actively transmitting to and from different base stations.

Another feature particularly interesting to reduce the UL and DL capacity imbalance is the use of decoupled UL and DL connections. Instead of performing the UL connection to the strongest BS signal received, it transmits information towards the base station that has highest received power in the UL. This means that, although the user is under the Mcell DL radio coverage, if it is closer to the SCell (i.e., is less attenuated, as the attenuation is related to the distance) it will transmit the UL signals to the SCell. Although DUDe can be useful to offload traffic from the MCell, SCells can be easily overloaded too, and in such conditions, the decoupled access towards another SCell (likely to be further from the user) needs to be evaluated.

The question then is, is it still a good idea to decouple the access? Even if the device has to connect to the 2nd, 3rd or even a further SCell? To this end, this thesis provides an in depth study of decoupled associations to the $n^th$ best SCell in the uplink. Also, since uplink transmissions need to be further improved in terms of capacity, decoupled associations are studied in a DC context.

## 1.2 Main contributions

The main objective of this thesis is to study how decoupling the access works once some SCells are unachievable. This is motivated because a device may not reach the closest SCell due to overload, other physical limitation like the fronthaul mechanism. Also, to study how DUDe works on dual connectivity.
To this end, a two-tier HetNet environment is studied in terms of two Key Performance Indicators (KPI's), Capacity and Outage probability, with the use of stochastic geometry. The two main contributions of this thesis are:

- In a Single Best Association scenario, it is considered that some Cells are not available to the user due to overloading and maximum capacity reach. In this environment, we have extended the association well studied in [23], to a generic case: $N^{th}$ best association. The two selected KPIs are compared to the traditional association, Downlink receive power (DRP), where the uplink is coupled to the cell that performs the best downlink. Our analytical study shows that in high dense scenarios, decoupling even to the 4-th cell improves the uplink capacity with respect to traditional cell association.

- In a Dual Connectivity scenario, we consider two uplink associations. The user is associated to the first and second best base stations, following uplink received power policies. In such conditions, we evaluate if decoupled associations offer improvements with respect to traditional downlink received power association rules. Moreover, the feasibility of DC in the UL is discussed, since user power limitations may impair the throughput performance, mainly due to multi-connectivity. Similar arguments where addressed in the community in the past with the use of Carrier Aggregation for cell edge users in the UL.

## 1.3 Thesis outline

The thesis has 6 chapters and is structured as follows:

- Chapter 2 reviews the theoretical aspects that sustain the developments of this thesis. It begins with a brief story of the mobile generations, from 1G

until the 4G and the evolution towards 5G. This chapter addresses main concepts required to understand the framework of this Master Thesis, such as HetNets, DC and decoupled associations.

- Chapter 3 goes through the main concepts of stochastic geometry, main mathematical tool used in this thesis to assess the performance of the mobile network. First, the main general definitions are shown. Subsequently the system model is explained: the two-tier network, void probability to $n$-th connection and interference modelling. Finally, the assumptions of the system model are also explained.

- Chapter 4 is the first of study of this thesis. The association probability to the $n$-th closest SCell is calculated and used to show how beneficial is to decouple the access based on two KPI's: the uplink capacity and the outage probability.

- Chapter 5 is the second study of the thesis. The probability regions of the decoupling on a Dual Connectivity scenario are computed and used to show if the decoupled access is beneficial to improve the overall uplink capacity.

- Finally, in Chapter 6 the final conclusions are extensively commented, followed by the future work.

# Chapter 2

# Background and State of the Art

This chapter resumes the background necessary for the study: In 2.1 a brief explanation of five generations of mobile communications is given. Then, in 2.2 it is more focused in 4G, specially in one of its main characteristics, HetNets. Although it brought a lot of advantages, the use of HetNets brought one huge disadvantage, uplink and downlink imbalance (2.3). Two possible solutions to this problem, Uplink and downlink decoupling (2.4) and dual connectivity (2.5) are briefly explained. The studies of decoupling and dual connectivity relevant to the study done so far are also mentioned

## 2.1 Towards 5G mobile networks

The first mobile generations (1G), back in the 80's, was the first mobile communications, although in 0G there were systems that preceded modern cellular mobile telephony technology. They used analogical networks and it was the first commercialization of mobile phones.
When it switched to digital network, we called it second generation (2G). It was launched on the GSM standard in Finland in 1991. Two benefits of 2G networks over their predecessors were:

- Phone conversations were digitally encrypted, allowing transferring of data in such a way that only the intended receiver can receive and read it.

- 2G introduced data services for mobile, starting with SMS text messages.

After 2G was launched, the previous mobile telephone systems were retroactively dubbed 1G.
The third generation of mobile telecommunications technology (3G), was released in 2002. The main changes from the previous generation was the spread of using Internet Access and starting to use video calls and mobile TV.
Although the data was shyly presented in 3G, it was not until the fourth generation (4G) where the data was exploited and even more used than the voice [4]. This is thanks to the high capacity achieved by the OFDM modulation and also for the spectral efficiency improvements as well.
For the first four generations a considerable change was needed in order to switch into the next generation. For the fifth generation (5G), however, we need more than this. The change to the next generation include interactivity between the machines, without the direct implication of the user, with things such Smart Cities applications, M2M communications, Internet Of Things and the innovative Tactile Internet. In spite of that, the most important and disruptive change for 5G is the unification of different technologies such LTE and WiFi to take the advantage of all these technologies and combine them to achieve all the challenging features that future applications requires [7].

## 2.2 Heterogeneous networks

To address the explosive growth in data demands driven by smart phones, tablets or new technologies involved in the Internet Of Things or Smart Cities, network operators will have to significantly increase the capacity of their networks (there are just too many devices demanding too much data), as well as to reduce the cost/bit delivered perhaps two orders of magnitude.
It becomes necessary to increase the number of Base stations (BS), which we call *macrocells* (MCell). However, in many situations, adding further MCells is not viable due to cost or the lack of available sites. The problem operators face is not coverage, which is nearly universal, but capacity. This means that more Cells are needed. Adding BS has been by far the most important factor historically in order to increasing capacity. When BS are added, each user competes with a smaller

number of users.
From all this, it comes the necessity to introduce other types of different BS. Smaller Cells that will provide more options to the users to perform their connections, with very little extra-cost as theses Cells are easy to install. However, these SCells has a very low power in a very low coverage. Their aim is to provide extra connections in very specific hotspots.
The implications of the coexistence of these two types of Cells, which we call Heterogeneous Networks (HetNets), are extensive. It changes the way the networks are deployed and opens a huge range of possibilities. When the HetNet has two different types of cells (as in our study) it is called a two-tier Network.

## 2.3 UL/DL Imbalance

When different type of Cells are used, in spite of all the advantages it brings, it carries some disadvantages as well. The most detrimental to the connection is what we call $Uplink - Downlink\ imbalance$. The problem with the Uplink-Downlink imbalance starts when a sector with the strongest downlink to a BS may not necessarily be the sector with the strongest uplink signal strength for that BS. This might not be so important if we would not require a higher capacity in the uplink, like internet or regular calls. However, with the 5G challenges, it will be necessary to achieve an equilibrium that new technologies such Smart cities applications or Tactile Internet require. Therefore this problem needs to be solved[9].

## 2.4 Downlink and Uplink Decoupling

In order to solve the Uplink-Downlink imbalance problem, one possibility is to perform the Uplink and the Downlink with different BS. This would solve the problem of not being in the best zone of the coverage zone of certain cell for both uplink and downlink connection [10]. Also, it would avoid the differences of gain between the devices that are close to the MCell and the ones that are inside the coverage zone but further form the MCell (which can be up to 300% lower) [11]. Up to now, the connection was performed depending on from which BS the device

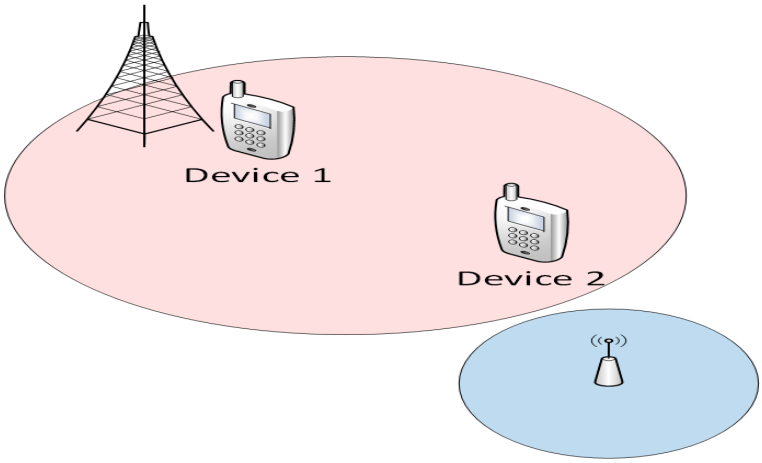


Figure 2.1: Uplink-Downlink imbalance. Device 2 would obtain a better uplink signal with the SCell although the best performance in the downlink is with the MCell.

received the most powerful signal [23].
Uplink and downlink decoupling (DUDe) proposes to hold this association rule for the downlink performance but for the uplink, perform the connection depending on the attenuation of the signal received by the device.
This means that, meanwhile the device keeps on performing the downlink with the strongest signal received from the Cell, it will perform the uplink depending on the distance between the device and SCell or the MCell. When the device is situated closer to a SCell than a MCell, but still inside the coverage zone of the MCell, it is situated in a decoupling zone. To evaluate how the decoupling behaves over the study, it will be compared with the suboptimal case 2.2. This, what we call Downlink Received Power (DRP), is to keep performing the connection with the MCell even in the decoupling zone.

In [11], the need of decoupling the access and how theoretically works is explained. The association probability is calculated in [21]. However, it only studies the single best association. In recent studies made on decoupling, like [10] and [23] calculate capacity and outage probability in a single best association. It does not take into account any further connection either.

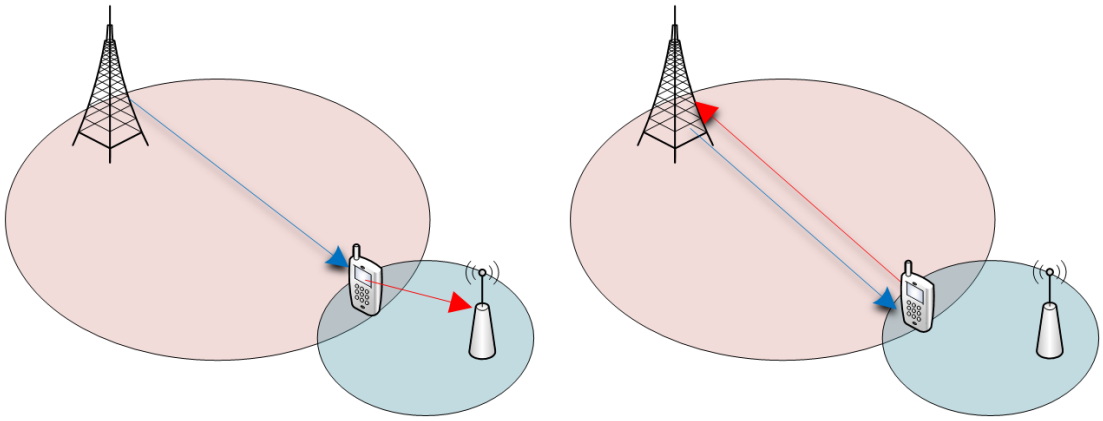

(a) DUDe (b) DRP

Figure 2.2: Comparison DUDe and DRP Association inside the decoupling zone

## 2.5 Dual Connectivity

The multiple connectivity is an operation where a device consumes radio resources provided by at least two different networks points [12]. In the case of Dual Connectivity (DC), two Cells are used to perform the connection. The information can be either split or transmit it twice. This network architecture with functionality separation is estimated to save more than one third of the current overall network power consumption [14]. DC is among the solutions standardized by 3GPP for release 12 [13].

In [14] the basic theory on the study is explained. In [12] the capacity in a dual connectivity scenario is calculated, although is based in the downlink connection. In the uplink is calculated in [14] But in a RSRP association without split the uplink and the downlink. In [16], the capacity to the Single best association, $n$-th single best association and Nth best association is calculated. However, every capacity is calculated individually instead of determine the final capacity of both connections.

# Chapter 3

# System model

In the past few years, it has been proved that stochastic geometry is the most convenient method to model communication systems. Traditionally, cellular networks have been modelled by placing the base stations on a grid, with users either randomly scattered or placed deterministically. However, these regular grids tend to overestimate the capacity of the networks [12]. Stochastic geometry appears to be a more realistic approach to evaluate the performance of wireless networks. Before the description of the system model itself, it is necessary to review some of the definitions and properties that will be used subsequently. These definitions are extracted from [18] and [19].

## 3.1 Poisson Point process: Main definitions

Let us consider a $d$-dimensional euclidean space, $\mathbb{R}^d$, with $d \geq 1$.

*Definition* **3.1** *A point process (PP) is a random and finite collection of points in the space* $\mathbb{R}^d$*, without accumulation points. A Poisson point process (PPP)* $\Phi$ *is a PPP where the points are randomly distributed following a Poisson pattern.*

*Definition* **3.2** *The intensity* $\lambda$ *is the number of random points of the process* $\Phi$*.*

A very useful property is the processes superposition. The sum of several point processes is another p.p.p. If we have $n$ independent p.p.p.'s $\Phi_1$, $\Phi_2$, $\Phi_3$... $\Phi_n$ with

intensities $\lambda_1$,$\lambda_2$,$\lambda_3$...$\lambda_n$ respectively:

*Definition* **3.3** *The sum of n PPP is another PPP* $\Phi_{TOTAL} = \sum_{i=1}^{n} \Phi_i$. *The intensity of this new process is* $\lambda_{TOTAL} = \sum_{i=1}^{n} \lambda_i$.

Let us consider another $d$-dimensional euclidean space, $\mathbb{R}^l$, with $l \geq 1$. This new space is a marking process. These marks can be either random values or deterministic numbers. Each mark $(m_i)$ is associated to a point$(x_i)$ of the PPP This marked process can be expressed as $\Phi_i = \sum_{i=1}^{n} \ x_i \cdot m_i$

*Definition* **3.4** *Kendall-like notation: A PP can be represented in a similar way of the queue theory models. It will be used ./. where the first parameter is the nature of the p.p. and the second one the nature of the marks. For a Poisson distribution it will be used letter M, for a deterministic placement letter D, and for a Rayleigh distribution a letter G.*

## 3.2 Our system model

Under the previous definitions, a simplified system model is deployed. Our system model is based on:

- Two independent and overlaid point processes $\Phi_s$ and $\Phi_m$ are being considered. $\Phi_s$, with intensity $\lambda_s$, represents the number of SCells. Likewise, $\Phi_m$ (with intensity $\lambda_m$), represents the number of MCells. Thus, we have a PPP $\Phi_v = \Phi_m + \Phi_s$. It is assumed to have one MCell ($\lambda_m = 1$) so if at any point it receives a stronger signal from a further MCell, the device will ignore it. In this point of view, this can be seen as a Poisson cluster process (PCP). The PCP models the random patterns produced by random clusters. The Poisson cluster processes are constructed from a parent PPP $\Phi = X_i$ ; i = 1, 2, 3,... by replacing each point $xi \in \Phi$ with a cluster of points $M_i$, $\forall$ $X_i \in \Phi$, where the points in $M_i$ are independently and identically distributed in the spatial domain [17]. Each cluster, in our case, is composed by one MCell and several SCells 3.1.

- A third PPP $\Phi_d$, with intensity $\lambda_d$, represents the users of the system. The number of users affect in a dramatic way as the BS are more occupied and

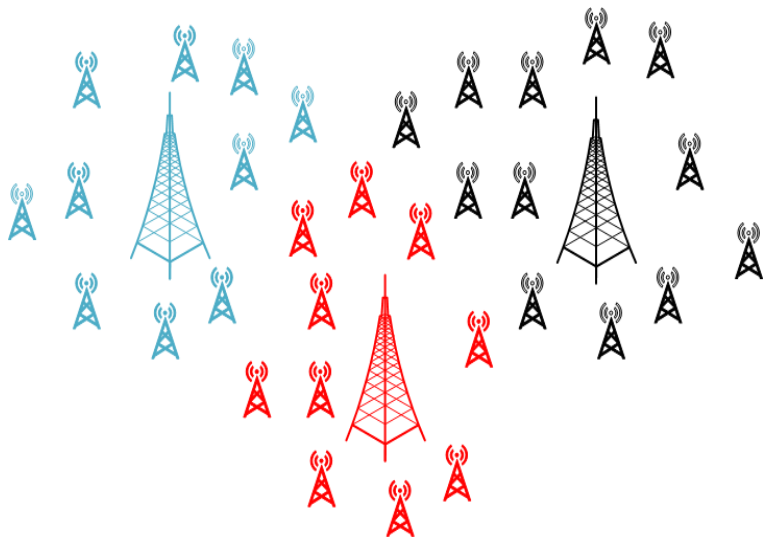

Figure 3.1: Two tier PPP with three PCP.

the interference increases. Normally $\lambda_d > \lambda_v$. Our study the system will hold 200 users per cluster.

The typical association for the device to perform is the RSRP (Reference Signal Received Power), which associates the device with the strongest signal received. This, in a mathematical model, is:

$$E_h[S_v{}^{DL}] \;=\; P_v \; \|X_v\|^{-\alpha_v} \tag{3.1}$$

Where $E_h[S_v]$ is the average signal received (we need to take the mean as the distance is a random variable), $P_v$ is the power of the Cell and $\|X_v\|$ is the distance from the device to the Cell, affected for the path-loss $\alpha_v$. In the DUDe Association, however, the devices associates the less attenuated signal for its point of view, instead of based on the power from the Cells. This expressed mathematically is:

$$E_h[S_v{}^{UL-DUDe}] \;=\; P_d \; \|X_v\|^{-\alpha_v} \tag{3.2}$$

Where $P_d$ is the power of the device. To compare the results we use as a baseline the downlink receive power association (DRP). With this association, the signal received is:

$$E_h[S_v{}^{UL-DRP}] \;=\; P_v \; \|X_v\|^{-\alpha_v} \tag{3.3}$$

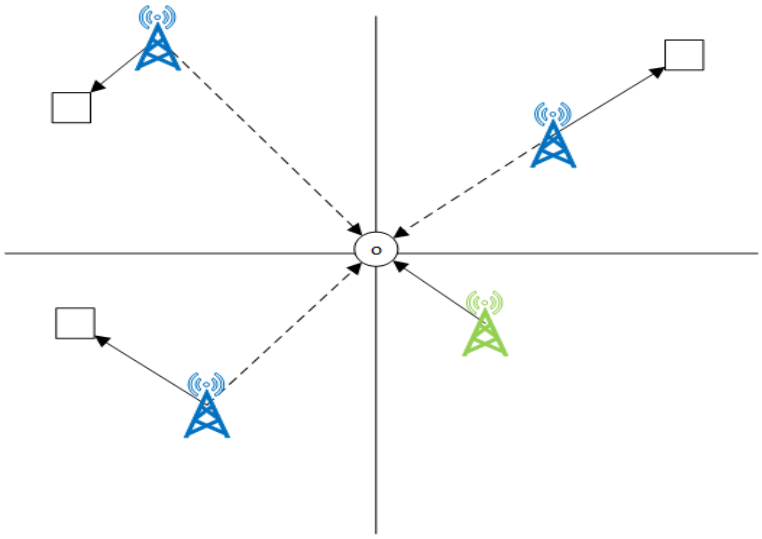

Figure 3.2: Centred device receiving signal from green Cell and interference from the signals emitted from blue Cells

.

Another assumptions made are:

- The network is viewed as a single snapshot in time for the purpose of characterizing its spatial statistics.
- The frequency of all the users transmitting are orthogonal among them, hence in the worst case is only possible to have $v - 1$ interferences, one per each Cell except the one the user is transmitting in.
- It will be considered a interference - limited system ($I_x >> \sigma^2$)

It will be considered a $\mathbb{R}^2$ space, with a device centred in the origin (3.2). the study will be focused on the uplink (UL) receiving power from the device, from both MCell and Scells. As it depends on the distance between the device and the Cells, it becomes extremely important to know which is the closest Cell to the device. In stochastic geometry, this is called *Void Probability*

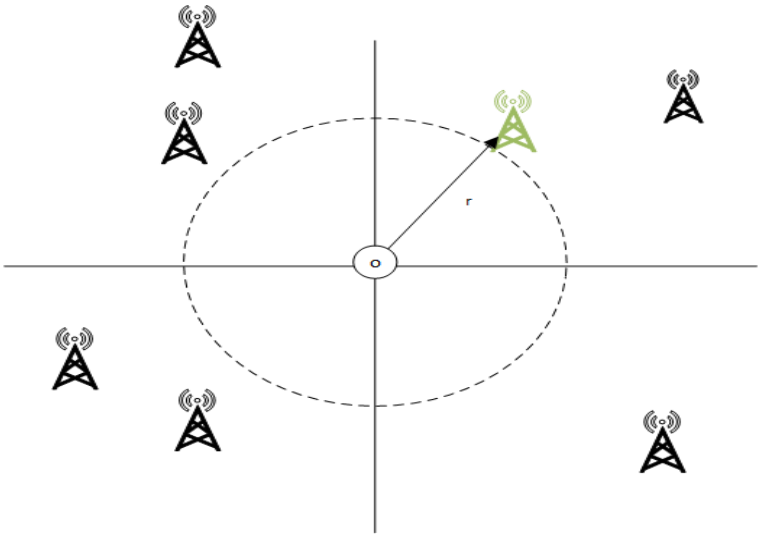


Figure 3.3: Void probability: Distance between the closest cell from the device and the device itself

.

## 3.3 Void Probability

The concept of void probability implies the consideration that the points are sorted. That means that considering a ppp $\Phi$ with $n$ points, we label all the points in order of increasing distance from the origin or the device $o$ with $|x_1| < |x_2| < ... < |x_n|$ . As the signal will be received from the closest Cell, we are interested in finding the probability of the distance from the closest Cell ($x_1$). In other words, the probability that there is no other Cell closer than $x_1$. To find out the probability, let us consider a $d$-dim ball ( $b_d$ ) centred in $o$ and with the radius r( $|x-c| < r$)(3.3):

*Definition* **3.5** *The volume of* $b_d$ *is* $c_d r^d$*, where* $c_d$ *is:*

$$c_d = \begin{cases} \frac{\pi^{\frac{d}{2}}}{(\frac{d}{2})!} & \text{if } d \text{ even} \\ \\ \frac{1}{(d)!}\pi^{\frac{d-1}{2}} 2^d (\frac{d-1}{2})! & \text{if } d \text{ odd} \end{cases} \tag{3.4}$$

In our case of interest, d = 2 and thus $c_d$ is:

$$c_2 = \frac{\pi^{\frac{2}{2}}}{(\frac{2}{2})!} = \pi. \tag{3.5}$$

The void probability is calculated by [18] :

$$P\ (\text{ There is no point inside } b_d\ ) = P(\Phi_{\lambda_v,d}(b_d(o,r)) = 0) = P(|x_1| > r) = e^{-\lambda_v c_d r^d} \tag{3.6}$$

As we are in a $\mathbb{R}^2$, with the result of (3.2), the void probability becomes:

$$P(|x_1| > r) = e^{-\lambda_v \pi r^2} \tag{3.7}$$

Where $\lambda_v$ can be either $m$ or $s$ depending on whether we are looking for the distance to the closest MCell or the distance to the closest SCell respectively. Considering the previous results, let us consider a random variable, $\|X_v\|$, that shows the distance from the device to the closest VCell. The cumulative distribution function (cdf) of this $\|X_v\|$ is:

$$F_{X_v}(x) = P(X_v \leq x) = 1 - (X_v > x) = 1 - P\ (\text{ There is no point inside } b_d\ ) = 1 - e^{-\lambda_v \pi x^2} \tag{3.8}$$

The probability density function (pdf) from the cdf is, by definition:

$$f_{X_v}(x) = \frac{\partial(F_{X_v}(x))}{\partial x} \tag{3.9}$$

With 3.8 and 3.9, the cdf and the pdf of the distance between the closest SCell and $o$ are, respectively:

$$F_{X_s}(x_s) = 1 - e^{-\lambda_s \pi x_s^2} \tag{3.10}$$

$$f_{X_s}(x_s) = 2\lambda_s \pi x e^{-\lambda_s \pi x_s^2} \tag{3.11}$$

Likewise, the cdf and the pdf of the distance between the closest MCell and $o$ are, respectively:

$$F_{X_m}(x_m) = 1 - e^{-\lambda_m \pi x_m^2} \tag{3.12}$$

$$f_{X_m}(x_m) = 2\lambda_s \pi x e^{-\lambda_m \pi x_m^2} \tag{3.13}$$

These results are very important, as the decision of decoupling the access or not is based on the position of the device and the relation of the closest SCell and MCell with it [21]. However, for the study in the Chapter 4, we have some SCells $(n-1)$ which are unavailable by the device. Due to being overload, the SCell is not available to the device, which will try to associate with another SCell, the problem becomes finding out the probability that there are $n-1$ points in a ball $b_d$, instead of none 3.4. The pdf of distance between the $n$-th closest SCell to the device is [22]:

$$f_{X_s}(x_s, n) = \frac{2(\lambda_s \pi)^n}{(n-1)!} x^{2n-1} e^{-\lambda_s \pi x^2} \tag{3.14}$$

It is noticeable that this PDF matches with a PDF of the generalized gamma function:

$$f_{X_s} = \frac{\frac{p}{a^d}}{\Gamma(\frac{d}{p})} x^{d-1} e^{-(\frac{x}{a})^p} \tag{3.15}$$

With $p = 2$, $d = 2n$ and $a = \frac{1}{\sqrt{\lambda\pi}}$. Thus, the CDF of distance between the $n$-th closest Scell to the device is:

$$F_{X_v}(x_s, n) = \frac{\gamma(\frac{d}{p}, (\frac{x_s}{a})^p)}{\Gamma(\frac{d}{p})} = \frac{\gamma(n, \lambda_s \pi x^2)}{(n-1)!} = \frac{\int_0^{\lambda\pi x^2} t^{n-1} e^{-t} \cdot dt}{(n-1)!} \tag{3.16}$$

Where $\gamma(a, x)$ is the lower incomplete gamma function and $\Gamma$(x) is the gamma function of $x$. For both 3.15 and 3.16, it is easily shown that, for $n$=1, the pdf and the cdf are the same as the void probability, 3.10 and 3.11. Only the functions related to the $n$-th Scell are considered as in our study only 1 MCell is assumed.

## 3.4 Interference modelling

In our system, it will be considered to have a PPP under a Rayleigh channel fading $(h_i)$. This channel is modelled as the marks of the PPP Therefore, following the

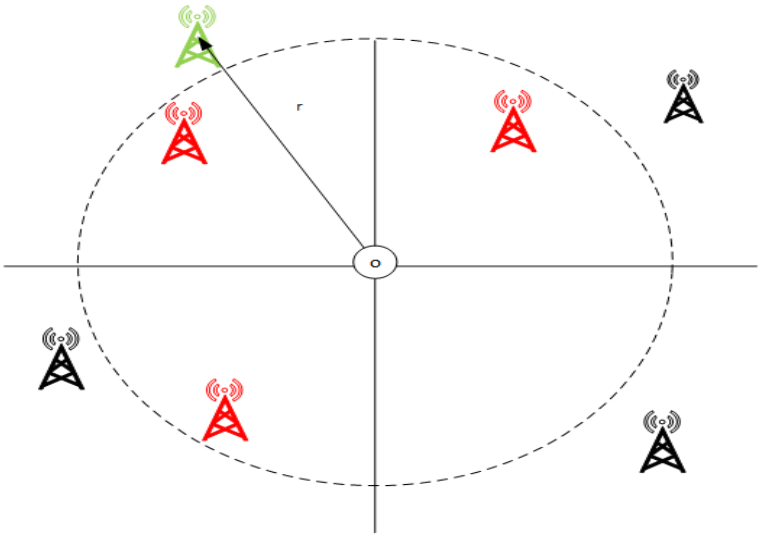


Figure 3.4: Distance between the $n$-th closest cell from the device and the device itself. In this example, $n = 4$

.

Notation Kendall-like notation we have a PPP M/G. The exponential response $X^{-\alpha}$, with $\alpha > 2$ is a common choice to model the attenuation due to path-loss in wireless communication. Our signal received, thus is:

$$S_v = P_d \cdot h_o \cdot \|X_v\|^{-\alpha_v} \tag{3.17}$$

In a similar way, the interferences received from all the others BS are:

$$\Phi_i = \sum_{i=1}^{n} P_d \cdot h_i \cdot \|X_i\|^{-\alpha_i} \tag{3.18}$$

For simplicity, from now onwards it will be considered that all the channels produce the same attenuation, so $\alpha_v = \alpha_i = \alpha$

Finally, we can express the Signal to Noise and Interference ratio (SINR) as:

$$\gamma = \frac{P_d \cdot h_o \cdot \|X_v\|^{-\alpha_v}}{\sum_{i=1}^{n} P_d \cdot h_i \cdot \|X_i\|^{-\alpha_i} + \sigma^2} \tag{3.19}$$

Where $\sigma^2$ is the noise of the system. The interference is calculated using the worst case. That means that the device receives a signal from every single BS.

According to [23], the uplink capacity for a device is:

$$C_{UL} = E[log_2(1 + SINR^{UL})] = \frac{1}{ln(2)} \int_0^{+\infty} P(ln(1 + SINR^{UL}) > dt = \\ \frac{1}{ln(2)} P(h_o > \frac{(e^t - 1)x_v^\alpha (I_x + \sigma^2)}{P_d}) = \\ \frac{1}{ln(2)} \int_0^{+\infty} \int_0^{+\infty} \underbrace{\frac{(e^t - 1)x_v^\alpha I_x}{P_d}}_{Interference} \underbrace{\frac{(e^t - 1)x_v^\alpha \sigma^2}{P_d}}_{Noise} f_x(x) dx dt \tag{3.20}$$

The interference then is:

$$I = \frac{(e^t - 1)x_v^\alpha I_x}{P_d} = \frac{(e^t - 1)x_v^\alpha \sum P_d h_i x_i}{P_d} = (e^t - 1)x_v^\alpha \sum h_i x_i \tag{3.21}$$

To compute the value of this interference, it will be used the Laplace transformation. The Laplace transformation of a PPP, in accordance with [27], is:

$$L(\Phi) = e^{2\pi\lambda_{ID} \int_0^{+\infty} (1 - \frac{1}{1 + f(x)x_j}) x_j dx j} \tag{3.22}$$

With the following variable change:

$$u = [(e^t - 1)x_v^\alpha]^{\frac{-2}{\alpha}} x_j \tag{3.23}$$

The interference results:

$$I = e^{-\pi\lambda_{ID}(e^t - 1)^{\frac{-2}{\alpha}} x_v^2 \int_0^{+\infty} \frac{1}{1 + v^{\frac{1}{2}}} dv} \tag{3.24}$$

It can be shown that is extendible to an $n$-th connection. As the devices are transmitting with the same power. If the device of interest transmits with $P_d$ / n, the interferences transmit with $P_d$ / n and the interference remains the same.

## 3.5 Notation

Through the following Chapters, several mathematical variables and functions are used, in the next table (3.5) there is a resume of these parameters and their values in case they have.

| Notation | Definition/Explanation | Value (if applicable) |
|---|---|---|
| P(A) | Probability of event A | |
| UL | Uplink connection | |
| DL | Downlink connection | |
| $f_x(x)$ | pdf RV x | |
| $F_x(x)$ | cdf RV x | |
| $F_{x_{\min}}(x_1, x_2)$ | cdf minimum RV'S x1 & x2 | |
| Lx (f(x)) | Laplace transform f(x) | |
| d | Dimension space | 2 |
| o | origin in $\mathbb{R}^d$ | |
| $\Phi_{\lambda_{v,d}}$ | p.p.p. in dimension d and intensity $\lambda$ | |
| $\lambda_v$ | Intensity p.p.p Cells | $\{m, s\}$ |
| $\lambda_d$ | Intensity p.p.p users | 200 |
| $\|X_s\|$ | RV distance from the device to the nth closest SCell | |
| $\|X_m\|$ | RV distance from the device to the MCell | |
| $\|X_1\|$ | RV distance from the device to the SCell 1 in DC | |
| $\|X_2\|$ | RV distance from the device to the SCell 2 in DC | |
| $P_s$ | Power Small Cell | 23 dBm |
| $P_m$ | Power Macro Cell | 46 dBm |
| $P_d$ | Power device | 20 dBm |
| $\alpha$ | Path loss exponent | >2, usually 3-4 |
| h | Channel fading | Rayleigh distribution |
| $\gamma^{UL}$ | SINR | |
| $B_x$ | Load balancing | |
| $\text{f(x)}_{\|\text{DUDe}}$ | pdf restricted to decoupling zone | |
| $\sigma^2$ | Noise power | $8^{-11}$ |
| $\tau$ | Threshold Outage probability | |
| OP | Outage probability | |
| CP | Coverage probability | |

Table 3.1: Notation

# Chapter 4

# The reliability of the decoupled access

## 4.1 Introduction

One of the main benefits of decoupling the access is to divide the uplink traffic among different SCells (instead of forcing the MCell to handle it all) to relieve the traffic congestion, and as well it constitutes a very good solution to address the uplink throughput and reliability improvements. However, due to various reasons SCells can become highly overloaded and users may be not able to access the SCell on their attempt. Reasons behind being overloaded and unavailable can stem from infrastructure limitation (as for example fronthaul based networks that limit the cell capacity) or impossibility of delivering the required QoS.

The reliability is usually used in networks to define how much is possible to ensure the communication from one point to another. Although if a node fails to transmit the data, we can find another path to achieve the transmission. The higher the probability to reach the final node, the more reliable the network is [20]. The aim of this Chapter is to evaluate the reliability of decoupling the access: How reliable is decoupling the access, and up to which extent is it better to decouple than to remain connected to the MCell, based on downlink received power information?

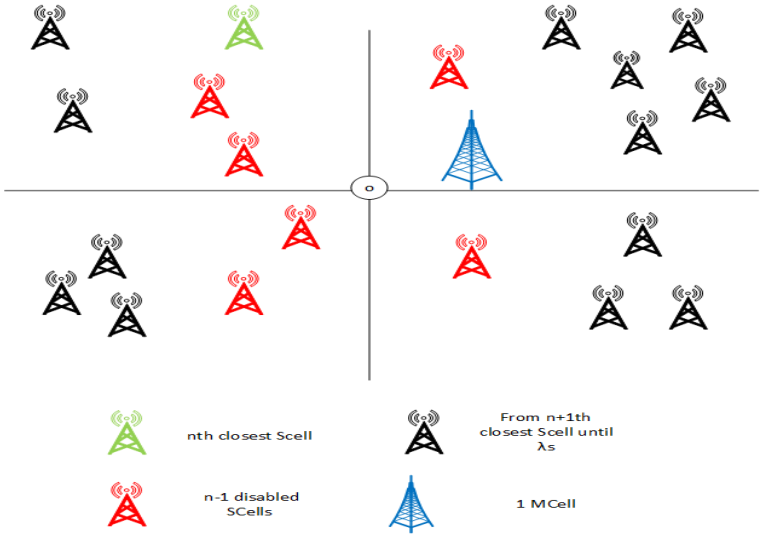


Figure 4.1: DUDe $n$-th Single Best Association Scenario

.

The rest of the chapter is organized as follows: in section 4.2, the association probability to the $n$-th closest SCell is calculated, by using the association probability regions defined for a single best association case, largely following study on [21], and deriving the generalized expression of the pdf of the $n$-th nearer neighbour [22]. The association probability is needed in order to compute the capacity. On one side, it affects the serving cell distance pdf and on the other side, the exact decoupling probability is needed. In section 4.3 the capacity of the decoupled access to the $n$-th closest SCell is determined, using the association probability calculated in 4.2. The same procedure is applied to the calculation of the outage probability in section 4.4. The performance evaluation and the conclusions obtained from it are shown in section 4.5.

## 4.2 Association probability

The scenario for this study, as shown in 4.1, is deployed by 1 MCell and several SCells ($\lambda_s$). From the closest SCell to the ($n$-*1*)-th are considered unavailable due to load conditions. In a DUDe environment, the DL transmission is still based on the power of the BS. It is performed by the MCell if the device is inside its radio coverage and by the $n$-th SCell otherwise (3.1). The radio coverage of the MCell

| Case | UL | DL |
|---|---|---|
| 1 | MCell | MCell |
| 2 | SCell | MCell |
| 3 | MCell | SCell |
| 4 | SCell | SCell |

Table 4.1: Probability regions *nth*-SBA

and SCells are given by their power $P_m$ and $P_s$ respectively. The uplink, however, is based on the signal received by the device (3.2). $X_m$ is a random variable that represents the distance between the device and the MCell. In a similar way, $X_s$ is a random variable that represents the distance between the device and the $n$-th closest SCell. This gives 4 possibilities for the connection to be performed. In 4.2 these possibilities are resumed. Afterwards, the probabilities will be calculated with details:

### Case 1 : Both UL/DL MCell

Following the previous reasoning, to be in that case 4.2 is needed that the device is situated inside the radio coverage of the MCell and closer from it than the nth SCell. In other words:

$$\left.\begin{array}{l} UL : P_d \left\|x_m\right\|^{-\alpha} > P_d \left\|x_s\right\|^{-\alpha} \\ DL : P_m \left\|x_m\right\|^{-\alpha} > \ P_s \left\|x_s\right\|^{-\alpha} \end{array}\right\} \left\|x_m\right\|^{-\alpha} > \left\|x_s\right\|^{-\alpha} \tag{4.1}$$

since $P_m$ / $P_s > 1$ so the Uplink condition is more restrictive. In order to compute the probability of being on Case 1, the CDF of nth nearest SCell and the pdf of MCell, together with the a probability theorem [2], are taken into account:

$$P_{Case1} \ = \ P(\left\|X_m\right\|^{-\alpha} > \left\|X_s\right\|^{-\alpha}) = P(\left\|X_m\right\| < \left\|X_s\right\|) = \int_0^{+\infty} (1 - F_{Xsn}(x_m)) \cdot f_{Xm}(x_m) \ dxm \tag{4.2}$$

This function is not integrable but, with an approximation of the incomplete Delta function [25], it is possible to calculate its value with Matlab.

### Case 2 : UL SCell nth Best and DL MCell

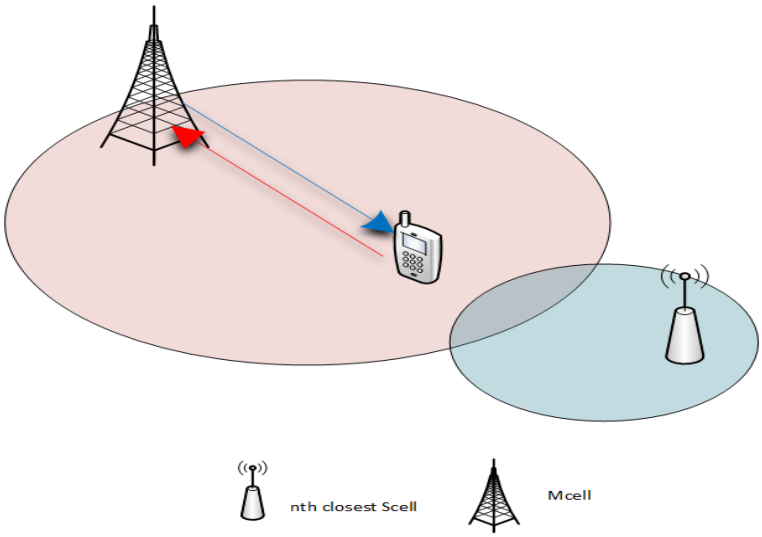


Figure 4.2: Case 1 nth SBA, UL/DL MCell

.

This is one of the cases in which the access is decoupled. For the device to be in that case, it has to be in the MCell radio coverage but closer from the nth SCell than the MCell. In terms of regions:

$$\begin{matrix} UL: P_d \|x_s\|^{-\alpha} > P_d \|x_m\|^{-\alpha} \\ DL: P_m \|x_m\|^{-\alpha} > P_s \|x_s\|^{-\alpha} \end{matrix} \} \|x_s\|^{-\alpha} > \|x_m\|^{-\alpha} \cap \|x_m\|^{-\alpha} > \frac{P_s}{P_m} \|x_s\|^{-\alpha} \}$$

$$\|x_s\|^{-\alpha} > \|x_m\|^{-\alpha} > \frac{P_s}{P_m} \|x_s\|^{-\alpha} \tag{4.3}$$

Similarly to the case 1, the probability of this intersection is calculated as:

$$P_{Case2} = P(\|x_s\|^{-\alpha} > \|x_m\|^{-\alpha} > \frac{P_s}{P_m} \|x_s\|^{-\alpha}) = P(\|x_s\| < \|x_m\| < \frac{P_m}{P_s}^{\frac{1}{\alpha}} \|x_s\|) =$$

$$\int_0^{+\infty} ((F_{Xm}(\frac{P_m}{P_s}^{\frac{2}{\alpha}} x_s)) - F_{Xm}(x_s)) \cdot f_{Xsn}(x_s)\, dxs =$$

$$\frac{(\lambda_s)^n}{(\lambda_s + \lambda_m)^n} - \frac{(\lambda_s)^n}{(\lambda_s + \frac{P_m}{P_s}^{\frac{2}{\alpha}} \lambda_m)^n} \tag{4.4}$$

It can be easily proved that for $n = 1$, the probability of decoupling is the same as for the single best association case [27]

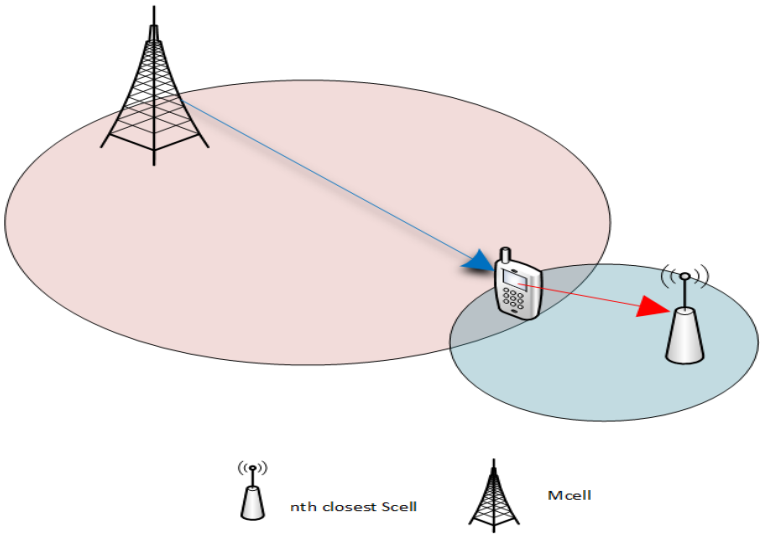


Figure 4.3: Case 2 nth SBA, UL SCell and DL MCell

### Case 3 : UL MCell and DL SCell nth Best

This is the other decoupled access case. The joint probability for associating the DL to the nth SCell and the UL to the MCell is satisfied by the following events:

$$\left.\begin{array}{l} UL : P_d \left\|x_m\right\|^{-\alpha} > P_d \left\|x_s\right\|^{-\alpha} \\ DL : P_s \left\|x_s\right\|^{-\alpha} > P_m \left\|x_m\right\|^{-\alpha} \end{array}\right\} \left\|x_m\right\|^{-\alpha} > \left\|x_s\right\|^{-\alpha} \cap \left\|x_s\right\|^{-\alpha} > \frac{P_m}{P_s} \left\|x_m\right\|^{-\alpha} \tag{4.5}$$

There is no possibility of accomplishing both events. If $\|x_m\|^{-\alpha}$ is bigger than $\|x_s\|^{-\alpha}$, $P_m/P_s$ (which is actually larger than 1) times $\|x_m\|^{-\alpha}$ can not be smaller than $\|x_s\|^{-\alpha}$ in any case. That would mean that although it is not in the MCell radio coverage, the device is still closer to the SCell than from the MCell. As the power of the MCell is always much higher than the power of the SCell, this situation is not suitable. This leads to a conclusion that the probability of the this case is zero.

$$P_{Case3} = 0. \tag{4.6}$$

### Case 4: Both UL/DL SCell

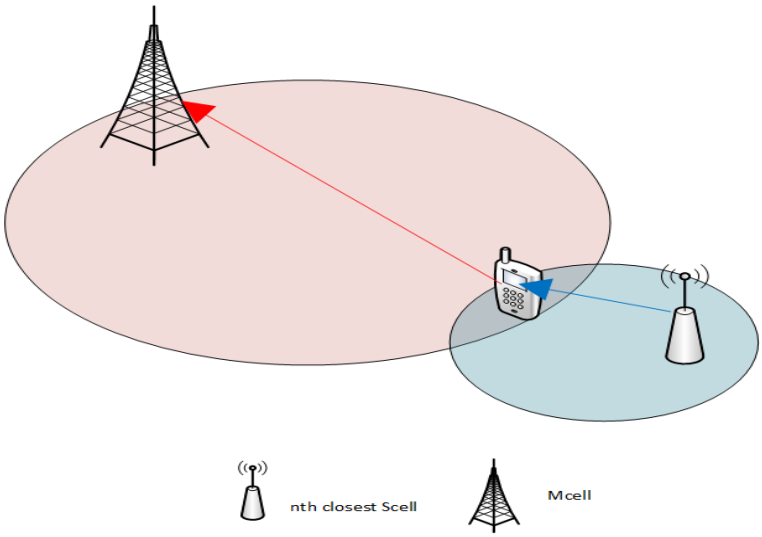


Figure 4.4: Case 3 nth SBA, UL MCell and DL SCell

This last case places the device closer to the SCell, close enough to be out of the MCell radio coverage. In terms of probability regions, this means that :

$$\left.\begin{array}{l} UL : P_d \left\|x_s\right\|^{-\alpha} > P_d \left\|x_m\right\|^{-\alpha} \\ DL : P_s \left\|x_s\right\|^{-\alpha} > P_m \left\|x_m\right\|^{-\alpha} \end{array}\right\} \left\|x_s\right\|^{-\alpha} > \frac{P_m}{P_s} \left\|x_m\right\|^{-\alpha} \tag{4.7}$$

Different from the Case 1, the most restrictive is the Downlink condition. If $\|x_s\|^{-\alpha}$ is bigger than $P_m/P_s \cdot \|x_m\|^{-\alpha}$ , it will be bigger than just $\|x_m\|^{-\alpha}$ , as $P_m/P_s > 1$. Similarly to previous cases, it can be calculated as:

$$\begin{aligned} P_{Case4} \;=\; & P(\|X_s\|^{-\alpha} > \frac{P_m}{P_s}\|X_m\|^{-\alpha}) = P(\|X_m\| > \frac{P_m}{P_s}^{\frac{1}{\alpha}} \|X_s\|) = \\ & \int_0^{+\infty} (1 - F_{Xm}(\frac{P_m}{P_s}^{\frac{1}{\alpha}} X_s)) \cdot f_{Xsn}(x_s)\; dxm = \\ & \frac{(\lambda_s)^n}{(\lambda_s + \frac{P_m}{P_s}^{\frac{2}{\alpha}} \lambda_m)^n} \end{aligned} \tag{4.8}$$

Once again, for *n=1*, is the same probability as the one to connect to an SCell in both UL and DL links in SBA scenario.

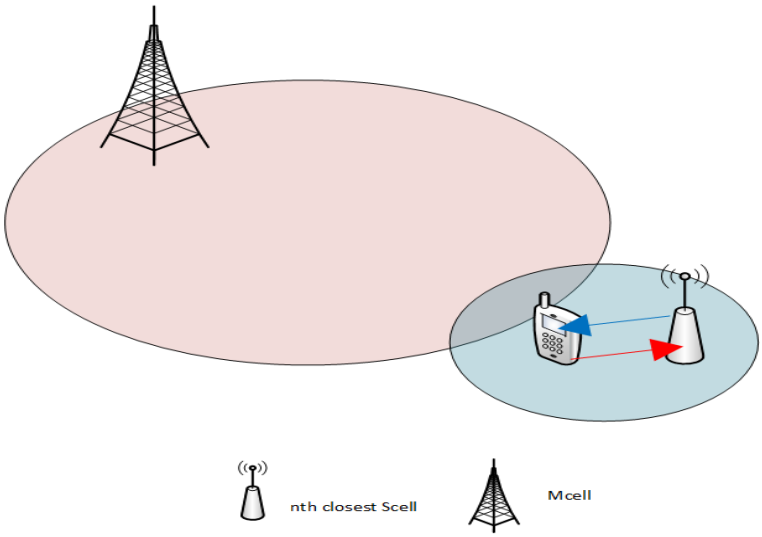


Figure 4.5: Case 4 nth SBA, UL/DL SCell

.

## 4.3 Capacity

The SINR is usually defined as the relation between the signal received by a certain device and all the interfering signals, coming either from the other system devices or the noise power. The typical SINR in the uplink received by a device responds to:

$$\gamma_v^{UL} = \frac{S_v^{UL}}{I_x + \sigma^2} \tag{4.9}$$

Where $S_v^{UL}$ is the signal received by the device (3.2), $I_x$ the signal received from the other devices (3.1) and $\sigma^2$ is the noise power. As it has been considered that it is an interference limited system, the SINR is simplified to:

$$\gamma_v^{UL} = \frac{P_d \cdot h_{xv} \cdot \|x_v\|^{-\alpha}}{\sum_{X_i \in \Phi_{Id}} P_i \cdot h_{xi} \cdot \|x_i\|^{-\alpha}} \tag{4.10}$$

We derive the distribution of the distance to the serving BS in UL for both DRP and DUDe association. From the decoupling probability [23], the region of being in Case 2 is obtained. The pdf of the distance to the serving BS, conditioned on

Case 2, is:

$$\widetilde{f_{X_v}(x)} = \frac{(e^{\pi\lambda_m x^2} - e^{\pi\lambda_m \frac{P_m}{P_s}^{\frac{2}{\alpha}} x^2}) \cdot fx_v(x)}{P_{case2}} \tag{4.11}$$

Where $v$ can be either $s$ or $m$ if it follows the DUDe association or the DRP association respectively. The spectral efficiency, defined by Shannon [23], is:

$$C_{UL} = E\left[log_2\left(1+\gamma_v^{UL}\right)\right] \tag{4.12}$$

The expected value is used because the SINR depends on the distance from the BS to the device, which is a random variable. The expected value of a random variable, can be computed as $E[T] = \int_0^{+\infty} P(T > t)dt$ for $T > 0$. Applying this property the spectral efficiency can be expressed as:

$$C_{UL} = \int_0^{+\infty}\int_0^{+\infty} P((log_2\left(1+\gamma_v^{UL}\right)) > t) \cdot \widetilde{f_{X_v}(x)} \cdot dt \cdot dx \tag{4.13}$$

in order to obtain the total throughput, the bandwidth assigned to computed. The criterion to assign the bandwidth [24] is fairer than simply divided it into all the Cells [23].

$$B_x = \frac{B}{1+\frac{1.28\cdot\lambda_D\cdot P_{av}}{\lambda_{av}}} \tag{4.14}$$

where $P_{av}$ is the probability of associating to the cell of interest(Case 2 and 4 for the decoupling load balancing and Case 1 in the sub-optimal association case) and $\lambda_{av}$ corresponds to the intensity of the cell of interest ($\lambda_s$ for the decoupled association and $\lambda_m$ sub-optimal one). If we multiply the spectral efficiency by the bandwidth assigned to the device, the final throughput or capacity in the uplink transmission is:

$$C_{UL}(n) = \frac{B}{1+\frac{1.28\cdot\lambda_D\cdot P_{av}}{\lambda_{av}}} \cdot \frac{log_2(e)}{P(Case2)} \int_0^{+\infty}\int_0^{+\infty} e^{-\pi\lambda_{ID}(e^t-1)^{\frac{2}{\alpha}}x^2} \int_0^{+\infty}\left(\frac{1}{1+v^{\frac{\alpha}{2}}}\right)dv$$
$$(e^{-\lambda_m x^2} - e^{-\lambda_m \frac{P_m}{P_s}^{\frac{2}{\alpha}} x^2}) \cdot (2(\pi\lambda_s)^n/(n-1)!) \cdot x^{2n-1} e^{-2\pi\lambda_s x^2} \cdot dt \cdot dx \tag{4.15}$$

In a similar way, for a DRP association, the capacity in the region of the Case 2 is calculated as:

$$C_{UL}\,(n) = \frac{B}{1+\frac{1.28\cdot\lambda_D\cdot P_{av}}{\lambda_{av}}} \cdot \frac{log_2(e)}{P(Case2)} \int_0^{+\infty} \int_0^{+\infty} e^{-\pi\lambda_{ID}(e^t-1)^{\frac{2}{\alpha}}x^2} \int_0^{+\infty} \left(\frac{1}{1+v^{\frac{\alpha}{2}}}\right) dv$$
$$(e^{-\lambda_m x^2} - e^{-\lambda_m \frac{P_m}{P_s}^{\frac{2}{\alpha}} x^2}) \cdot 2\pi\lambda_m\, x\, e^{-2\pi\lambda_m x^2} \cdot dt \cdot dx \tag{4.16}$$

## 4.4 Outage probability

The outage probability (OP) is the probability of, being established a target SINR $\tau$, drops the call if it is not capable of reaching $\tau$. This KPI is as important as the Capacity, as it ensures not only a high throughput but also a minimum quality of the call to be performed. It can be calculated trough the coverage probability (CP), as:

$$CP(\tau, n) = \int_0^{+\infty} (P(\gamma_v^{UL} > \tau)) \cdot \widetilde{f_{X_v}(x_v)}\, dx_v \tag{4.17}$$

The call can be either accepted or rejected, so:

$$OP(\tau, n) = 1 - CP(\tau, n) \tag{4.18}$$

In the case of decoupling the access, the outage probability in function of the target SINR and the number of SCells disabled is:

$$OP(\tau, n) = \int_0^{+\infty} e^{-\pi\lambda_{ID}(e^t-1)^{\frac{2}{\alpha}}\tau} \int_0^{+\infty} \left(\frac{1}{1+v^{\frac{\alpha}{2}}}\right) dv$$
$$(e^{-\lambda_m x^2} - e^{-\lambda_m \frac{P_m}{P_s}^{\frac{2}{\alpha}} x^2}) \cdot (2(\pi\lambda_s)^n/(n-1)!) \cdot x^{2n-1}\, e^{-2\pi\lambda_s x^2} \cdot dx \tag{4.19}$$

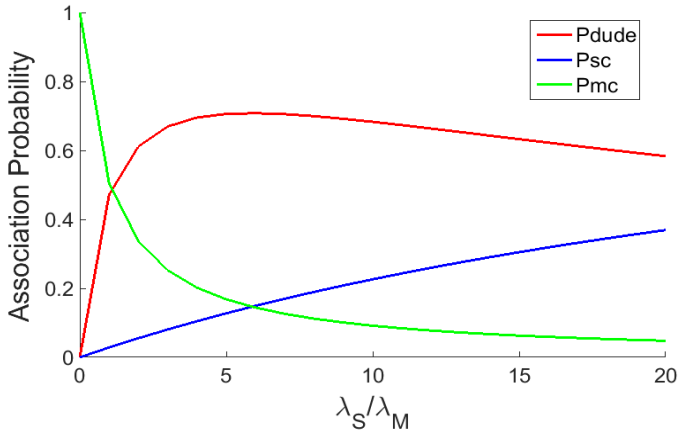


Figure 4.6: Association probability Best SBA. $P_m = 46$ dBm, $P_s = 23$ dBm, $\alpha = 3$, $\lambda_m = 1$.

.

In a similar way, we can calculate the outage probability in a DRP environment:

$$OP(\tau, n) = \int_0^{+\infty} e^{-\pi\lambda_{ID}(e^t-1)^{\frac{2}{\alpha}}\tau} \int_0^{+\infty} \left(\frac{1}{1+v^{\frac{\alpha}{2}}}\right) dv \cdot (e^{-\lambda_m x^2} - e^{-\lambda_m \frac{P_m}{P_s}^{\frac{2}{\alpha}} x^2}) \cdot 2\pi\lambda_m \, x \, e^{-2\pi\lambda_m x^2} \cdot dx \tag{4.20}$$

## 4.5 Performance evaluation

It can be easily shown that for $n$=1, the probability is the same that for an SBA situation (4.6). For $n > 1$, the trend of the three probabilities are similar each other. the main difference among them is that, as the $n$ increases, the decoupling probability and the UL/DL MCell probability increase in detriment of UL/DL SCell probability 4.7. The reason for this to happen is that as we are disabling SCell we decrease the probability on being in those zones (Case 4). However, the decoupling probability increase because although the SCell is involved, the device is in the MCell coverage zone. If we focus on the decoupling probability (4.8), we can see that it clearly depends on the $P_m/P_s$ relation. The decoupling is more beneficial when $P_m$ is much higher than $P_s$ the distance where the Uplink-Downlink imbalance can happen is bigger. On the contrary, as $P_s$ is getting closer to $P_m$ and the network tends to become more homogeneous, the decoupling is less suitable.

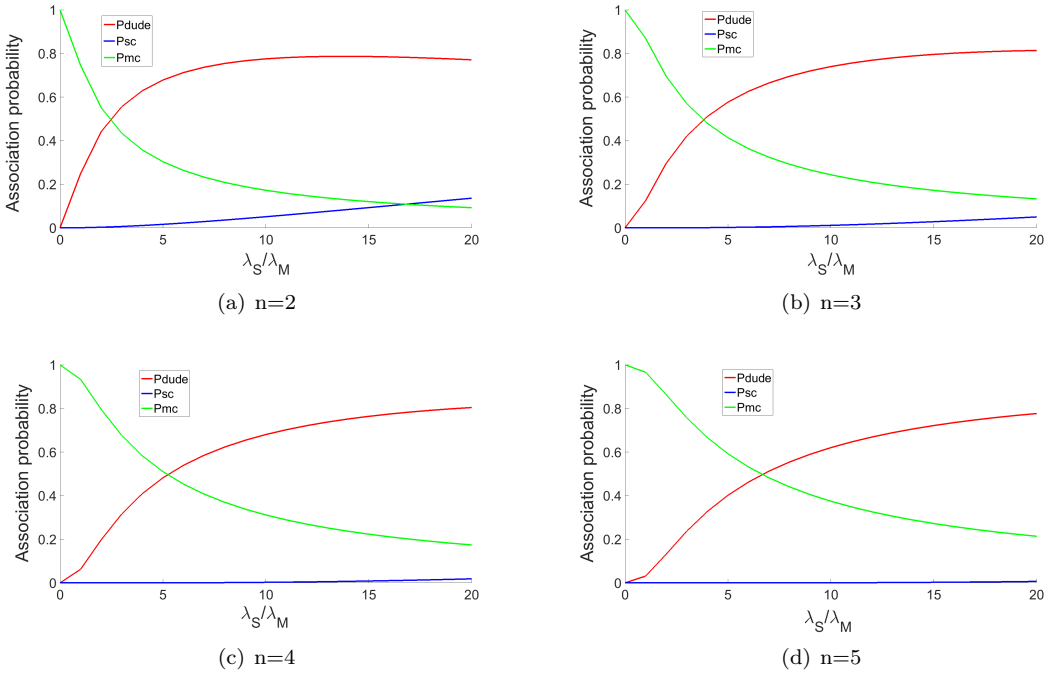


(a) n=2 (b) n=3

(c) n=4 (d) n=5

Figure 4.7: Association probability Nth SBA. $P_m = 46$ dBm, $P_s = 23$ dBm, $\alpha = 3$, $\lambda_m = 1$.

The connection will be more likely to be either to the MCell or the SCell in both UL/DL depending on the distance from the device to the Cell.
Regarding the capacity, the study is focused on the case where the access should be decoupled (4.3). To analyse the situation, there are taken two possibilities into account. On one side, it has been computed the uplink capacity of the decoupling access to the $n$-th SCell (i.e. performance the DL with the MC and the UL with the $n$-th closer SCell). On the other side, is computed the uplink capacity when is performed by the MCell. This comparison allows us to show if, even with a fronthaul limitation, the capacity of decoupling the access is still higher than the DRP environment in SBA. For $n = 1$ (4.5), The capacity decoupling the access is 10 times higher than in a DRP Association. However, as the fronthaul starts to disable SCells ($n$ increases) the decoupling capacity decreases and approaches the DRP capacity. For $n = 4$, the capacity of the decoupled access is similar to the DRP capacity. In (4.10), we can see that for $n = 4$ it is still worth to decoupling the access. for $n = 5$, however, the capacity for the DRP is higher than the DUDe. This means that 4 Cells can be unavailable and it is worth to decoupling

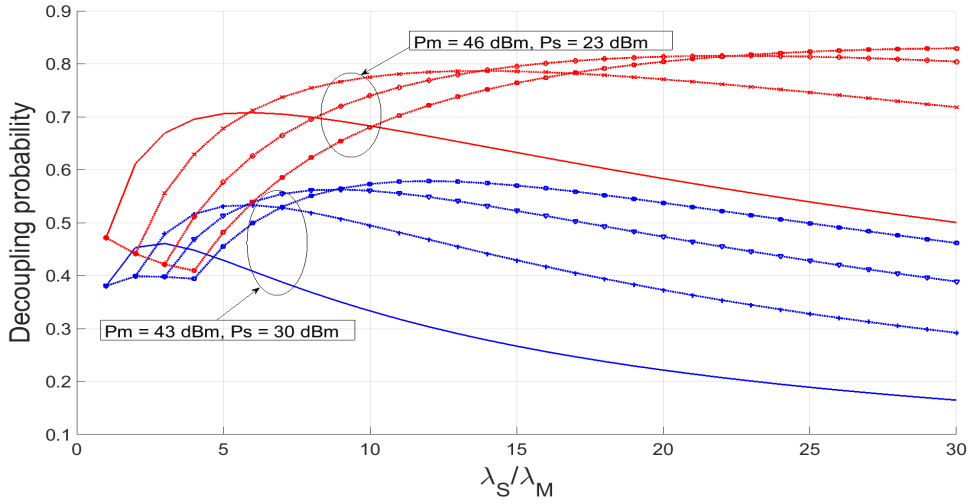


Figure 4.8: Decoupling probability for n=1,2,3,4 and Pm/Ps = 20,200. $P_m = 46$ dBm and $P_s = 23$ dBm for Pm/Ps = 200 and $P_m = 43$ dBm and $P_s = 30$ dBm for Pm/Ps =20, $\alpha = 3$, $\lambda_m = 1$.

.

the access.

The outage probability for $n = 4$ (4.11) is still better than in a DRP. We could go even further and see that until the 6th or the 7th SCell where in about 60 % of the threshold zone is worst on the decoupling and we can not consider it reliable. Therefore, if there is more interest in achieve a good OP, we can allow to connect the 6th or the 7th SCell. However, if we don't want to loose capacity, we only can reach the 4th Scell. These outage probability is achievable for the lower thresholds.

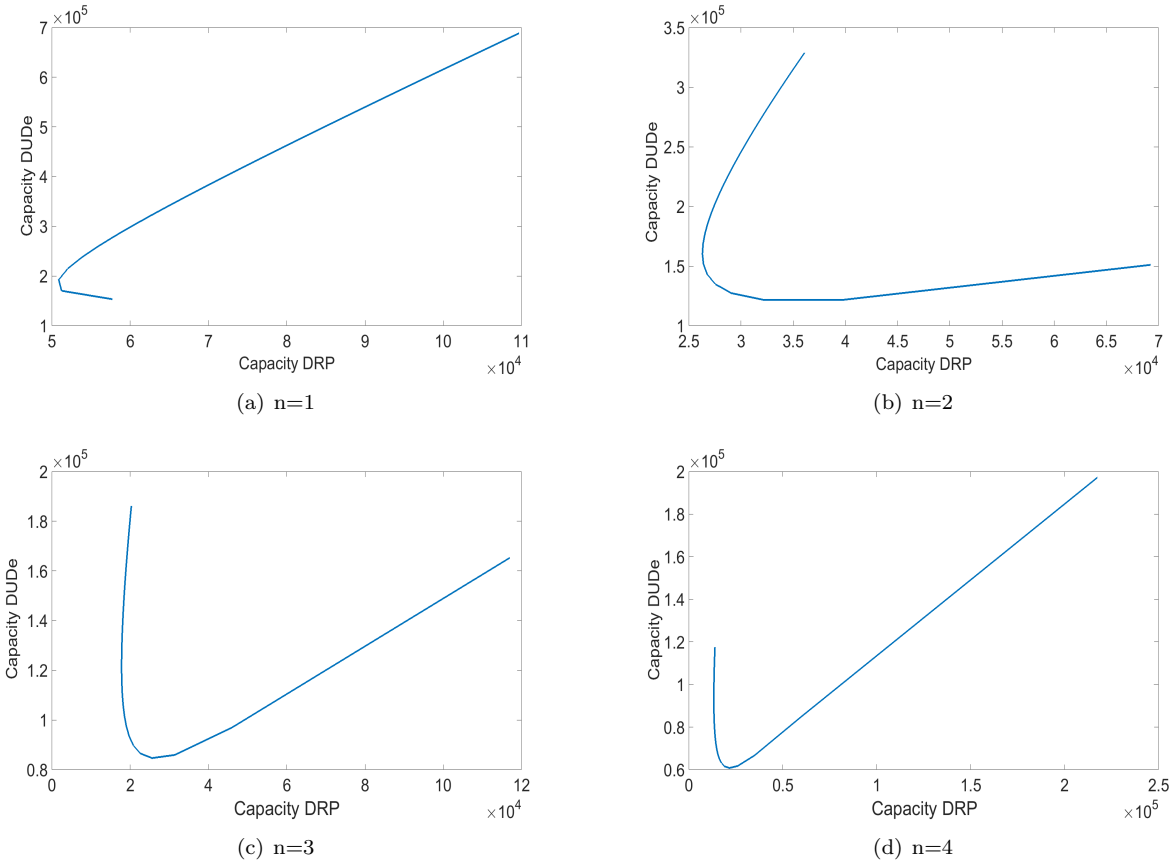


(a) n=1 (b) n=2

(c) n=3 (d) n=4

Figure 4.9: $P_m = 46$ dBm, $P_s = 23$ dBm, $\alpha = 4$, $\lambda_m = 1$.

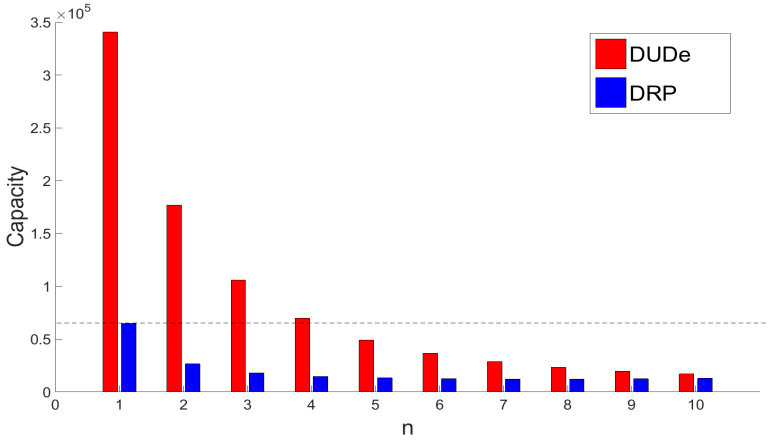


Figure 4.10: Capacity SBA Dude and DRP. $P_m = 46$ dBm, $P_s = 23$ dBm, $\alpha = 4$, $\lambda_m = 1$, $\lambda_s = 20$.

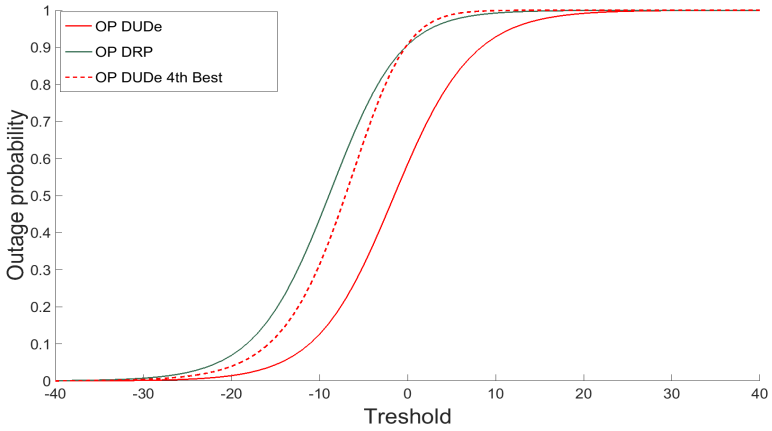


Figure 4.11: Outage probability nth SBA DUDe and DRP. $P_m = 46$ dBm, $P_s = 23$ dBm, $\alpha = 4$, $\lambda_m = 1$, $\lambda_s = 20$, n=4.

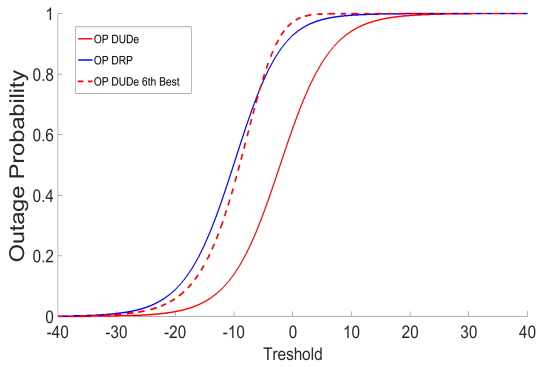


(a) n=6

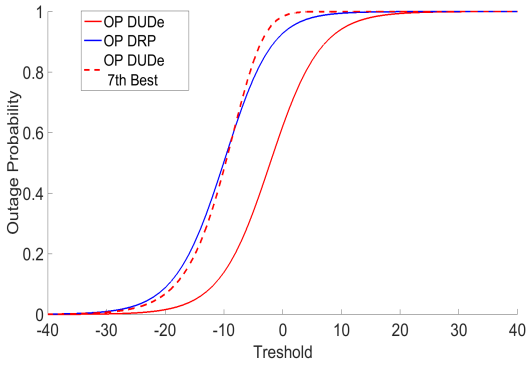


(b) n=7

Figure 4.12: Reliability Outage Probability. $P_m = 46$ dBm, $P_s = 23$ dBm, $\alpha = 4$, $\lambda_m = 1$.

# Chapter 5

# Decoupling access on Dual Connectivity scenario

## 5.1 Introduction

The Dual Connectivity (DC) allows to increase the Capacity of a transmission, as two channels are used to transmit information. The mechanism, however, is similar to the Single Connectivity: The device performs the first connection exactly as in a SBA performance. The main difference comes into when while it does this first connection, it also connects to the 2-nd nearest one.

In this situation 5.1, the system model is deployed by 1 MCell and several SCells ($\lambda_s$). It will be taken into account a Single Best Association, which means that the device will connect either the MCell or the two closest SCells (depending on its position) but never needs to connect any other further Cell. This gives a lot of possibilities for the connection to be performed.

The aim of the Chapter is to study the benefits of decouple the access once Dual connectivity is used and is organized as follows: in 5.2, the association probability is computed. In this scenario, the region in which the decoupling is performed is totally different than a single best association or nth-SBA Association. Therefore, the pdf of the distance serving is also different. In 5.3, both DUDe probability

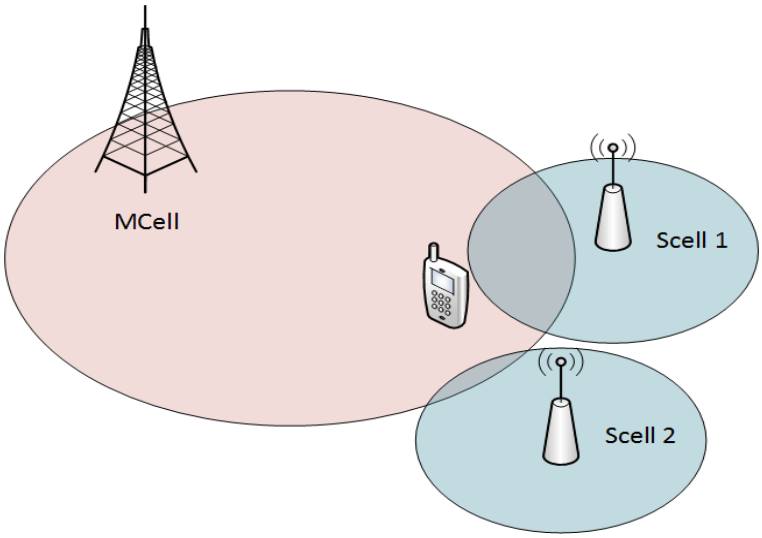


Figure 5.1: Dual Connectivity scenario

.

and pdf of distance serving are used to compute the probability. Finally, the performance evaluation and its conclusions are shown in 5.4.

## 5.2 Probability regions

In the scenario deployed in (5.1), it is possible to performance the connections among three Cells (1 MCell and 2 Scells). This 3 Cells are randomly distributed following a PPP. As described in the system model (Chapter 3), the distance from a device situated in the origin are:

$$MCell : f_{Xm} = 2\pi\lambda_m x_m e^{-\pi\lambda_m x_m^2} \tag{5.1}$$

$$SCell\ 1 : f_{X1} = 2\pi\lambda_s x_{S1} e^{-\pi\lambda_s x_{S1}^2} \tag{5.2}$$

$$SCell\ 2 : f_{X2} = 2\pi\lambda_s x_{S2} e^{-\pi\lambda_s x_{S2}^2} \tag{5.3}$$

The aim of this study is to calculate the probability of performing these connections. There are some connections, however, that are not suitable. Similarly to the Case 3 of the previous Chapter, any combination of connecting to a SCell in the DL and to a MCell in the UL. Furthermore, the only possibility for the UL to be decoupled is to perform the first connection with a SCell and decouple the access

| Case | Subcase | UL1 | DL1 | UL2 | DL2 | Duality DC-SBA |
|---|---|---|---|---|---|---|
| 1 | 1.1 | MCell | MCell | SCell 1 | SCell 1 | Pmc |
| | 1.2 | MCell | MCell | SCell 2 | SCell 2 | |
| 2 | 2.1 | SCell 1 | SCell 1 | MCell | MCell | |
| | 2.2 | SCell 2 | SCell 2 | MCell | MCell | |
| 3 | 3.1 | SCell 1 | SCell 1 | SCell 2 | MCell | PDude |
| | 3.2 | SCell 2 | SCell 2 | SCell 1 | MCell | |
| 4 | 4.1 | SCell 1 | SCell 1 | SCell 2 | SCell 2 | Psc |
| | 4.2 | SCell 2 | SCell 2 | SCell 1 | SCell 1 | |

Table 5.1: Probability regions in a Best Association Dual connectivity scenario

in the second one. The device can not decouple the access twice because only 1 connection with MCell is allowed. These constrains, leads to eight possibilities for the three Cells be associated. As the two SCells pdfs are similar, it can be reduced to four cases using symmetry. These four cases will be divided in 8 subcases for the 8 possibilities. The table 5.2 resumes which Cell performs every connection in different cases. Besides, the probabilities are compared with the nth SBA Case: Pmc if there is one connection performed by the MCell and other one performed by one of the SCells (both UL/DL with the same Cells), Psc if all the connections are performed by the SCells and PDude with any decoupling situation.

### Case 1 : 1st connection with MCell, 2nd connection with SCell (both UL/DL)

In this case 5.2, the first connection is performed by the MCell and the second one with either one SCell or another (both UL/DL). This leads to these conditions for the Case 2.1 and 2.2 respectively:

$$\left.\begin{array}{l} UL : P_d \left\|x_m\right\|^{-\alpha} > P_d \left\|x_1\right\|^{-\alpha} > P_d \left\|x_2\right\|^{-\alpha} \\ DL : P_m \left\|x_m\right\|^{-\alpha} > \ P_s \left\|x_1\right\|^{-\alpha} > \ P_s \left\|x_2\right\|^{-\alpha} \end{array}\right\} \left\|x_m\right\|^{-\alpha} > \left\|x_1\right\|^{-\alpha} > \left\|x_2\right\|^{-\alpha} \tag{5.4}$$

$$\left.\begin{array}{l} UL : P_d \left\|x_m\right\|^{-\alpha} > P_d \left\|x_2\right\|^{-\alpha} > P_d \left\|x_1\right\|^{-\alpha} \\ DL : P_m \left\|x_m\right\|^{-\alpha} > \ P_s \left\|x_2\right\|^{-\alpha} > \ P_s \left\|x_1\right\|^{-\alpha} \end{array}\right\} \left\|x_m\right\|^{-\alpha} > \left\|x_2\right\|^{-\alpha} > \left\|x_1\right\|^{-\alpha} \tag{5.5}$$

In both situations the Uplink condition is more restrictive, in a similar way than 4.1 . This can be reduced to:

$$\|x_m\|^{-\alpha} > (\|x_1\|^{-\alpha}, \|x_2\|^{-\alpha}) = \|x_m\| < (\|x_1\|, \|x_2\|) \tag{5.6}$$

Which means that $\|x_m\|$ needs to be smaller than both $\|x_1\|$ and $\|x_2\|$. In other words, it needs to be smaller than $min(x_1, x_2)$. The probability of being in that case can be calculated as:

$$P_{Case1} \;=\; P(\|X_m\| < min(x_1, x_2)) = \int_0^{+\infty} (1 - F_{min(X1,X2)}(x_m)) \cdot f_{Xm}(x_m)\; dxm \tag{5.7}$$

The cdf of $min(x_1, x_2)$ can be calculated using order statistics. This cdf, can be written as:

$$F_{min(X1,X2)} = 1 - ((1 - F_{x1}) * (1 - F_{x2})) \tag{5.8}$$

As $F_{x1}\ (xm) = F_{x2}\ (xm)$, the expression 5.8 can be written as:

$$F_{min(X1,X2)} = 1 - (1 - F_{x1})^2 = 1 - e^{-2\pi\lambda_s x_m^2} \tag{5.9}$$

Finally, with 5.1 , 5.7 and 5.9, the probability of be in Case 1 is:

$$P_{Case1} \;= \int_0^{+\infty} e^{-2\pi\lambda_s x_m^2} \cdot 2\pi\lambda_m x_m e^{-\pi\lambda_m x_m^2}\; dxm = \frac{\lambda_m}{2\lambda_s + \lambda_m} \tag{5.10}$$

**Case 2: 1st connection with SCell (both UL/DL), 2nd connection connection with MCell**

In Case 2 5.3, the connections performed by the device are the same than in Case 1. They only differ in the order of the connections. The first connection is with the SCell and the second one is with the MCell (UL/DL). To be in this case, the device has to accomplish:

$$\left.\begin{array}{l} UL : P_d \|x_1\|^{-\alpha} > P_d \|x_m\|^{-\alpha} > P_d \|x_2\|^{-\alpha} \\ DL : P_s \|x_1\|^{-\alpha} > \; P_m \|x_m\|^{-\alpha} > \; P_s \|x_2\|^{-\alpha} \end{array}\right\} \|x_1\|^{-\alpha} > \|x_m\|^{-\alpha} > \|x_2\|^{-\alpha} \tag{5.11}$$

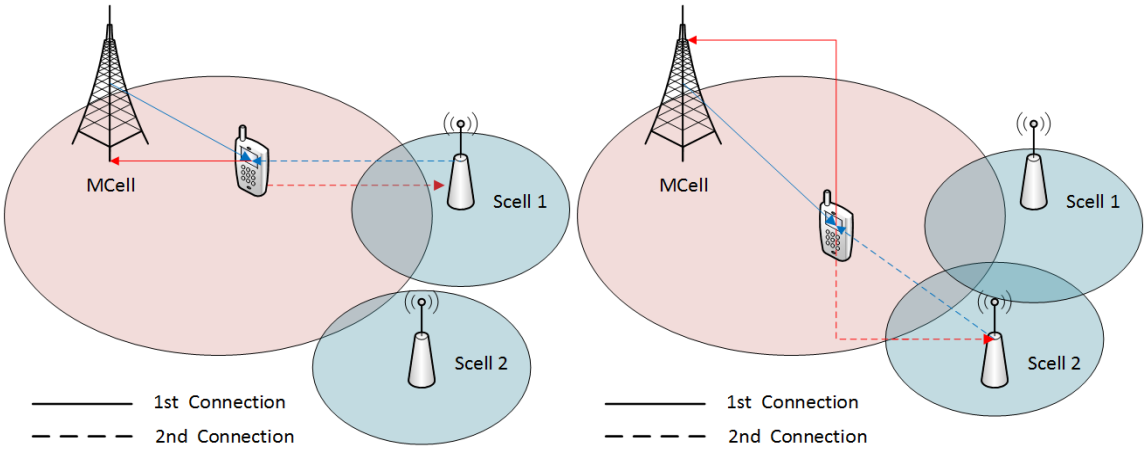


(a) Association Sub-case 1.1 (b) Association Sub-case 1.2

Figure 5.2: Association Case 1

$$\left.\begin{array}{l} UL: P_d \left\|x_2\right\|^{-\alpha} > P_d \left\|x_m\right\|^{-\alpha} > P_d \left\|x_1\right\|^{-\alpha} \\ DL: P_s \left\|x_2\right\|^{-\alpha} > \ P_m \left\|x_m\right\|^{-\alpha} > \ P_s \left\|x_1\right\|^{-\alpha} \end{array}\right\} \left\|x_2\right\|^{-\alpha} > \left\|x_m\right\|^{-\alpha} > \left\|x_1\right\|^{-\alpha} \tag{5.12}$$

Similarly to Case 1, the uplink condition is most restrictive. The difference between Case 2.1 (5.11) and Case 2.2 5.12) is the SCell to with the device performs the first connection. As the two pdf are similar, the probability of these sub cases will be the same. Thus, we can calculate the probability (5.12) and the probability of Case 2 will be twice the probability calculated. The probability of the device to be in (5.12) is:

$$\begin{array}{l} P(\left\|x_1\right\|^{-\alpha} > \left\|x_m\right\|^{-\alpha} > \left\|x_2\right\|^{-\alpha}) = P(\left\|x_1\right\| < \left\|x_m\right\| < \left\|x_2\right\|) = \\ \int_0^{+\infty} \int_{x_1}^{+\infty} \int_{x_m}^{+\infty} f_{X_m}(x_m) \cdot f_{X1}(x_1) \cdot f_{X2}(x_2) \cdot dx_2 \cdot dx_m \cdot dx_1 \end{array} \tag{5.13}$$

After few operations, it is found that, the probability for the device to be in Case 2.1 is:

$$P(\text{Case 2.1}) = \frac{\lambda_m \lambda_s}{(\lambda_m + \lambda_s)(\lambda_m + 2\lambda_s)} \tag{5.14}$$

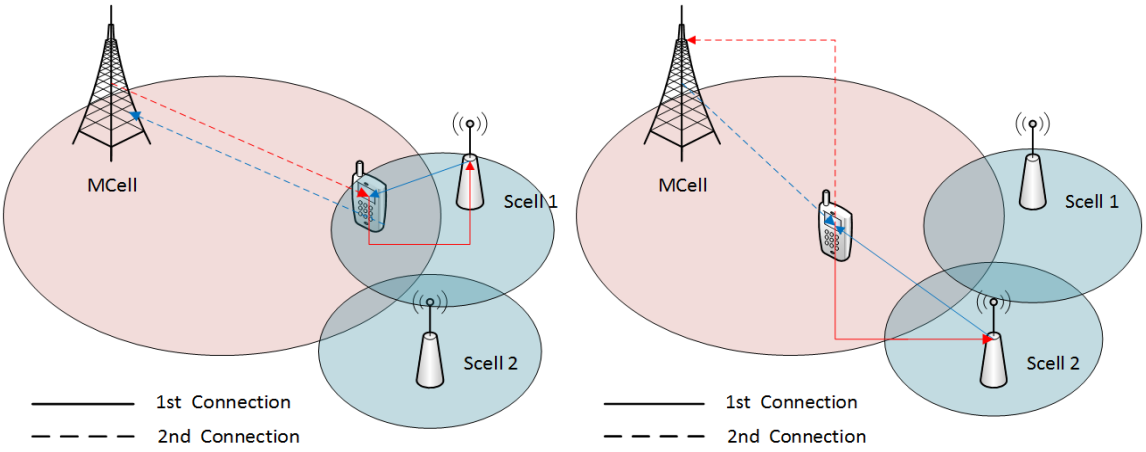


(a) Association Sub-case 2.1

(b) Association Sub-case 2.2

Figure 5.3: Association Case 2

As it was mentioned, the probability of the device for be in Case 2 is twice the probability for be in Case 2.1. Thus:

$$P(\text{Case 2}) = \frac{2\lambda_m\lambda_s}{(\lambda_m + \lambda_s)(\lambda_m + 2\lambda_s)} \tag{5.15}$$

These two cases performs 1 connection (both UL/DL) with the MCell so analogously to the study in Chapter 4, the sum of the four probabilities can be considered $Pmc$.

### Case 3 : 1st connection with SCell (both UL/DL), 2nd connection DL with MCell and UL with the other SCell

In this Case (5.4), the device is situated next to one of the SCells and inside the radio coverage of the MCell but closer from the other SCell than from the MCell. Therefore, performs the first connection with the closest SCell and the second one decoupling the access: the uplink with the other SCell and the downlink with the MCell. To proceed with the calculations, it will be considered that the closest SCell is SCell 1. However, by symmetry the probability coincides if the closest one is SCell 2 as long as the situation of all the other Cells is te same

mentioned before. This situation , mathematically is:

$$\left.\begin{array}{l} UL: P_d \|x_1\|^{-\alpha} > P_d \|x_2\|^{-\alpha} > P_d \|x_m\|^{-\alpha} \\ DL: P_s \|x_1\|^{-\alpha} > P_m \|x_m\|^{-\alpha} > P_s \|x_2\|^{-\alpha} \end{array}\right\} \|x_1\|^{-\alpha} > \frac{P_m}{P_s}\|x_m\|^{-\alpha} > \|x_2\|^{-\alpha} > \|x_m\|^{-\alpha} \tag{5.16}$$

This probability, $P(\|x_1\|^{-\alpha} > \frac{P_m}{P_s}\|x_m\|^{-\alpha} > \|x_2\|^{-\alpha} > \|x_m\|^{-\alpha})$ or which is the same: $P(\|x_1\| < \frac{P_s}{P_m}\|x_m\| < \|x_2\| < \|x_m\|)$ can be seen as the intersection of events: $\|x_1\|$ is the minimum value among the three Cells and also $\|x_2\|$ needs to be between $\frac{P_s}{P_m}\|x_m\|$ and $\|x_m\|$):

$$P(\|x_1\| < min(\|x_2\|, \|x_m\|)) \cap P(\frac{P_s}{P_m}\|x_m\| < \|x_2\| < \|x_m\|) \tag{5.17}$$

Since these two events are independent, the intersection of this is the multiplication of their probabilities for these events to happen:

$$P(\|x_1\| < min(\|x_2\|, \|x_m\|)) \cdot P(\frac{P_s}{P_m}\|x_m\| < \|x_2\| < \|x_m\|) \tag{5.18}$$

The first probability can be calculated similarly to 5.8:

$$P(1) = P(\|X_m\| < min(\|x_2\|, \|x_m\|)) = \int_0^{+\infty} (1 - F_{min(X2,Xm)}(x_1)) \cdot f_{X1}(x_1)\, dx_1 \tag{5.19}$$

The second probability, $P(\frac{P_s}{P_m}\|x_m\| < \|x_2\| < \|x_m\|)$ can be calculated as:

$$\begin{array}{l} P(\frac{P_s}{P_m}\|X_m\| < \|X_2\| < \|X_m\|) = \int_0^{+\infty} \int_0^{x_m} f_{xm}(x_m) \cdot f_{x2}(x_2) \cdot dx_2 dx_m = \\ \int_0^{+\infty} 2\pi\lambda_m x_m e^{-\lambda_m \pi x_m^2}\, dx_m \cdot \int_{\frac{P_s}{P_m}X_m}^{X_m} 2\pi\lambda_m x_m e^{-\lambda_m \pi x_m^2}\, dx_2 = \\ \int_0^{+\infty} 2\pi\lambda_m x_m e^{-\lambda_m \pi x_m^2} \cdot (e^{\lambda_s \frac{P_s}{P_m}\pi x^2} - e^{\lambda_s \pi x^2})\, dx_m = \frac{\lambda_m}{\lambda_m + \lambda_s \frac{P_s}{P_m}} - \frac{\lambda_m}{\lambda_m + \lambda_s} \end{array} \tag{5.20}$$

Thus, with 5.16, 5.2, 5.19 and 5.20, The probability for the device to be in Case 3 is: we can compute the probability for the device to be in Case 3:

$$P(\text{Case 3}) = 2P(1)(\frac{\lambda_m}{\lambda_m + \lambda_s \frac{P_s}{P_m}} - \frac{\lambda_m}{\lambda_m + \lambda_s}) \tag{5.21}$$

**Case 4 : 1st connection with SCell (both UL/DL), 2nd connection with**

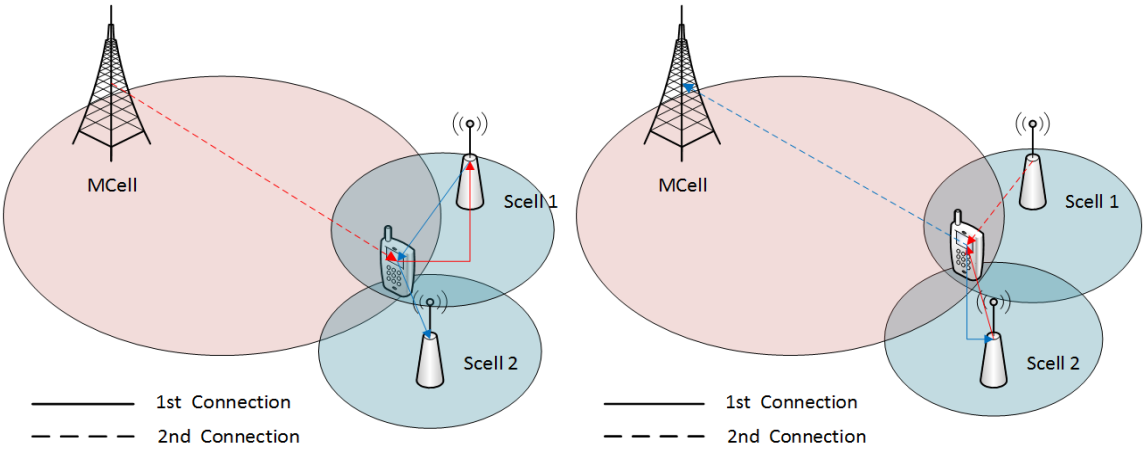


(a) Association Sub-case 3.1 (b) Association Sub-case 3.2

Figure 5.4: Association Case 3

**the other SCell (both UL/DL)**

In this last case 5.5, both connections are performed by the SCells. These means:

$$\left.\begin{array}{l} UL: P_d \|x_1\|^{-\alpha} > P_d \|x_2\|^{-\alpha} > P_d \|x_m\|^{-\alpha} \\ DL: P_s \|x_1\|^{-\alpha} > P_s \|x_2\|^{-\alpha} > P_m \|x_m\|^{-\alpha} \end{array}\right\} \|x_1\|^{-\alpha} > \|x_2\|^{-\alpha} > \frac{P_m}{P_s}\|x_m\|^{-\alpha} \tag{5.22}$$

$$\left.\begin{array}{l} UL: P_d \|x_2\|^{-\alpha} > P_d \|x_m\|^{-\alpha} > P_d \|x_1\|^{-\alpha} \\ DL: P_s \|x_2\|^{-\alpha} > P_m \|x_m\|^{-\alpha} > P_s \|x_1\|^{-\alpha} \end{array}\right\} \|x_2\|^{-\alpha} > \|x_1\|^{-\alpha} > \frac{P_m}{P_s}\|x_m\|^{-\alpha} \tag{5.23}$$

In that case, the downlink condition is the restrictive one. Similarly to Case 2, the two probabilities are the same due to the similarity of the pdf of the SCells.

$$\begin{aligned} &P(\|x_1\|^{-\alpha} > \|x_2\|^{-\alpha} > \frac{P_s}{P_m}\|x_m\|^{-\alpha}) = P(\|x_1\| < \|x_2\| < \frac{P_s}{P_m}\|x_m\|) = \\ &P(\|x_1\| < \|x_2\| < \|x_m\|) \cap P(\|x_2\| < \frac{P_s}{P_m}\|x_m\|) = \\ &P(\|x_1\| < \|x_2\| < \|x_m\|) \cdot P(\|x_2\| < \frac{P_s}{P_m}\|x_m\|). \text{ (Due to independence of events)} \end{aligned} \tag{5.24}$$

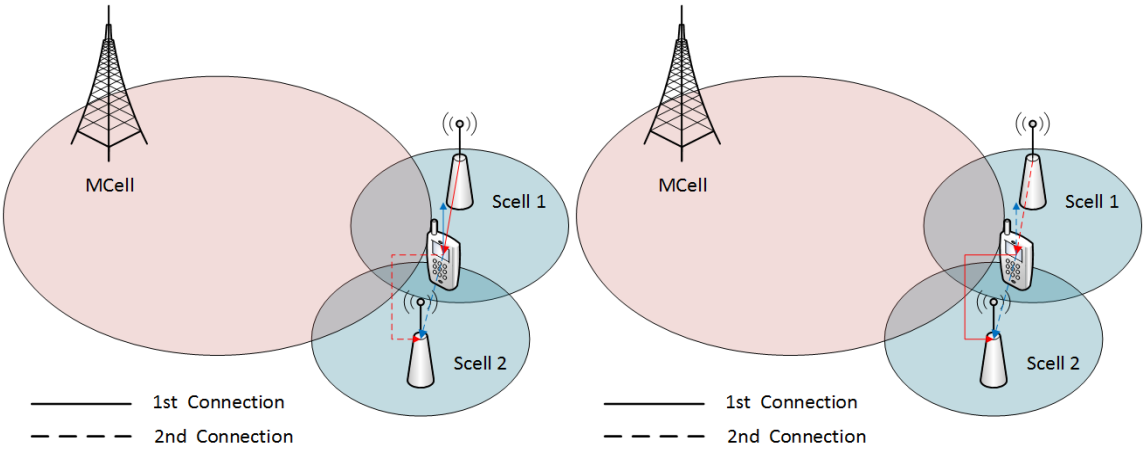


(a) Association Sub-case 4.1

(b) Association Sub-case 3.2

Figure 5.5: Association Case 4

The first probability is calculated, as 5.7 and 5.19:

$$P(\|x_1\| < \|x_2\| < \|x_m\|) = P(\|x_1\| < min(x_2, x_m)) \tag{5.25}$$

The second probability is:

$$\begin{aligned} P(\|x_2\| < \frac{P_s}{P_m}\|x_m\|) = \int_0^{+\infty} \int_{\frac{P_m}{P_s}}^{+\infty} f_{xm}(x_m) \cdot f_{x2}(x_2) \cdot dx_2 dx_m = \\ \int_0^{+\infty} \int_{\frac{P_m}{P_s}}^{+\infty} 2\pi\lambda_m x_m e^{-\pi\lambda_m x_m^2} \cdot 2\pi\lambda_s x_2 e^{-\pi\lambda_s x_2^2} \cdot dx_m dx_2 = \\ \int_0^{+\infty} 2\pi\lambda_s x_2 e^{-(\pi\lambda_s + \pi\lambda_s(\frac{P_m}{P_s})^2)x^2} \cdot dx_2 = \frac{\lambda_s}{\lambda_s + \frac{P_m}{P_S}\lambda_m} \end{aligned} \tag{5.26}$$

Thus, the probability for the device to be in Case 4 is:

$$P(\text{Case 4}) = 2 * P(2) * \frac{\lambda_s}{\lambda_s + \frac{P_m}{P_S}\lambda_m} \tag{5.27}$$

## 5.3 Capacity

In a DC scenario, there are two connections for any possibility computed in 5.2. This studio is focused in the capacity decoupling the access (Case 3). It will be calculated the capacity of the case 3.1. The capacity in Case 3.2 would be the same as the probabilities and the regions are the same for the two decoupling possibilities.

The capacities are calculated separately, one for each connection. Each capacity is calculated in a similar way to 4.15. The only thing that differs from this formula is the conditioned density function, as the region is different from the the SBA case. The region of this case satisfies that:

$$Fx_{|DUDe} = P(X_1 > x|\frac{P_s}{P_m}x_2^{-\alpha} < x_m^{-\alpha} < x_2^{-\alpha}) = \\ \int_x^{+\infty}(\frac{\lambda_m e^{-(\frac{P_s}{P_m}\lambda_s\pi+\lambda_m\pi)x^2}}{\lambda_m+\frac{P_s}{P_m}\lambda_s} - \frac{\lambda_m e^{-(\lambda_s\pi+\lambda_m\pi)x^2}}{\lambda_m+\lambda_s}) \cdot fx(x) \cdot \frac{1}{\text{P. Case 3.1}}\ dx \tag{5.28}$$

Solving the integral and applying the relation between cdf and pdf, the pdf of the distance serving to the SCell conditioned to Case 3.1 is:

$$fx_{s|Dude}(x) = (\frac{\lambda_m e^{-(\frac{P_s}{P_m}\lambda_s\pi+\lambda_m\pi)x^2}}{\lambda_m+\frac{P_s}{P_m}\lambda_s} - \frac{\lambda_m e^{-(\lambda_s\pi+\lambda_m\pi)x^2}}{\lambda_m+\lambda_s}) \cdot 2\pi\lambda_s x e^{-\pi\lambda_s x^2} \tag{5.29}$$

Analogously, the pdf of the distance serving tot the MCell for the same case is:

$$fx_{s|DRP}(x) = (\frac{\lambda_m e^{-(\frac{P_s}{P_m}\lambda_s\pi+\lambda_m\pi)x^2}}{\lambda_m+\frac{P_s}{P_m}\lambda_s} - \frac{\lambda_m e^{-(\lambda_s\pi+\lambda_m\pi)x^2}}{\lambda_m+\lambda_s}) \cdot 2\pi\lambda_m x e^{-\pi\lambda_m x^2} \tag{5.30}$$

The first connection performs the uplink and the downlink with the SCell 1. It will be the same capacity regardless the second connection. With 4.15 and 5.29,

the capacity of the first connection is:

$$C_{SCell} = \frac{B}{1+\frac{1.28\cdot\lambda_D\cdot P_{av}}{\lambda_{av}}} \cdot \frac{log_2(e)}{P(Case2)} \int_0^{+\infty}\int_0^{+\infty} e^{-\pi\lambda_{ID}(e^t-1)^{\frac{2}{\alpha}}x^2} \int_0^{+\infty}\left(\frac{1}{1+v^{\frac{\alpha}{2}}}\right)dv$$
$$\left(\frac{\lambda_m e^{-(\frac{P_s}{P_m}\lambda_s\pi+\lambda_m\pi)x^2}}{\lambda_m+\frac{P_s}{P_m}\lambda_s} - \frac{\lambda_m e^{-(\lambda_s\pi+\lambda_m\pi)x^2}}{\lambda_m+\lambda_s}\right) * 2\pi\lambda_s x e^{-\pi\lambda_s x^2}\cdot dt\cdot dx \tag{5.31}$$

The second connection, if the access is decoupled, is the same connection as 5.31, as the device is performing the uplink capacity with SCell 2. However, in the suboptimal Case, where the access is not decoupled, it performs the uplink capacity with the MCell. Thus, the pdf of the distance serving to the MCell (5.1) is needed. The capacity of the suboptimal Case is:

$$C_{MCell} = \frac{B}{1+\frac{1.28\cdot\lambda_D\cdot P_{av}}{\lambda_{av}}} \cdot \frac{log_2(e)}{P(Case2)} \int_0^{+\infty}\int_0^{+\infty} e^{-\pi\lambda_{ID}(e^t-1)^{\frac{2}{\alpha}}x^2} \int_0^{+\infty}\left(\frac{1}{1+v^{\frac{\alpha}{2}}}\right)dv$$
$$\left(\frac{\lambda_m e^{-(\frac{P_s}{P_m}\lambda_s\pi+\lambda_m\pi)x^2}}{\lambda_m+\frac{P_s}{P_m}\lambda_s} - \frac{\lambda_m e^{-(\lambda_s\pi+\lambda_m\pi)x^2}}{\lambda_m+\lambda_s}\right) * 2\pi\lambda_m x e^{-\pi\lambda_m x^2}\cdot dt\cdot dx \tag{5.32}$$

The final capacity is the sum of the capacities of both. In the case of decoupled access is 2 times $C_{SCell}$. In the suboptimal case, in a DRP association with the second connection is $C_{SCell} + C_{MCell}$.

## 5.4 Performance evaluation

It is easily shown that the probability trend of all the joint cases (Pmc,Psc and Pdude) is the same as the Single Best Association. However, as there are 4 possibilities more for the connection to be performed, every probability is lower. This can be specially in 5.7, where one of the decoupling probabilities (both are the same as it has been calculated), the probability is almost a half than Pdude in SBA.

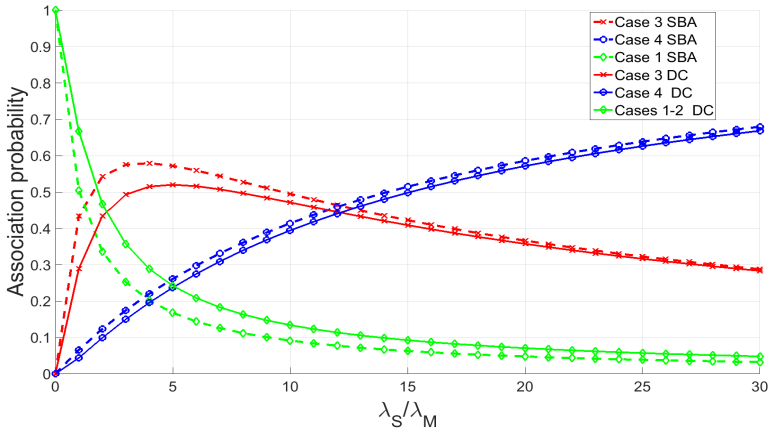


Figure 5.6: Association probability 2 Best Association. Joint probabilities of the four possible combinations. $P_m = 46$ dBm, $P_s = 23$ dBm, $\alpha = 3$, $\lambda_m = 1$.

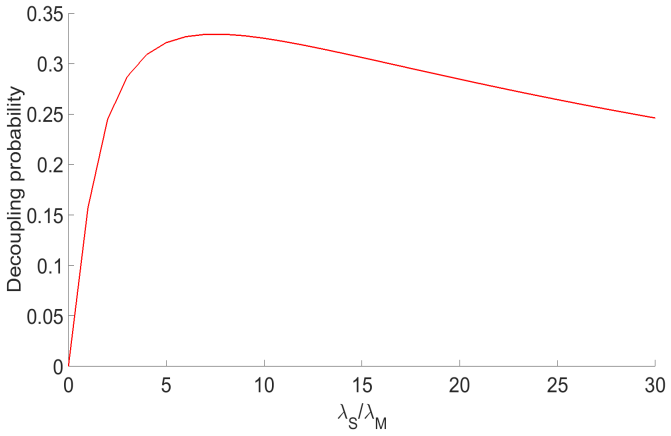


Figure 5.7: Decoupling probability 2 Best Association. $P_m = 46$ dBm, $P_s = 23$ dBm, $\alpha = 3$, $\lambda_m = 1$.

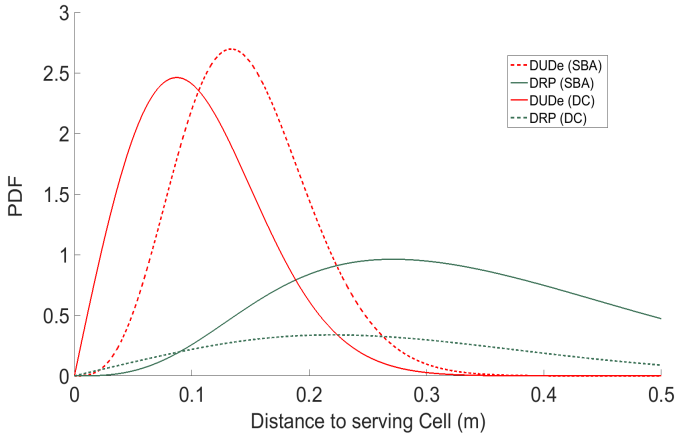


Figure 5.8: .
$P_m = 46$ dBm, $P_s = 23$ dBm, $\alpha = 3$, $\lambda_m = 1$.

In the figure 5.8, we can observe that the pdf of the distance serving in a DRP Association is smaller than in a SBA scenario. This means that the difference between the capacity performing the second connection in a DUDe Association and the capacity on DRP Association will be higher. We can check that on 5.9. As the number of SCells increase, the difference between the DUDe Capacity and the DRP Capacity also gets higher.

Finally, taken into account both connections, we can see a great improvement in comparison to SBA Capacity. It is five times higher and reaches almost 3Mb per second. The most important change is the slope of the line. It is much bigger in the DC scenario, so the capacity will increase also

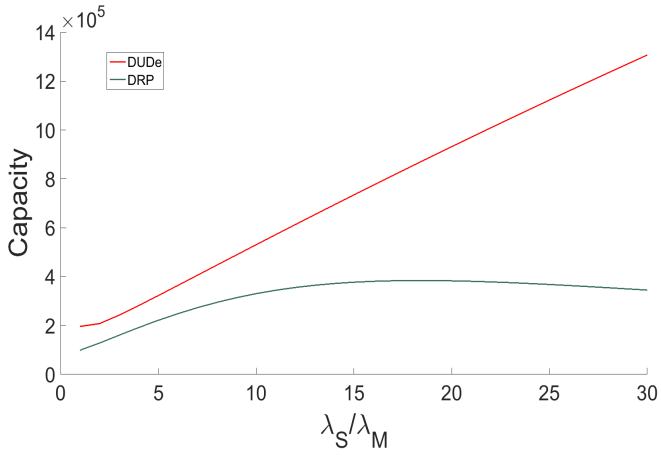


Figure 5.9: Capacity 2nd Association. Comparison DUDe/DRP. $P_m = 46$ dBm, $P_s = 23$ dBm, $\alpha = 4$, $\lambda_m = 1$.

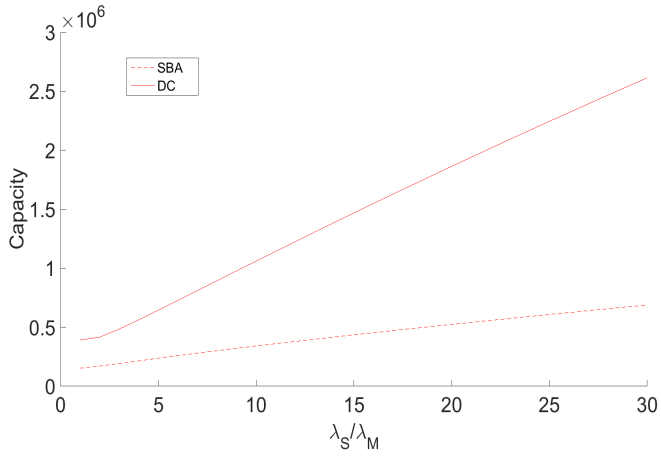


Figure 5.10: Capacity 2 Best Association. Comparison SBA/DC. $P_m = 46$ dBm, $P_s = 23$ dBm, $\alpha = 4$, $\lambda_m = 1$.

# Chapter 6

# Conclusions and further work

The main objective of this thesis has been to strengthen the DUDe technique. Starting from the basic theory and research done so far, two studies has been carried out.

The first study is focused on figure out if decoupling the access is worth if there are some Cells unreachable due to having achieved an amount of data prefixed. It has been observed that the decoupled access works perfectly even with that constraint. The device can not reach up to four SCells and keep obtaining a better capacity than in a DRP Association

In the second study it has been deployed the DUDe over a Dual connectivity scenario. After finding the region of decoupling region among the 3 Cells (2 SCells and 1 MCell) the capacity decoupling the access is has been calculated and it has been shown that is 5 times the capacity in a Best Single Best Association

To sum up, we can conclude that the two studies are satisfactory and we had obtained the results expected. On one side, we assure not to congest any SCell, as we assure that once a SCell starts to being overloaded we can appeal to the second nearest, and so on. On the other side, it has been shown that the decoupling works really good over one technique already being used: Dual Connectivity.

This thesis can be seen as a bridge between the basic theory developed about

DUDe technique so far and lots of work to improve the capacity on the uplink and reduce the uplink and downlink imbalance problem.

First of all, it has been proved that decoupling the access in a DC scenario improves clearly the capacity. However, the study has been made under the assumption of a Best Association. It should be necessary to analyse the situation in a $n$-th Best association to find out if it behaves the same way as the $n$-th Single Best Association. This, would give us the reliability of the DC scenario decoupling the access. If it is better than the SBA one, means that increasing the number of connections, the capacity increases as well.

However, the capacity increases but the interferences affects twice to the connection as every connection may have $v-1$ interferences. For this reason, is reasonable to think that the capacity will not increase forever. There will be certain point that the interference will compensate capacity that multi connectivity gives us. It would be interesting to find that point, $k$. Also, it should be necessary to find out if in any case of $k$ connections the reliability is maintained at the same $n$-th Best Association

Once we find out the $k$ connections of the $n$-th Best Associations, we can build an algorithm for the device to perform that number of connections automatically. For example, the highest capacity is performing 4 connections and the fronthaul can disable 3 of these connections and still have higher capacity than in a DRP Association.

This algorithm would accelerate the process and would gives us the best performance for the decoupled access. Moreover, it opens a wide range of possibilities for the reduction of the uplink and downlink imbalance problem...

# Appendices

# Appendix A

# Matlab code

The mathematical model has been simulated with Matlab software. In this chapter, the Matlab code used for the simulations is introduced for whoever is interested in continuing the research. These functions are attached to the PDF of this thesis as a comment. There are 5 functions that have been used to develop all the simulations:

- In capacity, association probability for $n$-th single best association and dual connectivity is computed. Also, the capacity for both scenarios is calculated for DUDe and DRP association.
- In reliability, the capacity and outage probability is compared among DUDe in $n$-th single best association, DUDe in best single best association and DRP in best single best association.
- In pdude, the decoupling probability for $n$-th single between $n_1$ and $n_2$ is calculated
- In regions, the regions of conditioned functions in DUDe and DRP association in both scenarios.
- In AproxGamma, the approximation used to compute the delta function used for the cdf of $n$-th Best association is proved.

These are the functions:

```
function [] = Capacity

Pm = 40; Ps = 0.2; sigma = 8e-11 ; alpha=4;
beta = ((Pm./Ps).^(2./alpha)); beta2=1./beta;
FIi = @(x) 1 ./ (1 +(x.^(alpha/2))); Ii = integral (FIi
    ,0,+inf);
Lm =1; Ld = 200; B = 10e6; N=30;
n=1; area = 1; Nd = area .* Ld;  Pd=0.2;
Lambda=0:1:N;

for ni=0:N

    Ls=ni*Lm; %number of femto eNBs

    %% Values to approximate Delta function

    p1 = 9.4368392235E-03;
    p2 = -1.0782666481E-04;
    p3 = -5.8969657295E-06;
    p4 = 2.8939523781E-07;
    p5 = 1.0043326298E-01;
    p6 = 5.5637848465E-01;
    q1 = 1.1464706419E-01;
    q2 = 2.6963429121E+00;
    q3 = -2.9647038257E+00;
    q4 = 2.1080724954E+00;
    r1 = 0.0;
    r2 = 1.1428716184E+00;
    r3 = -6.6981186438E-03;
    r4 = 1.0480765092E-04;
    s1 = 1.0356711153E+00;
    s2 = 2.3423452308E+00;
    s3 = -3.6174503174E-01;
    s4 = -3.1376557650E+00;
```

```
34      s5 = 2.9092306039E+00;
35
36      c1 = 1 + p1.*n + p2.*(n.^2) + p3*(n.^3) + p4.*(n.^4)+p5
            .*(exp(-p6*n)-1);
37      c2 = q1 + q2./n + q3./(n.^2) + q4./(n.^3);
38      c3 = r1 + r2.*n + r3.*(n.^2) + r4.*(n.^3);
39      c4 = s1 + s2./n + s3./(n.^2) + s4./(n.^3) + s5./(n.^4);
40
41      %% Association probability nth Single Best Association
42
43      fun3 = @(x) (exp(-x.^2 .* Lm .* pi .* ((Pm/Ps).^(2./
            alpha)))* ((2.*(Lm.*ni.*pi).^(n))/factorial(n-1))
            .*((x).^((2.*n)-1)).*(exp(-Lm.*ni.*pi.*x.^2)));
44      Psc (ni+1) = integral (fun3 , 0 , +inf);
45      fun1 = @(x) (((exp(-x.^2 .* Lm .* pi)-(exp(-x.^2 .* ((
            Pm/Ps).^(2./alpha)) .* Lm .* pi)))*((2.*(Ls.*pi).^(n
            ))/factorial(n-1)).*((x).^((2.*n)-1)).*(exp(-Ls.*pi
            .*x.^2))));
46      pdudesba (ni+1) = integral (fun1 , 0 , +inf);
47      fun2 = @(x) ((1-(((exp(-x.^2 .* Lm .* ni .* pi).*((x.^2
             .* Lm .* ni .* pi).^n).*(((1./n)+(c1.*(x.^2 .* Lm
            .* ni .* pi)./(n.*(n+1))))+(((c1.*(x.^2 .* Lm .* ni
            .* pi)).^2)./(n.*(n+1).*(n+2)))).*(1-(0.5+(0.5.*tanh
            (c2.*(x.^2 .* Lm .* ni .* pi-c3))))) + (factorial(n
            -1)).*((0.5+(0.5.*tanh(c2.*(x.^2 .* Lm .* ni .* pi-
            c3)))).*(1-(c4.^(-x.^2 .* Lm .* ni .* pi)))))./(
            factorial(n-1))))).*((2.*pi.*Lm.*x.*exp(-pi.*Lm.*x
            .^2))));
48      Pmc (ni+1) = integral (fun2, 0 , +inf);
49
50      %%Capacity nth Single Best Association
51
52      %%Dude
53
```

```
54      Nms(ni+1) = (Ls + Lm).* area;
55      Nm(ni+1) = Lm .* area;
56      p (ni+1) = (Nms(ni+1)-1)./ Nd;
57      Li(ni+1)= p(ni+1).* Ld;
58      p1(ni+1) = (pdudesba(ni+1)+Psc(ni+1));
59      Nxdude2 (ni+1) = B ./ (1 + ((1.28.*Ld.*p1(ni+1))./(Ls))
            );
60      KDUDE (ni+1) = log2(exp(1)) ./ pdudesba (ni+1) .*
            Nxdude2 (ni+1) ;
61      funCDUDE = @(x,t) KDUDE (ni+1) .* (exp(-(x.^alpha)
            .*(exp(t)-1).*sigma./Pd)) .* exp(-pi.*Li(ni+1).*x
            .^2.*Ii.*((exp(t)-1).^(2./alpha))) .* (((exp(-x
            .^2.*Lm.*pi)-((exp(-x.^2.*((Pm/Ps)^(2./alpha)).*Lm.*
            pi))))) .* ((2.*(Ls.*pi).^(n))./factorial(n-1).*((x
            ).^((2.*n)-1)).*(exp(-Ls.*pi.*x.^2)));
62      CDude (ni+1) = integral2 (funCDUDE, 0, +inf, 0, +inf);
63
64      %%DRP
65      pSBADRP (ni+1) = pdudesba (ni+1) + Pmc (ni+1);
66      Nxdlrp2 (ni+1) = B ./ (1 + (1.28.*Ld.*Pmc (ni+1))./(Lm)
            );
67      KDRP (ni+1) = log2(exp(1)) ./ pdudesba (ni+1) .*
            Nxdlrp2 (ni+1);
68      funCDRP = @(x,t) KDRP (ni+1) .* ((exp(-(x.^alpha) .* (
            exp(t)-1).*sigma./Pd)) .* exp(-pi.*Li(ni+1).*x.^2.*
            Ii.*(((exp(t)-1)).^(2./alpha))) .* ((((exp(-x.^2 .*
            ((Ps/Pm).^(2./alpha)) .* Lm.* ni .* pi)-(exp(-x.^2
            .* Lm .* ni .* pi)))))) .* (2.*Lm.*pi).*x.*(exp((-
            Lm.*pi.*x.^2)));
69      CDrp (ni+1) = integral2 (funCDRP, 0, +inf, 0, +inf);
70
71      %% Association probability DUDe on Dual Connectivity
72
73      f1 = @(x) (1-(2.*(1-(exp(-Lm.*ni.*pi.*x.^2))))+((1-(exp
```

```
    (-Lm.*ni.*pi.*x.^2)))).^2).*2.*Lm.*pi.*x.*exp(-Lm.*
    pi.*x.^2);
74  Pmin3(ni+1) = integral(f1,0,inf);
75  Pcase1(ni+1) = Lm ./ (Lm+2.*Ls);
76  Pcase2(ni+1) = 2.* Lm.*Ls ./ (Lm+(Ls)) ./(Ls+Lm+(Ls));
77  PmcDC(ni+1)= Pcase1(ni+1) + Pcase2(ni+1);
78
79  f2= @(x) (1-(1-(exp(-Lm.*ni.*pi.*x.^2)))-(1-(exp(-Lm.*
    pi.*x.^2)))+(1-(exp(-Lm.*ni.*pi.*x.^2))).*(1-(exp(-
    Lm.*pi.*x.^2)))) .* 2.* Ls .* pi .* x .* exp(-Ls.*pi
    .*x.^2);
80  Pmin1(ni+1) = integral (f2,0,inf);
81  P2(ni+1) = Ls ./ (Ls + (beta.*Lm));
82  Psc1(ni+1) = Pmin1(ni+1) .* P2(ni+1);
83  f3 = @(x)(1-(1-(exp(-Lm.*ni.*pi.*x.^2)))-(1-(exp(-Lm.*
    pi.*x.^2)))+(1-(exp(-Lm.*ni.*pi.*x.^2))).*(1-(exp(-
    Lm.*pi.*x.^2)))).* 2.* Ls .* pi .* x .* exp(-Ls.*pi
    .*x.^2);
84  Pmin2(ni+1) = integral (f3,0,inf);
85  Psc2(ni+1) = Pmin2(ni+1) .* P2(ni+1);
86  Pcase4(ni+1) = (Psc1(ni+1) + Psc2(ni+1));
87
88  P3(ni+1) = (Lm./(Lm + Ls./beta))-(Lm./(Lm+Ls));
89  Pdude1(ni+1) = Pmin1(ni+1) .* P3(ni+1);
90  Pdude2(ni+1) = Pmin2(ni+1) .* P3(ni+1);
91  Pcase3(ni+1) = Pdude1(ni+1) + Pdude2(ni+1);
92
93  % Capacity DC - DUDe
94
95  f2= @(x) (1-(1-(exp(-Lm.*ni.*pi.*x.^2)))-(1-(exp(-Lm.*
    pi.*x.^2)))+(1-(exp(-Lm.*ni.*pi.*x.^2))).*(1-(exp(-
    Lm.*pi.*x.^2)))) .* 2.* Ls .* pi .* x .* exp(-Ls.*pi
    .*x.^2);
96  Pmin1(ni+1) = integral (f2,0,inf);
```

```
97      P3(ni+1) = (Lm./(Lm + Ls./beta))-(Lm./(Lm+Ls));
98      pSBADUDE2 (ni+1) = Pmin1(ni+1) .* P3(ni+1);
99      PSC_DC(ni+1) =  Psc(ni+1)+Pcase3(ni+1);
100     KDUDE2 (ni+1) = log2(exp(1)) ./ pSBADUDE2 (ni+1) .* (B
            ./(1+((1.28.*Ld.*PSC_DC(ni+1))./Ls)))  ;
101     funCDUDE21 = @(x,t) KDUDE2 (ni+1).* (exp(-2.*(x.^alpha)
            .*(exp(t)-1).*sigma./Pd)).* exp(-pi.*Li(ni+1).*x
            .^2.*Ii.*((2.*(exp(t)-1)).^(2./alpha)))  .* ((Lm .*
            pi .* exp (-(Ls.*pi.*beta2+Lm.*pi).*x.^2) ./ (Lm.*pi
             + Ls.*pi.*beta2)) - (Lm .* pi .* exp (-(Ls.*pi+Lm.*
            pi).*x.^2) ./ (Lm.*pi + Ls.*pi))) .* 2.*pi.*Ls.*x.*
            exp(-pi.*Ls.*x.^2);
102     CDude21 (ni+1) = integral2 (funCDUDE21, 0, +inf, 0, +
            inf);
103     CDude2 (ni+1) =  2.* CDude21 (ni+1);
104
105     % Capacity DRP - DUDe
106
107     Pcase2(ni+1) = (Lm.*Ls ./ (Lm+(Ls)) ./(Ls+Lm+(Ls)));
108     PMC_DC(ni+1) = Pmc(ni+1);
109     KDRP2 (ni+1) = log2(exp(1)) ./ pSBADUDE2 (ni+1) .* (B
            ./(1+((1.28.*Ld.*PMC_DC(ni+1))./Ls)));
110     funCDrp = @(x,t) KDRP2 (ni+1) .*  (exp(-2.*(x.^alpha)
            .*(exp(t)-1).*sigma./Pd)).* exp(-pi.*Li(ni+1).*x
            .^2.*Ii.*((2.*(exp(t)-1)).^(2./alpha)))  .* ((Lm .*
            pi .* exp (-(Ls.*pi.*beta2+Lm.*pi).*x.^2) ./ (Lm.*pi
             + Ls.*pi.*beta2)) - (Lm .* pi .* exp (-(Ls.*pi+Lm.*
            pi).*x.^2) ./ (Lm.*pi + Ls.*pi))) .* 2.*pi.*Lm.*x.*
            exp(-pi.*Lm.*x.^2);
111     CDrp22 (ni+1) = integral2 (funCDrp, 0, +inf, 0, +inf);
112     CDrp2 (ni+1) =  CDrp22 (ni+1) + CDude21 (ni+1)  ;
113
114     % Gain DUDe - DRP
115
```

```
116     Gain (ni+1) = ((CDude2 (ni+1) - CDrp2 (ni+1)) / CDrp2 (
            ni+1)) .* 100;
117
118 end
119
120 %% Graphs
121
122 % Probability nth Single Best Association
123 figure
124 hold on
125 plot(Lambda,pdudesba,'r')
126 plot(Lambda,Psc,'b')
127 plot(Lambda,Pmc,'g')
128 legend('Pdude','Psc','Pmc');
129 xlabel('\lambda_S/\lambda_M');
130 ylabel('Association probability');
131 hold off
132
133 % Association probability DC (4 cases)
134 figure
135 hold on
136 plot(Lambda,PmcDC,'b')
137 plot(Lambda,Pcase2,'k')
138 plot(Lambda,Pcase3,'r')
139 plot(Lambda,Pcase4,'g')
140 xlabel('Lambda S/Lambda M');
141 ylabel('P(A)');
142 legend('Pcase1','Pcase2','Pcase3','Pcase4');
143 hold off
144
145 % Association probability DC (Pmc, Psc, Pdude) - SBA (Pmc,
        Psc, Pdude)
146 figure
147 hold on
```

```
148 plot(Lambda,pdudesba,'r')
149 plot(Lambda,Psc,'b')
150 plot(Lambda,Pmc,'g')
151 plot(Lambda,Pcase3,'r')
152 plot(Lambda,Pcase4,'b')
153 plot(Lambda,PmcDC,'g')
154 legend('DUDe SBA','SCell SBA','MCell SBA','DUDe DC','SCell
      DC','MCell DC');
155 hold off
156 xlabel('\lambda_S/\lambda_M');
157 ylabel('Association probability');
158 hold off
159
160 % Comparison Decoupling probability SBA - DC
161 figure
162 hold on
163 plot(Lambda,CDude,'r')
164 plot(Lambda,CDrp,'b')
165 plot(Lambda,CDude2,'g')
166 plot(Lambda,CDrp2,'y')
167 xlabel('\lambda_S/\lambda_M');
168 legend('DC','SBA');
169 ylabel('Decoupling probability');
170 hold off
171
172 % Capacity
173 figure
174 hold on
175 plot(Lambda,Pcase3,'r')
176 plot(Lambda,pdudesba,'b')
177 xlabel('\lambda_S/\lambda_M');
178 ylabel('Capacity (bps)');
179 hold off
180
```

```
% Relation Capacity DUDe and Capacity DRP in nth Single
    Best Association
figure
plot(CDrp,CDude);
xlabel('Capacity DLRP (bps)');
ylabel('Capacity DUDe (bps)');
hold off

% Gain
figure
hold on
plot(Lambda,Gain,'b');
hold off
xlabel('\lambda_S/\lambda_M');
ylabel('Gain (%)');
hold off

end
```

```
function [P] = pdude
%Lm = Number Mc / Cluster
%alfa = pathloss due to distance to MC/SC
%Pm = Macro-cell power
%Ps= Pico-cell power
%n = nth nearest
%N = number Sc / Mc
Lm = 1;
alfa = 3;
Pm = 40;
Ps = 0.2;
n1=1; n2=4;

% Decoupling probability for different "n"

```

```
for n = n1:n2
for ni = n:30
    fun = @(x) (((exp(-x.^2 .* Lm .* pi)-(exp(-x.^2 .* ((Pm
        /Ps).^(2./alfa)) .* Lm .* pi)))*((2.*(Lm.*ni.*pi).^(
        n))/factorial(n-1)).*((x).^((2.*n)-1)).*(exp(-Lm.*ni
        .*pi.*x.^2))));
    P(ni) = integral(fun, 0, +inf);
    hold on

end

plot(P,'r')
xlabel('\lambda_S/\lambda_M');
ylabel('Decoupling probability');
hold off
end

end
```

```
function [OpDUDEn] = Reliability

no=8;
psba = 0.3666; psban = 0.6630;
sinr_target_dB = -40:40; sinr_target= 10.^(sinr_target_dB
    ./10);
sigma = 8e-11; ni=20; alpha = 4;
Pm = 40; Ps = 0.2; Pd = 0.2;
Lm = 1; Ls = Lm .* ni;
Ld = 100;  area = 10; Nd = area .* Ld;
Nms = (Ls + Lm).* area; p  = (Nms-1)./ Nd;
FIi  = @(x) 1 ./ (1 + (x.^(alpha/2))); Ii = integral(FIi
    ,0,+inf);
Li = p.* Ld; B = 10e6;

```

```
% Capacity

for nr = 1:10

    p1 = 9.4368392235E-03;
    p2 = -1.0782666481E-04;
    p3 = -5.8969657295E-06;
    p4 = 2.8939523781E-07;
    p5 = 1.0043326298E-01;
    p6 = 5.5637848465E-01;
    q1 = 1.1464706419E-01;
    q2 = 2.6963429121E+00;
    q3 = -2.9647038257E+00;
    q4 = 2.1080724954E+00;
    r1 = 0.0;
    r2 = 1.1428716184E+00;
    r3 = -6.6981186438E-03;
    r4 = 1.0480765092E-04;
    s1 = 1.0356711153E+00;
    s2 = 2.3423452308E+00;
    s3 = -3.6174503174E-01;
    s4 = -3.1376557650E+00;
    s5 = 2.9092306039E+00;

    c1 = 1 + p1.*nr + p2.*(nr.^2) + p3*(nr.^3) + p4.*(nr
        .^4)+p5.*(exp(-p6*nr)-1);
    c2 = q1 + q2./nr + q3./(nr.^2) + q4./(nr.^3);
    c3 = r1 + r2.*nr + r3.*(nr.^2) + r4.*(nr.^3);
    c4 = s1 + s2./nr + s3./(nr.^2) + s4./(nr.^3) + s5./(nr
        .^4);

    fun3 = @(x) (exp(-x.^2 .* Lm .* pi .* ((Pm/Ps).^(2./
        alpha)))*((2.*(Lm.*ni.*pi).^(nr))/factorial(nr-1))
        .*((x).^((2.*nr)-1)).*(exp(-Lm.*ni.*pi.*x.^2)));
```

```
44      Psc (nr) = integral (fun3 , 0 , +inf);
45      fun1 = @(x) (((exp(-x.^2 .* Lm .* pi)-(exp(-x.^2 .* ((
            Pm/Ps).^(2./alpha)) .* Lm .* pi)))*((2.*(Lm.*ni.*pi)
            .^(nr))/factorial(nr-1)).*((x).^((2.*nr)-1)).*(exp(-
            Lm.*ni.*pi.*x.^2))));
46      pSBADUDE (nr) = integral (fun1 , 0 , +inf);
47      Nxdude = B ./ (Nd./Nms);
48      p1(nr) = (pSBADUDE(nr)+Psc(nr));
49      Nxdude2 (nr) = B ./ (1 + ((1.28.*Ld.*p1(nr))./(Ls)));
50      KDUDE2 (nr) = log2(exp(1)) ./ pSBADUDE (nr) .* Nxdude2
            (nr) ;
51      KDUDE (nr) = log2(exp(1)) ./ pSBADUDE (nr) .* 10e6 ./
            Nxdude;
52      fun2 = @(x) ((1-(((exp(-x.^2 .* Lm .* ni .* pi).*((x.^2
             .* Lm .* ni .* pi).^nr) .* (((1./nr)+(c1.*(x.^2 .*
            Lm .* ni .* pi)./(nr.*(nr+1))))+(((c1.*(x.^2 .* Lm
            .* ni .* pi)).^2)./(nr.*(nr+1).*(nr+2))))
            .*(1-(0.5+(0.5.*tanh(c2.*(x.^2 .* Lm .* ni .* pi-c3)
            )))) + (factorial(nr-1)).*((0.5+(0.5.*tanh(c2.*(x.^2
             .* Lm .* ni .* pi-c3)))).*(1-(c4.^(-x.^2 .* Lm .*
            ni .* pi))))))./(factorial(nr-1))))).*((2.*pi.*Lm.*x
            .*exp(-pi.*Lm.*x.^2))));
53      Pmc (nr) = integral (fun2, 0 , +inf);
54      Nxdrp2 (nr) = B ./ (1 + (1.28.*Ld.*Pmc (nr))./(Lm));
55      KDRP2 (nr) = log2(exp(1)) ./ pSBADUDE (nr) .* Nxdrp2 (
            nr);
56      funCDUDE = @(x,t) KDUDE2 (nr) .* (exp(-(x.^alpha).*(
            exp(t)-1).*sigma./Pd)).*exp(-pi.*Li.*x.^2.*Ii.*((exp
            (t)-1).^(2./alpha))).* (((exp(-x.^2.*Lm.*pi)-((exp(-
            x.^2.*((Pm/Ps)^(2./alpha)).*Lm.*pi))))) .* ((2.*(Ls
            .*pi).^(nr))./factorial(nr-1).*((x).^((2.*nr)-1))
            .*(exp(-Ls.*pi.*x.^2))));
57      CDude (nr) = integral2 (funCDUDE, 0, +inf , 0, +inf);
58      funCDRP = @(x,t) KDRP2 (nr) .* ((exp(-(x.^alpha).*(exp
```

```
        (t)-1).*sigma./Pd)) .* exp(-pi.*Li.*x.^2.*Ii.*(((exp
        (t)-1)).^(2./alpha))) .* ((((exp(-x.^2 .* ((Ps/Pm)
        .^(2./alpha)) .* Lm.* ni .* pi)-(exp(-x.^2 .* Lm .*
        ni .* pi)))))))) .* (2.*Lm.*pi).*x.*(exp((-Lm.*pi.*x
        .^2)));
59      CDlrp (nr) = integral2 (funCDRP, 0, +inf, 0, +inf);
60
61  end
62
63  Y = [CDude(1),CDlrp(1);CDude(2),CDlrp(2);CDude(3),CDlrp(3);
    CDude(4),CDlrp(4);CDude(5),CDlrp(5);CDude(6),CDlrp(6);
    CDude(7),CDlrp(7);CDude(8),CDlrp(8);CDude(9),CDlrp(9);
    CDude(10),CDlrp(10)];
64
65  % Outage probability
66
67  for t=1:81
68
69      FIi = @(u) 1 ./ (1 + (u.^(alpha/2)));
70      Ii (t) = integral (FIi, (sinr_target(t).^(-2/alpha)),
            inf);
71      funDUDE = @(x) (1 ./ psba) .* (exp(-(x.^alpha) .*
            sinr_target(t).* sigma.*(1./Pd))).* (exp (-(x.^2.*Li
            .*pi.*((((sinr_target(t)).^ (2./alpha))).*Ii(t)))))
            .* (((exp(-x.^2 .* Lm .* pi)-(exp(-x.^2 .* ((Pm/Ps)
            ^(2/alpha)) .* Lm .* pi)))) .* ((2.*(Lm.*ni.*pi.*x))
            ) .* (exp(-Lm.*ni.*pi.*(x.^2))));
72      funDLR = @(x) (1 ./ psba) .* (exp(-(x.^alpha) .*
            sinr_target(t).* sigma.*(1./Pd)).*(exp (-(x.^2.*Li.*
            pi.*((sinr_target(t)).^(2./alpha)) .*Ii(t)))) .* (((
            exp(-x.^2 .* ((Ps/Pm)^(2/alpha)) .* Lm .* ni .* pi)
            -(exp(-x.^2 .* Lm .* ni .* pi)))) .* ((2.*(Lm.*pi.*x
            ))) .* (exp(-Lm.*pi.*x.^2))));
73      funDUDEn = @(x) (1 ./ psban) .* (exp(-(x.^alpha) .*
```

```
        sinr_target(t).*sigma.*(1./Pd))) .* exp(-x.^2.*Li.*
        pi.*((sinr_target(t)).^(2./alpha)).*Ii(t)).*(((exp(-
        x.^2 .* Lm .* pi)-(exp(-x.^2 .* ((Pm/Ps).^(2./alpha)
        ) .* Lm .* pi)))).*((2.*(Lm.*ni.*pi).^(no))/
        factorial(no-1)).*((x).^((2.*no)-1)).*(exp(-Lm.*ni.*
        pi.*x.^2)));
74          CpDUDE(t) = integral(funDUDE, 0, inf);
75      OpDUDE(t) = 1 - CpDUDE(t);
76      CpDLR(t) = integral(funDLR, 0, inf);
77      OpDLR(t) = 1 - CpDLR(t);
78      CpDUDEn(t) = integral(funDUDEn, 0, inf);
79      OpDUDEn(t) = 1 - CpDUDEn(t);
80
81  end
82
83  % Maximums and minimums values for Outages probabilities
84
85  max1 = max(OpDUDE);
86  min1 = min(OpDUDE);
87  max2 = max(OpDLR);
88  min2 = min(OpDLR);
89  max3 = max(OpDUDEn);
90  min3 = min(OpDUDEn);
91
92  % Comparison among OP Dude nth SBA, DUDe Best SBA and DRP
        Best SBA
93
94  %% Graphs
95
96  %Capacity
97
98  figure
99  hold on
100 bar(Y);
```

```
101 xlabel('n');
102 ylabel('Capacity');
103 legend('dude','drp');
104 hold off;
105
106 % Outage probability
107
108 figure
109 hold on
110 plot(sinr_target_dB,OpDUDE,'r');
111 plot(sinr_target_dB,OpDLR,'b');
112 plot(sinr_target_dB,OpDUDEn,'y');
113 xlabel('Treshold');
114 ylabel('OP')
115 legend('dude','drp','dude Nth best');
116 hold off
117
118 end
```

```
1 function [areadudesba,areamcsba,areasc,areadude,areamc] =
      regions
2
3 x=linspace(0,0.5,1000);
4
5 Lm = 1; ni=20; Ls = ni.*Lm; Pm=40; Ps=0.2; alfa=4; beta = (
      Pm./Ps).^(2./alfa); beta2=1./beta;
6
7 pdf_dude = ( exp (-pi.*Lm.*x.^2) - exp (-pi.*beta.*Lm.*x
      .^2) ) .* 2.*pi.*Ls.*x.*exp(-pi.*Ls.*x.^2);
8 pdf_sc =  2.*pi.*Ls.*x.*exp(-pi.*Ls.*x.^2);
9 pdf_drp =  (exp (-pi.*Ls.*beta2.*x.^2) - exp (-pi.*Ls.*x
      .^2) ).* 2.*pi.*Lm.*x.*exp(-pi.*Lm.*x.^2);
10 pdf_dudedc = ((Lm .* pi .* exp (-(Ls.*pi.*beta2+Lm.*pi).*x
      .^2) ./ (Lm.*pi + Ls.*pi.*beta2)) - (Lm .* pi .* exp (-(
```

```
    Ls.*pi+Lm.*pi).*x.^2) ./ (Lm.*pi + Ls.*pi))) .* 2.*pi.*
    Ls.*x.*exp(-pi.*Ls.*x.^2) ;
pdf_drpdc = ((Lm .* pi .* exp (-(Ls.*pi.*beta2+Lm.*pi).*x
    .^2) ./ (Lm.*pi + Ls.*pi.*beta2)) - (Lm .* pi .* exp (-(
    Ls.*pi+Lm.*pi).*x.^2) ./ (Lm.*pi + Ls.*pi))) .* 2.*pi.*
    Lm.*x.*exp(-pi.*Lm.*x.^2) ;
pdf_mc = 2.*pi.*Lm.*x.*exp(-pi.*Lm.*x.^2);

figure
hold on
plot(x,pdf_dude ,'k');
plot(x,pdf_drp,'g');
plot(x,pdf_dudedc,'r');
plot(x,pdf_drpdc,'b');
xlabel('Distance');
ylabel('PDF');
legend('PdudeSBA','PDRPSBA','PDUDEDC','PDRPDC');
hold off

end
```

```
function [matlb,aprox] = Aprox_Gamma(n,x)

matlb = gammainc(x,n) .* gamma(n) ;
p1 = 9.4368392235E-03;
p2 = -1.0782666481E-04;
p3 = -5.8969657295E-06;
p4 = 2.8939523781E-07;
p5 = 1.0043326298E-01;
p6 = 5.5637848465E-01;
q1 = 1.1464706419E-01;
q2 = 2.6963429121E+00;
q3 = -2.9647038257E+00;
q4 = 2.1080724954E+00;
```

```
14 r1 = 0.0;
15 r2 = 1.1428716184E+00;
16 r3 = -6.6981186438E-03;
17 r4 = 1.0480765092E-04;
18 s1 = 1.0356711153E+00;
19 s2 = 2.3423452308E+00;
20 s3 = -3.6174503174E-01;
21 s4 = -3.1376557650E+00;
22 s5 = 2.9092306039E+00;
23
24 c1 = 1 + p1.*n + p2.*(n.^2) + p3*(n.^3) + p4.*(n.^4)+p5.*(
       exp(-p6*n)-1);
25 c2 = q1 + q2./n + q3./(n.^2) + q4./(n.^3);
26 c3 = r1 + r2.*n + r3.*(n.^2) + r4.*(n.^3);
27 c4 = s1 + s2./n + s3./(n.^2) + s4./(n.^3) + s5./(n.^4);
28
29 aprox = exp(-x).*((x).^n).*(((1./n)+(c1.*(x)./(n.*(n+1))))+
       ...
30 (((c1.*(x)).^2)./(n.*(n+1).*(n+2)))).*(1-(0.5+(0.5.*tanh(c2
       .*(x-c3))))) ...
31 + (factorial(n-1)).*((0.5+(0.5.*tanh(c2.*(x-c3)))).*(1-(c4
       .^(-x))));
32
33 end
```

# Appendix B

# Scientific paper related to the thesis

# Flexible Dual-Connectivity Spectrum Aggregation for Decoupled Uplink and Downlink Access in 5G Heterogeneous Systems

Maria A. Lema*, Enric Pardo*, Olga Galinina§, Sergey Andreev§, Mischa Dohler*, *Fellow, IEEE*

*Centre for Telecommunications Research, Dept. of Informatics
King's College London,

§Department of Electronics and Communications Engineering
Tampere University of Technology

{maria.lema_rosas; enric.pardo; mischa.dohler@kcl.ac.uk}

**Abstract**

Maintaining multiple connections is an attractive solution to boost capacity in 5G networks, where the user is able to consume radio resources from more than one serving cell and ultimately aggregate bandwidth from all of them. Such a dual connectivity paradigm can be seen as an attractive access feature in dense heterogeneous 5G networks, where bandwidth sharing and cooperative techniques are likely to evolve to satisfy the increased capacity requirements. Dual connectivity in the uplink is highly controversial, since the user has limited power to share between two different access points, especially when placed close to the cell edge. However, in an attempt to enhance the uplink communications, the concept of uplink and downlink decoupling has been recently introduced. Leveraging on these developments, our work significantly advances prior art by introducing and investigating the concept of flexible cell association in dual connectivity scenarios with users able to aggregate traffic from more than one serving cell and with association policies for the uplink not following those of the downlink, thereby allowing for a complete decoupled access. With the use of stochastic geometry, the dual connectivity association regions for decoupled access are derived and performance is evaluated in terms of capacity gains with respect to traditional downlink received power access policies.

**Index Terms**

Dual-Connectivity, UL/DL Split, Bandwidth Aggregation, UL Communications

## I. Introduction

The deployment of a feasible high speed spectral efficient network needs a variety of innovative features, given that link level solutions have evolved to near Shannon limit capacity with the use of advanced Modulation and Coding Schemes (MCS) [1]. With the purpose of improving per-user throughput and overall system capacity, the third generation partnership project (3GPP) organization has introduced the concept of Dual-Connectivity in Heterogeneous Networks (HetNets) in Release 12 [2], defined as the simultaneous use of spectrum from macro and small cells (MCell and SCell) connected via non-ideal backhaul link over the X2 interface. In this sense, Dual-Connectivity is a new feature that allows to contribute to the large bandwidth demand to achieve high data rates by allowing the user to hold two simultaneous connections. On the other hand, multi-connectivity solutions allow to improve the user session continuity, enhancing the user connectivity experience as well as the overall communication reliability.

Spectrum aggregation techniques are in general almost directly applicable in the downlink (DL), where power availability to face increased bandwidth allocations is not an issue, given that the evolved Node B (eNB) is in charge of the transmission. The most restrictive link is always the uplink (UL), as it relies on the user terminal for transmission procedures. Given this, an extension in the allocated bandwidth may not be beneficial owing to the User Equipment (UE) power limitations. Similar assumptions where already made in the context of Carrier Aggregation, and multiple works have studied and evaluated the feasibility of spectrum aggregation in the UL transmissions [3]. In the scope of Dual-Connectivity, holding more than one UL connection can be less power efficient for users that are placed near the cell edge [4], [5], due to the increased path-loss experienced to the serving cells.

On a separate effort of offloading the MCell and improving the UL performance the 3GPP introduces the idea of the UL and DL split in [2]. As a result of the strong transmit power disparities among macro and small cells, the cell that provides the best received power in the DL may not be the same that receives the highest power in the UL. Traditional cell association schemes, based on DL received power, result in a sub-optimal association solution for the UL. Thus, allowing novel cell association rules in heterogeneous deployments, where energy

saving and constant user satisfaction along the cell radius are pursued, can contribute to a more fair UL rate.

The increased flexibility provided by decoupled UL and DL associations provides advantages when selecting UL and DL cooperative transmissions or receptions with the use of Dual-Connectivity. This flexible association, and the interoperability of DUDe with Dual-Connectivity goes one step further in the multi-connectivity network, since the UE can select independently the number and position of DL and UL serving cells, according to several input parameters, as backhaul capacity, power limitation, throughput maximization, among others. In this sense, spectrum aggregation with the use of Dual-Connectivity becomes highly efficient and flexible, allowing to maximize the user spectral efficiency.

This work addresses the user association problem in a HetNet system, where users are allowed to aggregate bandwidth with the use of Dual-Connectivity. With the aim of improving the UL capacity and spectral efficiency in aggregated transmissions, users should follow a per link maximum received power association rule, allowing to eventually decouple both links. Adding this level of flexibility in a multi-connectivity context allows to bring all the benefits of decoupled associations and enhance both UL and DL communications.

This document is organised as follows. This section continues with a literature survey that covers the prior art in both multi-site spectrum aggregation and decoupled associations, and closes with the main contributions presented in this work. Section II describes the system model and assumptions for the stochastic geometry mathematical analysis. In Section III, the association regions and probabilities are derived, and in Section IV the decoupled capacity expressions are developed. Performance evaluation is done in Section IV, followed by the conclusions.

### *A. State of the Art Review*

Dual connectivity is one of the 3GPP potential solutions to improve user performance by combining the benefits of the MCell coverage and the SCell capacity [2] where release 10 Carrier Aggregation is applied to aggregate carriers in co-channel HetNets. The technology potential has been widely studied by the 3GPP in [2], where significantly improved capacity gains where recognised.

The research community has well studied the performance improvements brought by the use of inter-site resource aggregation with the use of Carrier Aggregation. Work in [6] studies

the inter-site aggregation in a DL scenario where MCells share resources with other cells. This study proposes a Carrier Aggregation window to determine if Carrier Aggregation-compliant UEs should be selected to consume resources from both cells. This study considers a dedicated frequency deployment, where each cell is assumed to be operating at different frequencies. The benefit of aggregating resources from both cells is verified for different traffic patterns and cell load situations. The previous study is further extended with a focus in the UL in [7], where results show improvements of the UL throughput in low load situations due to larger bandwidth accessibility.

In the context of Dual-Connectivity, several works undertake the numerous open challenges and analyse the performance improvements. Work in [8] tackles the DL scheduling challenges and proposes a *downlink traffic scheduling* mechanism that aims at maximizing the network throughput when deciding the traffic splitting to the SCell. Moreover, work in [9] studies the Dual-Connectivity with a Control/User Plane split and proposes a flexible network configuration, which uses the channel state information reference signal (CSI-RS) information for SCell association purposes. Similarly, authors in [10] study the association as an optimization problem: the optimal combination of macro and small cells and the optimal traffic split between both serving cells. The improvements in the user performance with the use of shared resources provides a strong indication that cooperative techniques are becoming mandatory to maximize both spectrum utilization and efficiency.

One step further in the optimization of HetNets is the relationship between UL and DL and how the association policies affect the performance on both links. Both UL/DL power and MCell/SCell load and power imbalance motivates the decoupling of both links, which is particularly beneficial in co-channel heterogeneous deployments. In Release 12, 3GPP provided an initial evaluation of the HetNet performance when including UL and DL split, results show improvements particularly at the cell edge for both low and medium load scenarios [2], [11]. The literature has tackled the power and load imbalance problem recently and some relevant references can be identified. Authors in [12] present the path-loss cell association solution to the power imbalance problem. Results in terms of gain that can be achieved in the UL capacity are very promising. A detailed analysis of the decoupled access in terms of association probability, coverage and capacity are presented in [5]. Here, prior work is extended by adding the analytical evaluation using stochastic geometry and architectural considerations. Results show same trend between the stochastic geometry analysis and the real world experimental data. Work in [13] introduces cell load and

the backhaul limitation into the cell association process. SINR variance is reduced with the enhanced DUDe solution presented; also, the interference-aware UL power control applied allows a further improvement in the UL throughput. Finally, [14] analyses the UL SINR and rate distributions as a function of the association rules considering UL power control design parameters. Results show that minimum path-loss association leads to identical load distribution across all cells which is also optimal in terms of rate, irrespective of power control parameters. When both UL and DL joint coverage must be maximized, the decoupled association is the optimal solution. It is beneficial because it reduces the QoS imbalance between both links.

### *B. Main Contributions*

This work significantly extends the prior art of decoupled association in [5], [12], [14] by proposing and investigating the concept of flexible cell association in Dual-Connectivity scenarios, where users are allowed to aggregate spectrum to boost the capacity. Given that decoupled associations have been proposed to improve the UL communications, this work is focused on analysing the improvements over this link. Dual-Connectivity improvements in the DL are therefore left out of scope of this study.

In a Dual-Connectivity scenario, we consider two uplink associations. The user will attach to the first and second best base stations, following UL received power policies. In such conditions, we evaluate if decoupled associations offer improvements with respect to traditional downlink received power association rules. Moreover, the feasibility of Dual-Connectivity in the UL is discussed, since device power limitations may impair the throughput performance. The main novelties presented in this paper can be summarized as:

- recognition of different user association cases considering Dual-Connectivity aggregated transmissions;
- stochastic geometry modelling of a two tier co-channel HetNet with flexible associations in a Dual-Connectivity context; and
- comprehensive mathematical analysis and derivation of the association probabilities and capacity performance metrics for Dual-Connectivity aggregated transmissions.

## II. Dual Connectivity Association System Model

Let us consider two independent and overlaid poisson point processes (PPP) $\Phi_s$ and $\Phi_m$: $\Phi_s$ with intensity $\lambda_s$ represents the number of SCells; likewise, $\Phi_m$ with intensity $\lambda_m$ represents

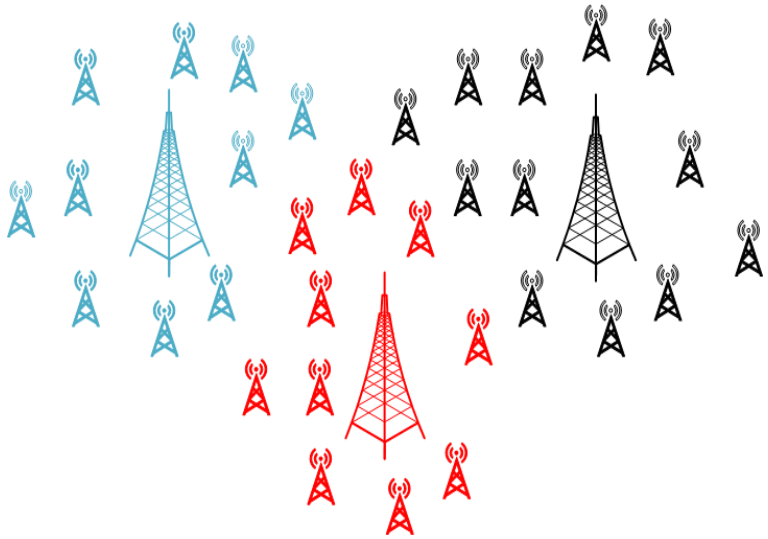

Fig. 1: Two tier PPP with three PCP

the number of MCells. Thus, $\Phi_v$ can be defined as $\Phi_v = \Phi_m + \Phi_s$.

This system model can be seen as a Poisson cluster process (PCP), which models the random patterns produced by random clusters. PCPs are constructed from a parent PPP $\Phi = \{x_i; i = 1, 2, 3, ...\}$ by replacing each point $x_i \in \Phi$ with a cluster of points $M_i$, $\forall$ $x_i \in \Phi$, where the points in $M_i$ are independently and identically distributed in the spatial domain [15]. Without loss of generality, in our system model each cluster is assumed to be composed by one MCell and several SCells, and signals coming from MCells belonging to other clusters are less dominant for association purposes. An example of the PCP used in this work is shown in figure 1.

Traditionally, users will associate in both UL and DL using the RSRP information, therefore attaching to the base station from which receives the strongest transmit power. Received signal in the DL can be expressed as:

$$E_h[S_v{}^{\mathrm{DL}}] = P_v \ \|X_v\|^{-\alpha} \tag{1}$$

where $E_h[S_v]$ is the average DL signal received power, $P_v$ is the transmit power of the cell, $\|X_v\|$ is the distance from the device to the cell, and $\alpha$ is the path-loss exponent. When allowing for decoupled associations, a more flexible policy is introduced, where the user is allowed to attach to the cell which receives the strongest signal from the user. The received signal power in the UL is expressed as:

$$E_h[S_v{}^{\mathrm{UL}}] \ = \ P_d \ \|X_v\|^{-\alpha} \tag{2}$$

where $P_d$ is the transmit power of the device, which follows the rules of the open loop power control (OLPC) mechanism defined in [16]. The user establishes an operation point using the open loop part, where it compensates the mean path loss and its slow variations; the user transmit power is expressed as:

$$P_d = P_0 L_x^{\gamma} \tag{3}$$

where $L_x$ corresponds to the distance dependent user path loss; $P_0$ and $\gamma$ are the OLPC parameters. For simplicity in the analysis, we are going to consider that all users transmit with the same power, and there is no path-loss compensation. Moreover, the network is viewed as a single snapshot in time for the purpose of characterizing its spatial statistics.

The mobile user locations are placed according to the homogeneous PPP $\Phi_d$, with intensity $\lambda_d$. Considering the uplink of LTE-A, intra-cell interference is null and so just inter-cell interferences are present. The interference model in this work largely follows the approach in [17]. Assuming a single dominant interference source per cell, the number of interfering devices equals to the number of cells; $\Phi_{I_d}$ is the point process denoting the locations of the interfering users. Following the analysis in [17], the net interference at a randomly chosen base station is the sum of powers from all transmitting mobiles lying farther than $X_v$, where $X_v$ is the random variable that describes the distance from the serving base station to the typical UE. This power will depend on the distance of the interfering UEs to its corresponding eNBs, which is described as $R_j$. Moreover, the system is considered to be interference limited.

A $\mathbb{R}^2$ space is considered, with a device centred in the origin, as shown in figure 2. This study focuses on the UL received power from both MCells and SCells, which depends on the distance distribution of the device towards the closest cell in the cluster located at a distance $x_1$ which follows the *Void Probability*; for our specific study this is expressed as:

$$P(|x_1| > r) = e^{-\lambda_v \pi r^2} \tag{4}$$

Therefore, the probability density and cumulative distribution functions can be expressed as:

$$f_{X_v}(x) = 2\pi\lambda_v x e^{-\pi\lambda_v x^2}, x \geq 0 \tag{5}$$

$$F_{X_v}(x) = 1 - e^{-\pi\lambda_v x^2}, x \geq 0 \tag{6}$$

For the Dual-Connectivity association probability a simplified scenario as the one shown in figure 3 is modelled following the assumptions explained earlier in this section. Connections

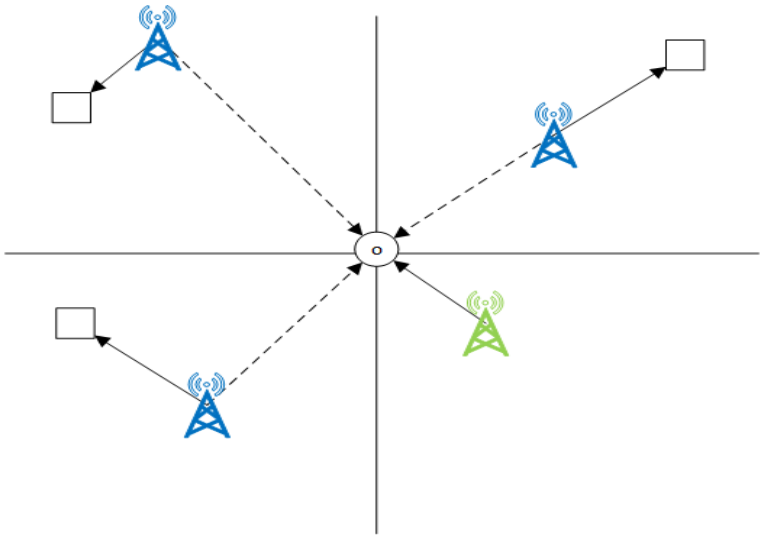

Fig. 2: Centred device receiving signal from closest cell and interference from the rest of the cells.

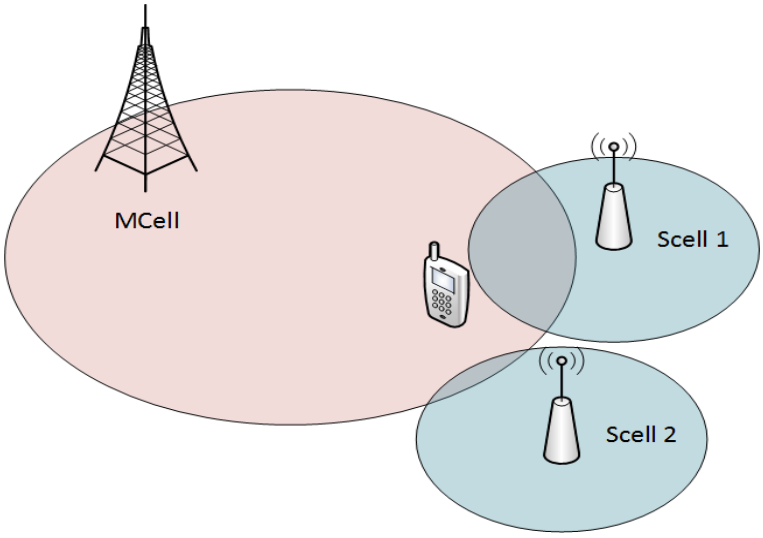


Fig. 3: Dual-Connectivity scenario

towards two cells are considered, and the cluster considered is formed of three cells: one MCell and two SCells. The distance distribution from a device situated in the origin is given by:

$$\text{MCell} : f_{X_m} = 2\pi\lambda_m x_m e^{-\pi\lambda_m x_m^2} \tag{7}$$

$$\text{SCell}_1 : f_{X_1} = 2\pi\lambda_s x_{S_1} e^{-\pi\lambda_s x_{S_1}^2} \tag{8}$$

$$\text{SCell}_2 : f_{X_2} = 2\pi\lambda_s x_{S_2} e^{-\pi\lambda_s x_{S_2}^2} \tag{9}$$

Table I summarises the notation used for the variables and functions across the study.

| Notation | Definition |
|---|---|
| P(A) | Probability of event A |
| UL | Uplink connection |
| DL | Downlink connection |
| $f_x(x)$ | pdf of random variable x |
| $F_x(x)$ | cdf of random variable x |
| $F_{x_{\min}}(x_1, x_2)$ | cdf minimum random variables'S $x_1$ & $x_2$ |
| Lx (f(x)) | Laplace transform f(x) |
| $\Phi_{\lambda,n}$ | PPP in dimension n and intensity $\lambda$ |
| $\lambda_m$ | Intensity PPP MCells |
| $\lambda_s$ | Intensity PPP SCells |
| $\lambda_d$ | Intensity PPP users |
| $\|X_m\|$ | Random variable distance from the device to the MCell |
| $\|X_1\|$ | Random variable distance from the device to the SCell 1 in DC |
| $\|X_2\|$ | Random variable distance from the device to the SCell 2 in DC |
| $P_s$ | Small Cell transmit power |
| $P_m$ | Macro Cell transmit power |
| $P_d$ | Device transmit power |
| $\gamma$ | OLPC Path loss compensation factor |
| $P_0$ | OLPC Device transmit power |
| $\alpha$ | Path loss exponent |
| $h$ | Channel fading |
| $B$ | System bandwidth |
| $N_a$ | Cell load |
| $\text{f(x)}_{\text{\|DUDe}}$ | pdf conditioned decoupling case |
| $\sigma^2$ | Noise power |

TABLE I: Notation

## III. Association Probability based on Decoupled Access

The aim of this study is to calculate the probability of decoupled events while having simultaneous UL and DL connections towards two cells in the cluster. As explained in [5], there are some decoupled association combinations which are not possible following the assumptions of this study, in particular all those combinations where the DL is connected to a SCell and the UL to a MCell, since there is no probability region that covers this event. Also, users will decouple a maximum of one link, since one MCell is considered per cluster.

Considering the above assumptions, there are eight association possibilities for the three cells in the cluster. As the two SCells density functions (pdf) are similar, association possibilities are reduced to four cases using symmetry, which are divided into 8 subcases, a summary of the associations considered is shown in table II. The mathematical derivation for the association probability is explained in the following sections.

| Case | Subcase | UL 1st Connection | DL 1st Connection | UL 2nd Connection | DL 2nd Connection |
|---|---|---|---|---|---|
| 1 | 1.1 | MCell | MCell | SCell 1 | SCell 1 |
| | 1.2 | MCell | MCell | SCell 2 | SCell 2 |
| 2 | 2.1 | SCell 1 | SCell 1 | MCell | MCell |
| | 2.2 | SCell 2 | SCell 2 | MCell | MCell |
| 3 | 3.1 | SCell 1 | SCell 1 | SCell 2 | MCell |
| | 3.2 | SCell 2 | SCell 2 | SCell 1 | MCell |
| 4 | 4.1 | SCell 1 | SCell 1 | SCell 2 | SCell 2 |
| | 4.2 | SCell 2 | SCell 2 | SCell 1 | SCell 1 |

TABLE II: Probability regions in a Best Association Dual connectivity scenario

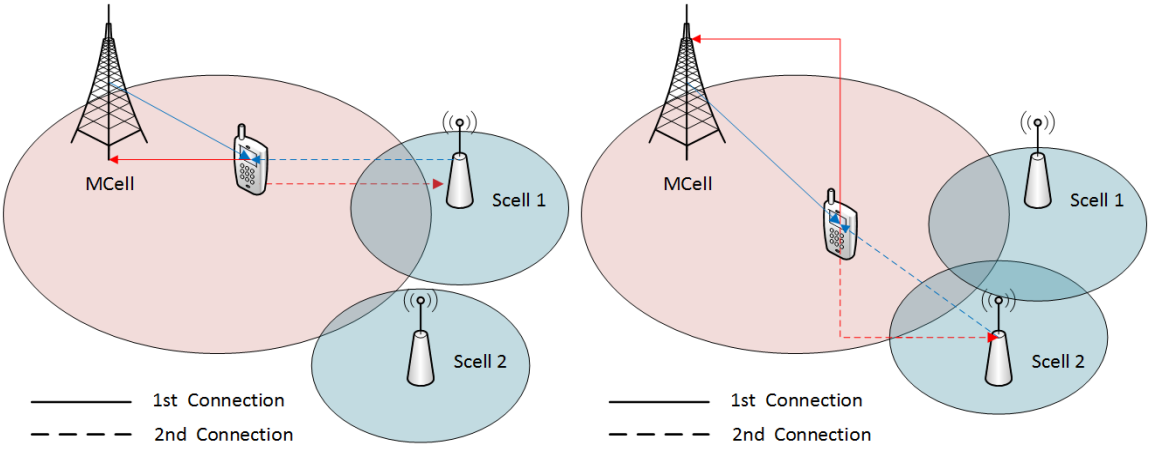


(a) Association Sub-case 1.1 (b) Association Sub-case 1.2

Fig. 4: Association Case 1

### A. *Case 1: Connection with MCell and SCell in UL and DL*

This case considers the probability region where the first connection is towards the MCell and the second one with either of the SCells in both UL and DL. Figure 4 shows a graphical representation of this association case.

This leads to the following conditions for sub-cases 1.1 and 1.2 respectively:

$$\begin{aligned} &\text{UL} : P_d \left\|x_m\right\|^{-\alpha} > P_d \left\|x_1\right\|^{-\alpha} > P_d \left\|x_2\right\|^{-\alpha} \\ &\text{DL} : P_m \left\|x_m\right\|^{-\alpha} > \ P_s \left\|x_1\right\|^{-\alpha} > \ P_s \left\|x_2\right\|^{-\alpha} \end{aligned} \quad ; \ \left\|x_m\right\|^{-\alpha} > \left\|x_1\right\|^{-\alpha} > \left\|x_2\right\|^{-\alpha} \tag{10}$$

$$\begin{aligned} &\text{UL} : P_d \left\|x_m\right\|^{-\alpha} > P_d \left\|x_2\right\|^{-\alpha} > P_d \left\|x_1\right\|^{-\alpha} \\ &\text{DL} : P_m \left\|x_m\right\|^{-\alpha} > \ P_s \left\|x_2\right\|^{-\alpha} > \ P_s \left\|x_1\right\|^{-\alpha} \end{aligned} \quad ; \ \left\|x_m\right\|^{-\alpha} > \left\|x_2\right\|^{-\alpha} > \left\|x_1\right\|^{-\alpha} \tag{11}$$

In both situations the UL condition is more restrictive, therefore the events of this association

case can be reduced to:

$$\|x_m\|^{-\alpha} > (\|x_1\|^{-\alpha}, \|x_2\|^{-\alpha}) = \|x_m\| < (\|x_1\|, \|x_2\|) \tag{12}$$

which means that $\|x_m\|$ needs to be smaller than both $\|x_1\|$ and $\|x_2\|$, which means it needs to be smaller than $\min(x_1, x_2)$. Hence, the probability of Case 1 can be calculated as:

$$P_{\text{Case 1}} \;=\; P(\|X_m\| < \min(x_1, x_2)) = \int_0^{+\infty} (1 - F_{\min(X_1,X_2)}(x_m)) \cdot f_{Xm}(x_m)\ \mathrm{d}x_m \tag{13}$$

The cdf of $\min(x_1, x_2)$ can be calculated using order statistics, and is given by:

$$F_{\min(X1,X2)} = 1 - ((1 - F_{x1})(1 - F_{x2})) \tag{14}$$

As $F_{x1}\ (x_m)$ = $F_{x2}\ (x_m)$, the expression (14) can be written as:

$$F_{\min(X_1,X_2)} = 1 - (1 - F_{x_1})^2 = 1 - e^{-2\pi\lambda_s x_m^2} \tag{15}$$

Finally, with (7) , (13) and (15), the probability of being in Case 1 can be simplified to the following expression:

$$P_{\text{Case 1}} \;= \int_0^{+\infty} e^{-2\pi\lambda_s x_m^2} \cdot 2\pi\lambda_m x_m e^{-\pi\lambda_m x_m^2}\ \mathrm{d}x_m = \frac{\lambda_m}{2\lambda_s + \lambda_m} \tag{16}$$

### *B. Case 2 : Connection with SCell and MCell for UL and DL*

In Case 2, the connections performed by the device are the same than in Case 1, but in a different order. The user will attach first to the SCell and then to the MCell, for both UL and DL. Figure 5 shows a graphical representation of this association case.

The events of this case can be expressed as:

$$\begin{array}{l} \text{UL} : P_d \|x_1\|^{-\alpha} > P_d \|x_m\|^{-\alpha} > P_d \|x_2\|^{-\alpha} \\ \text{DL} : P_s \|x_1\|^{-\alpha} > \ P_m \|x_m\|^{-\alpha} > \ P_s \|x_2\|^{-\alpha} \end{array} \;;\; \|x_1\|^{-\alpha} > \|x_m\|^{-\alpha} > \|x_2\|^{-\alpha} \tag{17}$$

$$\begin{array}{l} \text{UL} : P_d \|x_2\|^{-\alpha} > P_d \|x_m\|^{-\alpha} > P_d \|x_1\|^{-\alpha} \\ \text{DL} : P_s \|x_2\|^{-\alpha} > \ P_m \|x_m\|^{-\alpha} > \ P_s \|x_1\|^{-\alpha} \end{array} \;;\; \|x_2\|^{-\alpha} > \|x_m\|^{-\alpha} > \|x_1\|^{-\alpha} \tag{18}$$

Similarly to Case 1, the uplink condition is most restrictive. The difference between Case 2.1 (17) and Case 2.2 (18) is the SCell to which the device performs its first connection. As the two distance probabilities distributions are similar, equation (8) the probability of both sub-cases will be the same. Thus, the probability of Case 2 is twice the probability expressed

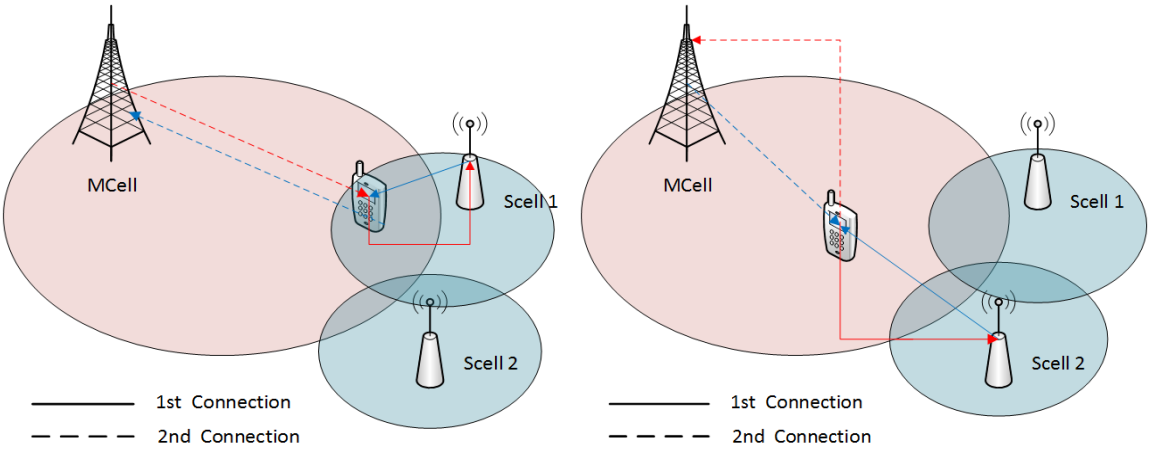


(a) Association Sub-case 2.1 (b) Association Sub-case 2.2

Fig. 5: Association Case 2

in equation (18):

$$P(\|x_1\|^{-\alpha} > \|x_m\|^{-\alpha} > \|x_2\|^{-\alpha}) = P(\|x_1\| < \|x_m\| < \|x_2\|) = \int_0^{+\infty} \int_{x_1}^{+\infty} \int_{x_m}^{+\infty} f_{X_m}(x_m) \cdot f_{X_1}(x_1) \cdot f_{X_2}(x_2) \cdot \mathrm{d}x_2 \cdot \mathrm{d}x_m \cdot \mathrm{d}x_1 \tag{19}$$

Finally, the probability for the device to be in Case 2.1 can be simplified to:

$$P(\text{Case 2.1}) = \frac{\lambda_m \lambda_s}{(\lambda_m + \lambda_s)(\lambda_m + 2\lambda_s)} \tag{20}$$

Since the probability of Case 2 is twice the probability of sub-case 2.1, the final association probability of Case 2 is:

$$P(\text{Case 2}) = \frac{2\lambda_m \lambda_s}{(\lambda_m + \lambda_s)(\lambda_m + 2\lambda_s)} \tag{21}$$

### *C. Case 3 : UL and DL connection to SCell, DL with MCell and UL with the other SCell*

This association case is the one that considers the decoupling event. The device is close to one SCell and the first association is done towards it. However, when choosing the second serving cell, the UE receives higher power from the MCell and the UL received power is better towards the second SCell of the cluster; hence, the user will decouple its second connection. Figure 6 shows a graphical representation of this association case.

For the derivations it is considered that the closest cell is SCell 1. However, by symmetry the association probability remains equal if the closest one is SCell 2, as long as the situation

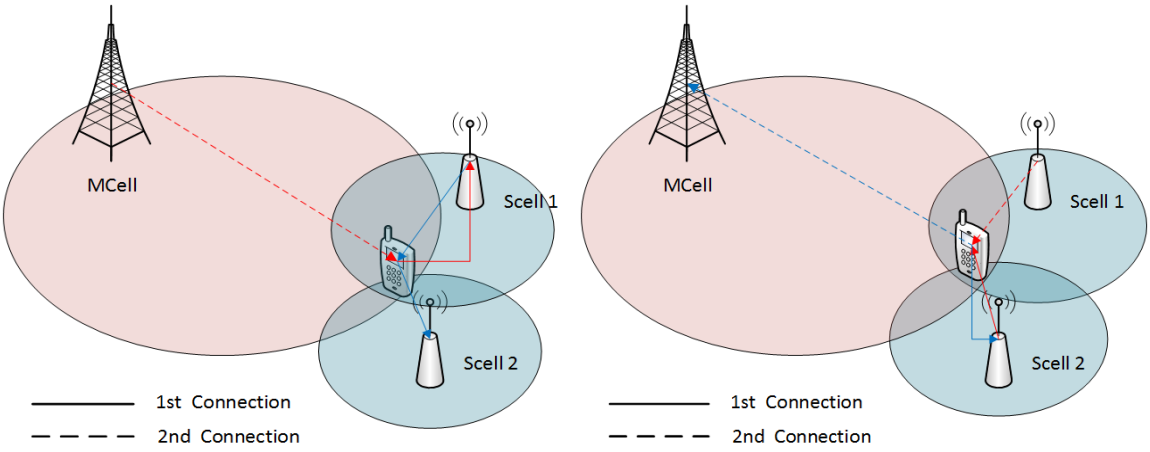


(a) Association Sub-case 3.1 (b) Association Sub-case 3.2

Fig. 6: Association Case 3

of all the other cells is the same as the one described before. This is mathematically expressed as:

$$\begin{aligned} &\text{UL}: P_d \|x_1\|^{-\alpha} > P_d \|x_2\|^{-\alpha} > P_d \|x_m\|^{-\alpha} \\ &\text{DL}: P_s \|x_1\|^{-\alpha} > P_m \|x_m\|^{-\alpha} > P_s \|x_2\|^{-\alpha} \end{aligned} \; ; \; \|x_1\|^{-\alpha} > \frac{P_m}{P_s}\|x_m\|^{-\alpha} > \|x_2\|^{-\alpha} > \|x_m\|^{-\alpha} \tag{22}$$

This probability, $P(\|x_1\|^{-\alpha} > \frac{P_m}{P_s}\|x_m\|^{-\alpha} > \|x_2\|^{-\alpha} > \|x_m\|^{-\alpha})$ or what is the same $P(\|x_1\| < \frac{P_s}{P_m}\|x_m\| < \|x_2\| < \|x_m\|)$ can be seen as the intersection of events: $\|x_1\|$ is the minimum value among the three cells and also $\|x_2\|$ needs to be between $\frac{P_s}{P_m}\|x_m\|$ and $\|x_m\|$):

$$P(\|x_1\| < \min(\|x_2\|, \|x_m\|)) \cap P(\frac{P_s}{P_m}\|x_m\| < \|x_2\| < \|x_m\|) \tag{23}$$

Since these two events are independent, the intersection of both is the multiplication of the probabilities of these events to happen:

$$P(\|x_1\| < \min(\|x_2\|, \|x_m\|)) \cdot P(\frac{P_s}{P_m}\|x_m\| < \|x_2\| < \|x_m\|) \tag{24}$$

The first probability can be calculated similarly to equation (14):

$$P(1) = P(\|X_m\| < \min(\|x_2\|, \|x_m\|)) = \int_0^{+\infty} (1 - F_{\min(X_2, Xm)}(x_1)) \cdot f_{X_1}(x_1)\, \mathrm{d}x_1 \tag{25}$$

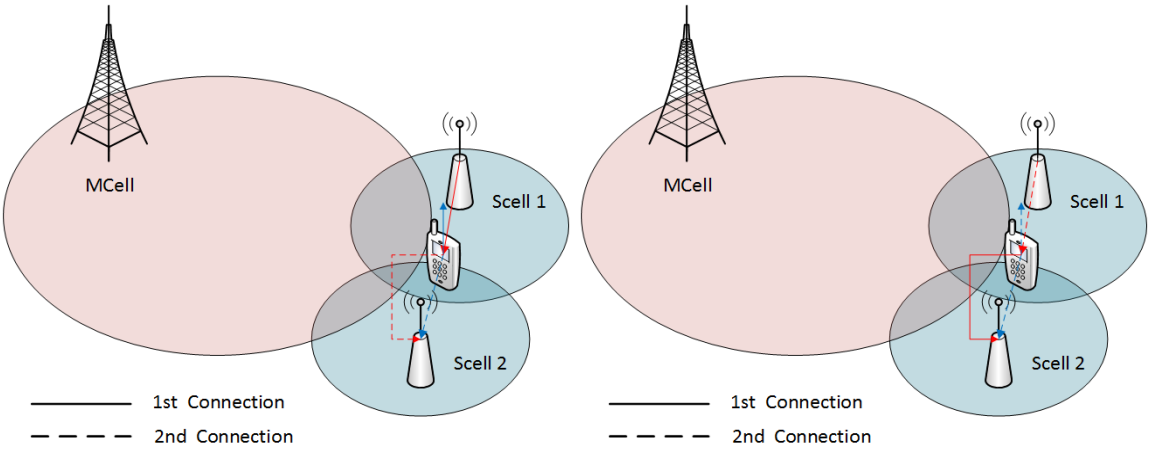


(a) Association Sub-case 3.1 (b) Association Sub-case 3.2

Fig. 7: Association Case 4

The second probability, $P(\frac{P_s}{P_m}\|x_m\| < \|x_2\| < \|x_m\|)$ can be calculated as:

$$P(\frac{P_s}{P_m}\|X_m\| < \|X_2\| < \|X_m\|) = \int_0^{+\infty}\int_0^{x_m} f_{x_m}(x_m)\cdot f_{x_2}(x_2)\cdot \mathrm{d}x_2\mathrm{d}x_m = \tag{26}$$
$$\int_0^{+\infty} 2\pi\lambda_m x_m e^{-\lambda_m\pi x_m^2}\, dx_m \cdot \int_{\frac{P_s}{P_m}X_m}^{X_m} 2\pi\lambda_m x_m e^{-\lambda_m\pi x_m^2}\, dx_2 =$$
$$\int_0^{+\infty} 2\pi\lambda_m x_m e^{-\lambda_m\pi x_m^2}\cdot (e^{\lambda_s\frac{P_s}{P_m}\pi x^2} - e^{\lambda_s\pi x^2})\,\mathrm{d}x_m = \frac{\lambda_m}{\lambda_m+\lambda_s\frac{P_s}{P_m}} - \frac{\lambda_m}{\lambda_m+\lambda_s}$$

Thus, with (22), (24), (25) and (26), the probability for the device to be in Case 3 is:

$$P(\text{Case 3}) = 2P(1)(\frac{\lambda_m}{\lambda_m+\lambda_s\frac{P_s}{P_m}} - \frac{\lambda_m}{\lambda_m+\lambda_s}) \tag{27}$$

### *D. Case 4 : Connection to both SCells both UL and DL*

In this last case, the user associates to both SCells of the cluster. Figure 7 shows a graphical representation of this association case.

The events that satisfy this are expressed as:

$$\begin{aligned}&\text{UL}: P_d\,\|x_1\|^{-\alpha} > P_d\,\|x_2\|^{-\alpha} > P_d\,\|x_m\|^{-\alpha}\\ &\text{DL}: P_s\,\|x_1\|^{-\alpha} > P_s\,\|x_2\|^{-\alpha} > P_m\,\|x_m\|^{-\alpha}\end{aligned} \;;\; \|x_1\|^{-\alpha} > \|x_2\|^{-\alpha} > \frac{P_m}{P_s}\|x_m\|^{-\alpha} \tag{28}$$

$$\begin{aligned}&\text{UL}: P_d\,\|x_2\|^{-\alpha} > P_d\,\|x_m\|^{-\alpha} > P_d\,\|x_1\|^{-\alpha}\\ &\text{DL}: P_s\,\|x_2\|^{-\alpha} > P_m\,\|x_m\|^{-\alpha} > P_s\,\|x_1\|^{-\alpha}\end{aligned} \;;\; \|x_2\|^{-\alpha} > \|x_1\|^{-\alpha} > \frac{P_m}{P_s}\|x_m\|^{-\alpha} \tag{29}$$

In this case the downlink condition is the restrictive one; and similarly to Case 2 derivation,

the two sub-cases probabilities are the same due to the similarity of the pdf of the SCells. Therefore,

$$P(\|x_1\|^{-\alpha} > \|x_2\|^{-\alpha} > \frac{P_s}{P_m}\|x_m\|^{-\alpha}) = P(\|x_1\| < \|x_2\| < \frac{P_s}{P_m}\|x_m\|) = \tag{30}$$
$$P(\|x_1\| < \|x_2\| < \|x_m\|) \cap P(\|x_2\| < \frac{P_s}{P_m}\|x_m\|) =$$
$$P(\|x_1\| < \|x_2\| < \|x_m\|)P(\|x_2\| < \frac{P_s}{P_m}\|x_m\|). \text{ (Due to independence of events)}$$

The first probability is calculated, as in equations (13) and (25):

$$P(2) = P(\|x_1\| < \|x_2\| < \|x_m\|) = P(\|x_1\| < \min(x_2, x_m)) \tag{31}$$

The second probability can be derived as:

$$P(\|x_2\| < \frac{P_s}{P_m}\|x_m\|) = \int_0^{+\infty} \int_{\frac{P_m}{P_s}}^{+\infty} f_{xm}(x_m) \cdot f_{x_2}(x_2) \cdot dx_2 dx_m = \tag{32}$$
$$\int_0^{+\infty} \int_{\frac{P_m}{P_s}}^{+\infty} 2\pi\lambda_m x_m e^{-\pi\lambda_m x_m^2} \cdot 2\pi\lambda_s x_2 e^{-\pi\lambda_s x_2^2} \cdot \mathrm{d}x_m \mathrm{d}x_2 =$$
$$\int_0^{+\infty} 2\pi\lambda_s x_2 e^{-(\pi\lambda_s + \pi\lambda_s(\frac{P_m}{P_s})^2)x^2} \cdot \mathrm{d}x_2 = \frac{\lambda_s}{\lambda_s + \frac{P_m}{P_S}\lambda_m}$$

Finally, the probability for the device to be in Case 4 is simplified to:

$$P(\text{Case 4}) = 2P(2)\frac{\lambda_s}{\lambda_s + \frac{P_m}{P_S}\lambda_m} \tag{33}$$

## IV. Uplink Capacity Derivation

Following the analysis detailed in the previous section, in a Dual-Connectivity scenario a user will attach to two cells in the cluster following the cases remarked in table II. However, since this study is focused on studying the benefits of flexible user association schemes, the capacity expressions are derived specifically for Case 3, the decoupling case. To evaluate the gains of allowing this level of flexibility, the capacity of the decoupled link is compared to that of an association based on the downlink received power policy, where the UL is transmitted to the MCell, instead of the SCell.

To calculate the link capacity it is first necessary to derive the distance distribution to the serving cell. In this particular case of Dual-Connectivity the conditioned density function is different to that of a single association case, since the probability region to which is

conditioned depends on the probability region of three different cells. This is expressed as:

$$Fx_{|\text{DUDe}} = P(X_1 > x|\frac{P_s}{P_m}x_s^{-\alpha} < x_m^{-\alpha} < x_s^{-\alpha}) = \tag{34}$$
$$\int_x^{+\infty}(\frac{\lambda_m e^{-(\frac{P_s}{P_m}\lambda_s\pi+\lambda_m\pi)x^2}}{\lambda_m+\frac{P_s}{P_m}\lambda_s} - \frac{\lambda_m e^{-(\lambda_s\pi+\lambda_m\pi)x^2}}{\lambda_m+\lambda_s})fx(x)\underbrace{\frac{1}{\text{P. Case 3.1}}}\ \mathrm{d}x$$

Operating the above expression and differentiating the cdf, the pdf of the distance to the serving cell conditioned to the events on Case 3.1 can be calculated as:

$$fx_{s|\text{DUDe}}(x) = (\frac{\lambda_m e^{-(\frac{P_s}{P_m}\lambda_s\pi+\lambda_m\pi)x^2}}{\lambda_m+\frac{P_s}{P_m}\lambda_s} - \frac{\lambda_m e^{-(\lambda_s\pi+\lambda_m\pi)x^2}}{\lambda_m+\lambda_s})2\pi\lambda_s x e^{-\pi\lambda_s x^2} \tag{35}$$

Similarly, for the sub-optimal association case the pdf of the distance to the serving cell, in this case being the MCell, is expressed as:

$$fx_{s|\text{DRP}}(x) = (\frac{\lambda_m e^{-(\frac{P_s}{P_m}\lambda_s\pi+\lambda_m\pi)x^2}}{\lambda_m+\frac{P_s}{P_m}\lambda_s} - \frac{\lambda_m e^{-(\lambda_s\pi+\lambda_m\pi)x^2}}{\lambda_m+\lambda_s})2\pi\lambda_m x e^{-\pi\lambda_m x^2} \tag{36}$$

The UL capacity is derived following the Shannon formula, and the user transmit bandwidth is estimated by approximating the cell load. Therefore, the user UL throughput is dependent on $B$, the carrier bandwidth and $N_a$, which corresponds to the average number of associated users, which follows the approximation derived in [18]:

$$N_a = 1 + \frac{1.28\lambda_d P_{av}}{\lambda_{av}}, \tag{37}$$

where $P_{av}$ is the probability of associating to the cell of interest (Case 2 and 4 for the decoupling load balancing and Case 1 in the sub-optimal association case) and $\lambda_{av}$ corresponds to the intensity of the cell of interest ($\lambda_s$ for the decoupled association and $\lambda_m$ sub-optimal one).

The UL signal received in cell $v$ expressed as:

$$S_v = P_d \cdot h_v \cdot \|X_v\|^{-\alpha} \tag{38}$$

And the PPP of the UL interference perceived from all the other users in the scenario is expressed as:

$$\Phi_{I_d} = \sum_{i=1}^{n} P_d/2 \cdot h_i \cdot \|R_j\|^{-\alpha} \tag{39}$$

Finally, the Signal to Noise and Interference ratio (SINR) is given by:

$$\text{SINR}_{\text{UL}} = \frac{P_d/2 \cdot h_v \cdot \|X_v\|^{-\alpha}}{\sum_{i=1}^{n} P_d/2 \cdot h_i \cdot \|X_i\|^{-\alpha} + \sigma^2} \tag{40}$$

where $\sigma^2$ is the thermal noise power and the interference is modelled following the assumptions defined in section II. The UL throughput can be defined as:

$$C_{UL} = E[(\frac{B}{N_a}) \log_2(1 + \text{SINR}_{\text{UL}})] = (\frac{B}{N_a}) \frac{1}{\ln(2)} \int_0^{+\infty} P(\text{SINR}^{\text{UL}} > e^t - 1)\text{d}t = \tag{41}$$
$$(\frac{B}{N_a}) \frac{1}{\ln(2)} \int_0^{+\infty} P(h_v > \frac{(e^t - 1)x_v^{\alpha}(I_x + \sigma^2)}{P_d/2})\text{d}t$$

Since the distance distribution to both SCells in the cluster is the same, the capacity towards each SCell is also considered to be equal. Also, the total throughput of one user is considered to be the aggregation of each link, so the approach is to calculate each link independently following the same procedure as in [19]. Taking equation (35), the UL throughput of the first connection is derived as:

$$C_{SCell} = \frac{B}{1 + \frac{1.28 \cdot \lambda_d \cdot P_{av}}{\lambda_{av}}} \cdot \frac{\log_2(e)}{\text{P(Case3)}} \int_0^{+\infty} \int_0^{+\infty} e^{-\pi \lambda_{I_d} (e^t - 1)^{\frac{2}{\alpha}} x^2} \int_0^{+\infty} \left( \frac{1}{1 + v^{\frac{\alpha}{2}}} \right) \text{d}v \tag{42}$$
$$(\frac{\lambda_m e^{-(\frac{P_s}{P_m}\lambda_s \pi + \lambda_m \pi)x^2}}{\lambda_m + \frac{P_s}{P_m}\lambda_s} - \frac{\lambda_m e^{-(\lambda_s \pi + \lambda_m \pi)x^2}}{\lambda_m + \lambda_s}) 2\pi \lambda_s x e^{-\pi \lambda_s x^2} \cdot \text{d}t \cdot \text{d}x$$

The total aggregate interference is calculated using the Laplace transform following the assumptions in section II and the approach in [17], but assuming that all interfering users are transmitting in Dual-Connectivity. The reader is referred to [17] for further proof of the interference derivation. The final expression of the interference component is:

$$I_x = e^{-\pi \lambda_{I_d} (e^t - 1)^{\frac{-2}{\alpha}} x_v^2 \int_0^{+\infty} \frac{1}{1 + v^{\frac{1}{2}}} \text{d}v} \tag{43}$$

Note that the dependencies with the OLPC parameter $\gamma$ have been neglected, since this study considers no fractional path-loss compensation.

Following the same procedure and using the sub-optimal distance distribution derived in

(36), the capacity of the sub-optimal associated link is:

$$C_{\text{MCell}} = \frac{B}{1+\frac{1.28\cdot\lambda_d\cdot P_{av}}{\lambda_{av}}} \cdot \frac{\log_2(e)}{\text{P(Case2)}} \int_0^{+\infty} \int_0^{+\infty} e^{-\pi\lambda_{I_d}(e^t-1)^{\frac{2}{\alpha}}x^2} \int_0^{+\infty} \left(\frac{1}{1+v^{\frac{\alpha}{2}}}\right) \mathrm{d}v \tag{44}$$
$$\left(\frac{\lambda_m e^{-(\frac{P_s}{P_m}\lambda_s\pi+\lambda_m\pi)x^2}}{\lambda_m+\frac{P_s}{P_m}\lambda_s} - \frac{\lambda_m e^{-(\lambda_s\pi+\lambda_m\pi)x^2}}{\lambda_m+\lambda_s}\right) 2\pi\lambda_m x e^{-\pi\lambda_m x^2} \cdot \mathrm{d}t \cdot \mathrm{d}x$$

## V. Performance evaluation

The performance of decoupled associations in Dual-Connectivity is evaluated by representing the metrics mathematically derived in the previous sections, and comparing them to different baselines. The first baseline is the non-decoupled association, when the user is not allowed to split the UL towards the SCell and therefore, while being in a region suitable for splitting the UL, the user will attach to the MCell, as in traditional user association schemes. In this baseline it is considered that the user has still the SCell primary connection. The second baseline is the decoupled association for a single cell scheme. In this case, the user is allowed to decouple, however it does not aggregate bandwidth, and one single connection is considered. This scenario is interesting to assess the gains of Dual-Connectivity, even in power limited cases. Finally, the last baseline is the use of Carrier Aggregation with no decoupled connections. In this case the user is aggregating spectrum from the same cell, in this case the comparison is done with respect to the MCell.

First, the association probability is evaluated. Figure 8 shows the probability of the cases shown in table II. Since the probability of each sub-case is equal, the joint case probability is represented. Case 3 is the one that represents the events of having decoupled associations, and in Dual-Connectivity the probability of this event happening is certainly not to be neglected. As the SCell density increases, decoupled associations are 10% more probable than MCell associations (Cases 1 and 2), and nearly 30% more probable than SCell coupled associations (Case 3). However, as the SCell density further increases and reaches 12 SCells per MCell, there is a higher probability of having both UL and DL connected to the SCell. In this case, decoupled association probabilities are still much higher than MCell associations.

Since the association regions depend largely on the user distance to the serving cell, comparing the association probabilities in Dual-Connectivity with the Carrier Aggregation baseline will be exactly the same as comparing it with the association of single carrier with one cell. In Dual-Connectivity the number of association possibilities increases when compared to a single cell attachment, the probability region is more spread.

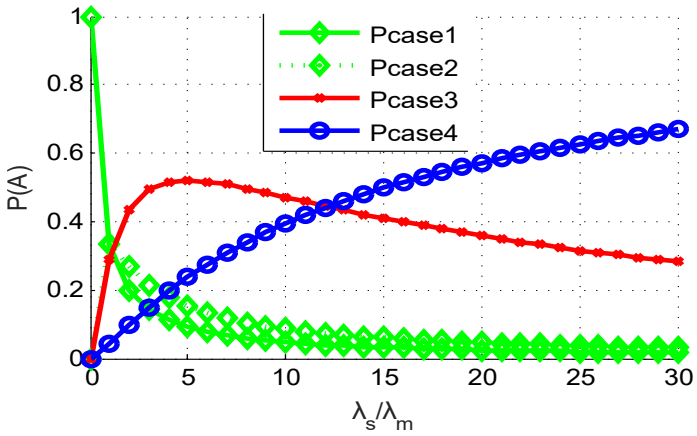


Fig. 8: Association probability for Dual-Connectivity association $P_m$ = 46 dBm, $P_s$ = 23 dBm, $\alpha = 3$, $\lambda_m = 1$.

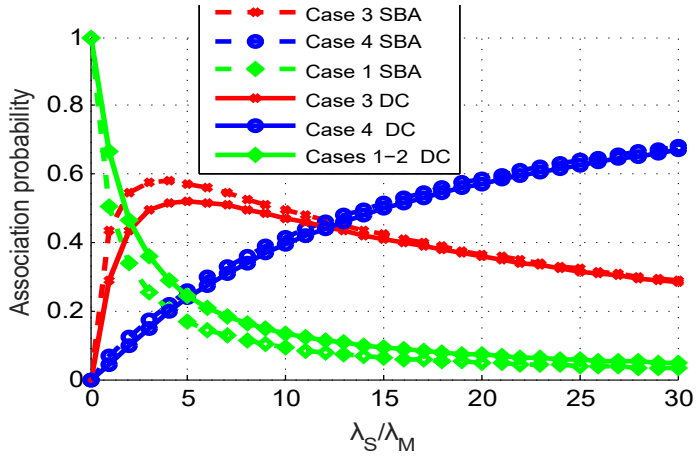


Fig. 9: Association probabilities of decoupled Dual-Connectivity vs Single Connectivity. $P_m$ = 46 dBm, $P_s$ = 23 dBm, $\alpha = 3$, $\lambda_m = 1$.

UL throughput gains depend largely on the distance distribution to the serving cell, shown in figure 10, where it is compared to that of a single cell for both association policies, the decoupled and the DL received power. In this case, the distance distribution represented is conditioned to the decoupling case, which correspond to equations (35) and (36) in the analysis. If multi-connectivity is considered by having a cluster with more than one SCell suitable for association, the distance distribution to the MCell is much more flattened. As well, this difference in distance distributions is also due to the fact that the user is considered to have as a first association option one SCell, and the second association is the decoupled one, as explained in section III-C, which forces the user to be close to the SCell.

The major advantage of Dual-Connectivity is the capacity increase that the user is entitled

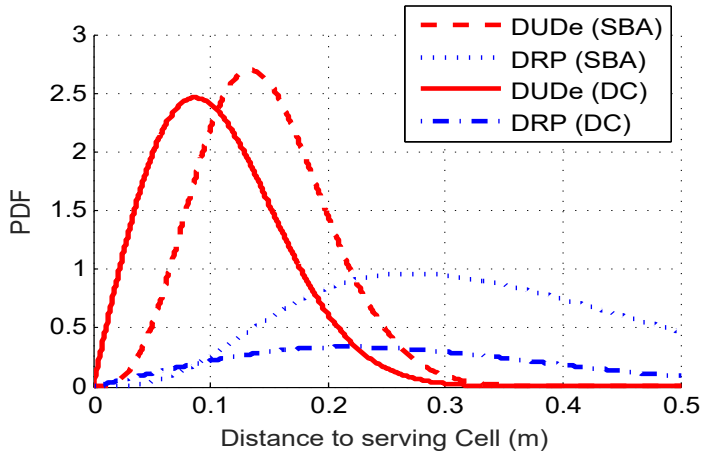


Fig. 10: Conditioned distance distribution to serving cell, $P_m$ = 46 dBm, $P_s$ = 23 dBm, $\alpha = 3$, $\lambda_m = 1$.

to. Figure 11 shows the UL throughput for one user, and it compares the decoupled association with respect to the sub-optimal association towards the MCell. In particular, figure 11(a) focuses on the capacity of the decoupled link, while figure 11(b) shows the aggregated throughput considering both connections. It is clear that changing the association policy in the UL and allowing to decouple its second connection towards the SCell, allows to boost capacity and to further improve the gains of Dual-Connectivity.

It is interesting to highlight the saturation point of the UL throughput in the sub-optimal case, shown in figure 11(a). Since the capacity of this case is conditioned to the probability of Case 3, that as well depends on the SCell density, there is a shy increase of throughput with the SCell density that quickly saturates. However, if the aggregated spectrum is compared, this saturation point is not as easily reached since the user is connected to a SCell, whose distance distribution narrows as the SCell density increases. This is well reflected in figure 12, where the percentage of gain of decoupled associations is represented. Two things are interesting to highlight in this graph: the first is that the gain continues to increase as the number of SCells density increases, which is simply due to the narrower distance distribution; the second is that the gain has a minimum, which is close to $\lambda_s/\lambda_m = 7$, which coincides with the change of slope in the capacity for the sub-optimal case in figure 11(b).

Finally, Dual-Connectivity is compared to a single connectivity. Figure 13 shows the comparison of the UL throughput of Dual-Connectivity, with respect to a decoupled association towards one single cell. In particular, figure 13(a) justifies the gain of Dual-Connectivity, since no spectrum aggregation is considered for the single best association case; it is shown

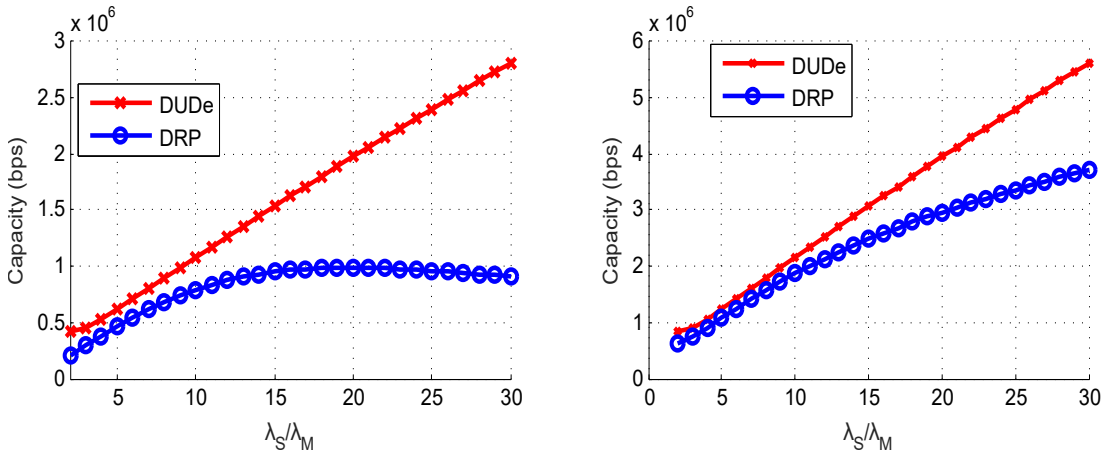


(a) UL Capacity for decoupled link

(b) UL Capacity for aggregated bandwidth

Fig. 11: UL Capacity: decoupled association versus sub-optimal associations, $P_m$ = 46 dBm, $P_s$ = 23 dBm, $\alpha = 4$, $\lambda_m = 1$

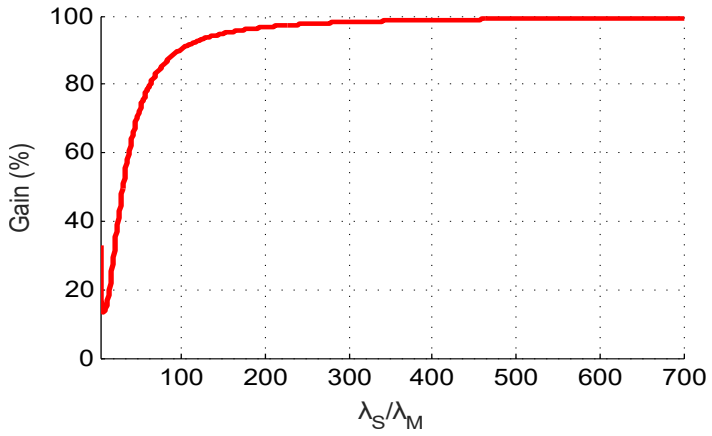


Fig. 12: UL Capacity gain for aggregated bandwidth, $P_m$ = 46 dBm, $P_s$ = 23 dBm, $\alpha = 3$, $\lambda_m = 1$.

that even though the user is forced to divide its transmit power between two cells, the result is a high throughput gain. Moreover, figure 13(b) compares two spectrum aggregation cases, being the baseline a Carrier Aggregation towards the MCell. It is seen that if the user aggregates spectrum in Carrier Aggregation towards a sub-optimal cell, the gain in capacity is going to be impaired, mainly due to the distance towards the serving cell. On the contrary, if decoupled associations are allowed, users can access to a more flexible aggregation of spectrum, which allows to maximize the UL capacity.

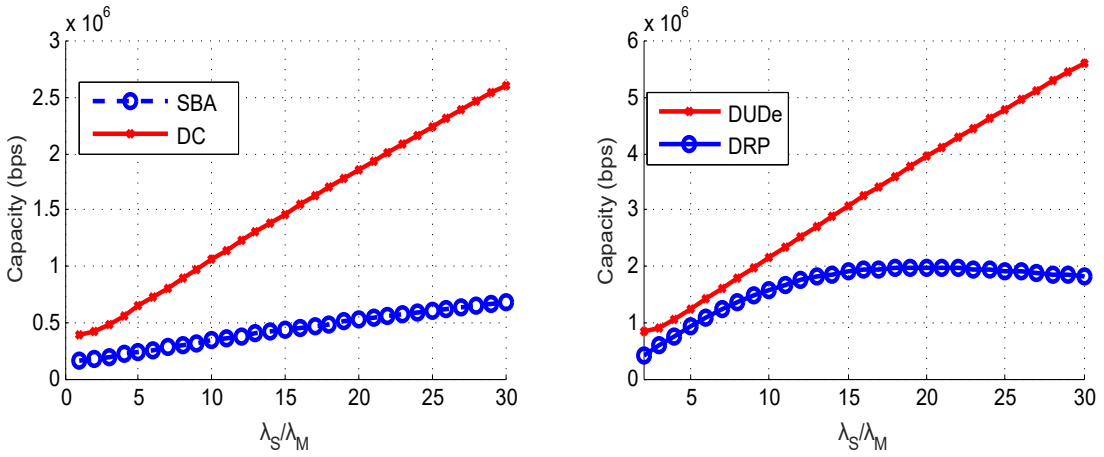


(a) UL Capacity for decoupled link: aggregation gain (b) UL Capacity for decoupled link: decoupling gain

Fig. 13: UL Capacity: comparison of single connectivity and Dual-Connectivity, $P_m$ = 46 dBm, $P_s$ = 23 dBm, $\alpha = 4$, $\lambda_m = 1$.

## VI. Conclusions

This work has studied the advantages of allowing decoupled associations in Dual-Connectivity scenarios, where the users are allowed to simultaneously consume radio resources from two cells. With the aim of improving the user throughput as well as the overall connectivity experience, it is proposed that the user decouples the UL connection and introduce UL specific association rules in the context of multi-connectivity in HetNets. This allows the user to experience maximum flexibility when deciding which cells to aggregate spectrum from. The system has been modelled using stochastic geometry and a poisson cluster process of two SCells and one MCell has been considered; it has been recognised that the probability of the decoupled events is certainly high. Overall, the main conclusions of this work can be summarised as:

1) Dual-Connectivity scenarios have a total of 8 sub-cases of association regions, that can be generally reduced to four, one of them being the decoupled association case. We have comprehensively studied each of these association regions and derived closed form expressions for the probabilities, considering three different cells in the cluster.
2) We have derived the distance distributions to the serving cell conditioned to the decoupled association case, which shows a clear reduction on the user path-loss when connecting to a SCell.
3) We have studied the UL throughput gains of multiple connections towards two different serving cells, by comparing the outcomes of the mathematical analysis with several

baseline solutions: DL received power-based association rule in Dual-Connectivity, Single-Connectivity with decoupled association and Carrier Aggregation towards the MCell. Conclusions highlight that the best form of spectrum aggregation for users in the decoupled region is to allow to split the UL from the DL, since significant gains can be obtained.

## ACKNOWLEDGEMENT

This work is supported by Ericsson 5G and Tactile Internet industry grant to King's College London as well as by the ICT-SOLDER project, www.ict-solder.eu, FP7 project number 619687

## REFERENCES

[1] S. Sesia, I. Toufik, and M. Baker, *LTE The UMTS Long Term Evolution, from Theory to Practice*. Wiley Online Library, 2009.

[2] 3GPP, "Study on Small Cell Enhancements for E-UTRA and E-UTRAN; Higher Layer Aspects," 3rd Generation Partnership Project (3GPP), TR 36.842, Sep. 2014. [Online]. Available: http://www.3gpp.org/dynareport/36842.htm

[3] M. A. Lema, M. Garcia-Lozano, S. Ruiz, and D. G. Gonzalez, "Improved Component Carrier Selection Considering MPR Information for LTE-A Uplink Systems," in *2013 IEEE 24th International Symposium on Personal Indoor and Mobile Radio Communications (PIMRC)*, Sept 2013, pp. 2191–2196.

[4] Huawei, "Handling of UL Traffic of a DL Split Bearer," 3GPP TSG-RAN, Tech. Rep. R2-140054, 2014.

[5] K. Smiljkovikj, P. Popovski, and L. Gavrilovska, "Analysis of the Decoupled Access for Downlink and Uplink in Wireless Heterogeneous Networks," 2014, Available online at http://arxiv.org/abs/1407.0536.

[6] H. Wang, C. Rosa, and K. Pedersen, "Dedicated Carrier Ceployment in Heterogeneous Networks with Inter-Site Carrier Aggregation," in *2013 IEEE Wireless Communications and Networking Conference (WCNC)*, April 2013, pp. 756–760.

[7] ——, "Uplink Inter-Site Carrier Aggregation between Macro and Small Cells in Heterogeneous Networks," in *2014 IEEE 80th Vehicular Technology Conference (VTC Fall)*, Sept 2014, pp. 1–5.

[8] M. S. Pan, T. M. Lin, C. Y. Chiu, and C. Y. Wang, "Downlink traffic scheduling for lte-a small cell networks with dual connectivity enhancement," *IEEE Communications Letters*, vol. 20, no. 4, pp. 796–799, April 2016.

[9] A. Zakrzewska, D. Lpez-Prez, S. Kucera, and H. Claussen, "Dual connectivity in lte hetnets with split control- and user-plane," in *2013 IEEE Globecom Workshops (GC Wkshps)*, Dec 2013, pp. 391–396.

[10] W. Zhouyun, X. Weiliang, Y. Fengyi, and B. Qi, "User association in heterogeneous network with dual connectivity and constrained backhaul," *China Communications*, vol. 13, no. 2, pp. 11–20, Feb 2016.

[11] S. Ericsson, "Further Discussions on UL/DL Split," 3GPP TSG-RAN, Tech. Rep. R2-131678, May 2013.

[12] H. Elshaer, F. Boccardi, M. Dohler, and R. Irmer, "Downlink and Uplink Decoupling: a Disruptive Architectural Design for 5G Networks," 2014, 2014 IEEE Global Telecommunications Conference (GLOBECOM 2014).

[13] ——, "Load & Backhaul Aware Decoupled Downlink/Uplink Access in 5G Systems," 2014, Available online at http://arxiv.org/abs/1405.1853.

[14] S. Singh, X. Zang, and J. Andrews, "Joint Rate and SINR Coverage Analysis for Decoupled Uplink-Downlink Biased Cell Associations in HetNets," 2014, Available online at http://arxiv.org/abs/1412.1898.

[15] H. ElSawy, E. Hossain, and M. Haenggi, "Stochastic Geometry for Modeling, Analysis, and Design of Multi-Tier and Cognitive Cellular Wireless Networks: A Survey," *IEEE Communications Surveys Tutorials*, vol. 15, no. 3, pp. 996–1019, Third 2013.

[16] 3GPP, "Physical Layer Procedures," 3rd Generation Partnership Project (3GPP), TS 36.213, Sep. 2009. [Online]. Available: http://www.3gpp.org/ftp/Specs/html-info/36213.htm

[17] T. Novlan, H. Dhillon, and J. Andrews, "Analytical Modeling of Uplink Cellular Networks," *IEEE Transactions on Wireless Communications*, vol. 12, no. 6, pp. 2669–2679, June 2013.

[18] S. Singh and J. Andrews, "Joint resource partitioning and offloading in heterogeneous cellular networks," *Wireless Communications, IEEE Transactions on*, vol. 13, no. 2, pp. 888–901, February 2014.

[19] K. Smiljkovikj, H. Elshaer, P. Popovski, F. Boccardi, M. Dohler, L. Gavrilovska, and R. Irmer, "Capacity Analysis of Decoupled Downlink and Uplink Access in 5G Heterogeneous Systems," 2014, Available online at http://arxiv.org/abs/1410.7270.

# Bibliography


[1] A. Aijaz, M. Dohler, A. H. Aghvami, V. Friderikos and M. Frodigh, Realizing The Tactile Internet: Haptic Communications over Next Generation 5G Cellular Networks, *arXiv preprint arXiv:1510.02826, 2015.*

[2] M.Lema, Contribution to the Optimization of 4G Mobile Communications by Means of Advanced Carrier Aggregation Strategies, *Doctoral dissertation,2015.*

[3] G. Nigam, P. Minero, and M. Haenggi, Coordinated multipoint in heterogeneous networks: A stochastic geometry approach. *Globecom Workshops (GC Wkshps), pp. 145-150, December 2013*

[4] D. Astely, E. Dahlman, A. Furuskr, Y. Jading, M. Lindstrm and S. Parkvall, LTE: the evolution of mobile broadband, *IEEE Communications Magazine, vol. 47, no. 4, pp. 44-51, April 2009.*

[5] J. G. Andrews, S. Buzzi, W. Choi, S. Hanly, A. C. K. Soong, J. C. Zhang and A. Lozano, What Will 5G Be? *Institute of Electrical and Electronics Engineers (IEEE), April 2014.*

[6] A. Ghosh et al., Heterogeneous cellular networks: From theory to practice, *IEEE Communications Magazine, vol. 50, no. 6, pp. 54-64, June 2012.*

[7] J. G. Andrews, Seven ways that hetnets are a cellular paradigm shift *IEEE Communications Magazine, vol 51, no. 3, pp. 136-144, 2013.*

[8] M. Y. Arslan, K. Sundaresan and S. Rangarajan, Software-defined networking in cellular radio access networks: potential and challenges," *IEEE Communications Magazine, vol. 53, no. 1, pp. 150-156, January 2015.*

[9] D. Ghosh and C. Lott, Uplink-Downlink Imbalance in Wireless Cellular Networks,emphCommunications, 2007. ICC '07. IEEE International Conference on, Glasgow, pp. 4275-4280, 2013.

[10] H. Elshaer, F. Boccardi, M. Dohler and R. Irmer, Downlink and Uplink Decoupling: A disruptive architectural design for 5G networks, *Global Communications Conference (GLOBECOM), 2014 IEEE, Austin, TX, pp. 1798-1803, 2014.*

[11] H. Elshaer, F. Boccardi, M. Dohler and R. Irmer, Load and backhaul aware decoupled downlink/uplink access in 5G systems, *Communications (ICC), 2015 IEEE International Conference on, London, pp. 5380-5385, 2015.*

[12] S. Kim, J. H. Na, D. S. Kwon, Performance analysis of Heterogeneus Cellular Networks with multiple Connectivity, *International Journal of Electrical, Energetic, Electronic and Communication engineering, Vol 9, no. 2, pp. 320-325, 2015.*

[13] H. Wang, C. Rosa, and K. I. Pedersen, Dual Connectivity for LTE-Advanced Heterogeneous Networks, *Wireless Networks (2015).*

[14] A. Zakrzewska, D. Lpez-Prez, S. Kucera and H. Claussen, Dual connectivity in LTE HetNets with split control- and user-plane, *Globecom Workshops (GC Wkshps), pp. 391-396. 2013 IEEE, Atlanta, GA, 2013.*

[15] X. Tao, X. Xu and Q. Cui, An overview of cooperative communications, *IEEE Communications Magazine 50, pp. 65-71, 2012).*

[16] S. Yan, w. Wang, Z. Zhao and A. Ahmed, *Investigation of cell association techniques in uplink cloud radio access networks, Trans. Emerging Tel. Tech. 2014.*

[17] H. ElSawy, E. Hossain and M. Haenggi, Stochastic Geometry for Modeling, Analysis, and Design of Multi-Tier and Cognitive Cellular Wireless Networks: A Survey, *IEEE Communications Surveys and Tutorials, vol. 15, no. 3, pp. 996-1019, Third Quarter 2013.*

[18] F.Bacelli, Stochastic Geometry and Wireless Networks: Volume I Theory, 2009.

[19] S.Weber and J. Andrews, Transmission capacity of wireless networks,2012.

[20] M. Médard and S. S. Lumetta, Network reliability and fault tolerance. *Encyclopedia of Telecommunications, 2003.*

[21] K. Smiljkovikj, P. Popovski and L. Gavrilovska, Analysis of the Decoupled Access for Downlink and Uplink in Wireless Heterogeneous Networks,*IEEE Wireless Communications Letters, vol. 4, no. 2, pp. 173-176, April 2015.*

[22] D. Moltchanov, Distance distributions in random networks, *Ad Hoc Networks, vol. 10, no. 6, pp. 1146-1166, 2012.*

[23] K. Smiljkovikj, H. Elshaer, P. Popovski, F. Boccardi, M. Dohler, L. Gavrilovska, R. Irmer, Capacity Analysis of Decoupled Downlink and Uplink Access in 5G Heterogeneous Systems. *2014.*

[24] S. Singh, Load balancing in heterogeneous cellular networks *Doctoral dissertation,2014.*

[25] U. Blahak, Efficient approximation of the incomplete gamma function for use in cloud model applications, *Geoscientific Model Development, vol. 3, no. 2, pp. 329-336, (2010).*

[26] J. Goldsmith and P. P. Varaiya, Capacity of fading channels with channel side information, *IEEE Transactions on Information Theory, vol. 43, no. 6, pp. 1986-1992, November 1997.*

[27] H. S. Jo, Y. J. Sang, P. Xia and J. G. Andrews, Heterogeneous Cellular Networks with Flexible Cell Association: A Comprehensive Downlink SINR Analysis, *IEEE Transactions on Wireless Communications, vol. 11, no. 10, pp. 3484-3495, October 2012.*